The Role of Phospholamban Cysteines in the Activation of the Cardiac Sarcoplasmic Reticulum Ca^{2+} Pump by Nitroxyl (HNO)

Chevon Nichole Thorpe

Dissertation submitted to the faculty of the Virginia Polytechnic Institute and State University in partial fulfillment of the requirements for the degree of

Doctor of Philosophy
In
Biochemistry

James E. Mahaney, Chair
David R. Bevan
Pablo Sobrado
Richard P. Wyeth

June 8, 2012
Blacksburg, VA

Keywords: Phospholamban, SERCA, Nitroxyl, Angeli's Salt, Heart failure

The Role of Phospholamban Cysteines in the Activation of the Cardiac Sarcoplasmic Reticulum Ca^{2+} Pump by Nitroxyl (HNO)

Chevon Nichole Thorpe

ABSTRACT

Phospholamban (PLN) is an integral membrane protein that regulates the sarco(endo)plasmic Ca^{2+}-ATPase (SERCA2a) within the cardiac sarcoplasmic reticulum (CSR). SERCA2a regulates intracellular Ca^{2+}- handling and thus plays a critical role in initiating cardiac contraction and relaxation. It is believed that dysregulation of SERCA2a is a contributing factor in human heart failure patients. Even though there have been substantial advancements in understanding heart failure pharmacological therapies, patient prognosis remains poor. Nitroxyl (HNO), a new candidate heart failure drug therapy, has been shown to enhance overall cardiovascular function in both healthy and failing hearts, at least in part, by increasing Ca^{2+} re-uptake into the CSR. Previous research has shown that activation of SERCA2a by HNO is PLN-dependent; however, the mechanism of action of HNO remains unknown. We propose that HNO, a thiol oxidant, modifies one or more of the three PLN cysteine residues (C36, C41, C46) affecting the regulatory potency of PLN toward SERCA2a. To test this hypothesis, a series of PLN mutants were constructed containing single, double and triple cysteine substitutions. Using the baculovirus expression insect cell system, each PLN cysteine mutant was expressed alone and co-expressed with SERCA2a in insect cells and isolated in cellular endoplasmic reticulum (ER) microsomes. Samples were treated with Angeli's salt (an HNO donor) to determine the role of each PLN cysteine residue in the mechanism of SERCA2a activation by nitroxyl. Using a standard phosphate activity assay and SDS-PAGE/immunoblot techniques, we determined that the PLN cysteine residues at positions 41 and 46 are important in HNO activation of SERCA2a. Both SERCA2a + 41C PLN and SERCA2a + 46C PLN microsomal samples showed a $\Delta K_{0.5}$ of ~0.33 μM and evidence of reversible HNO induced disulfide bond formation. These studies provide important new insight into the mechanism of action of HNO on cardiac SR and thereby help evaluate the drug as a candidate therapy for congestive heart failure.

ACKNOWLEDGEMENTS

First and foremost, I will like to acknowledge that without God none of this would have been possible. There were many times throughout this journey when I knew without a shadow of a doubt that I was not going to make it. In amidst the marriage woes, the birth of a baby, the loss of a second baby, the death of grandparents, the suicide attempts of loved ones, and the many days when there was not enough money to eat, I made it. To tell the full story would be to write another dissertation, but know that I have a testimony in my heart of God's grace, love, and mercy from my experience here at Virginia Tech. Thank you to my praying family that lifted me up when I couldn't bear to stand and the road ahead was cloudy because of my tears. Thank you for the phone calls, e-mails, scriptures, and most of all just being there to listen. Dad, I know this is a proud moment for you and I wish that you could be here to share it with me. Thank you for watching over me in heaven and sending angels to comfort me when I needed them the most.

I would be remiss if I did not send a very special, heartfelt thank you to my family. To my husband, Leemar, for the never ending words of encouragement and love. These mere words cannot ever do justice for how much I appreciate you and your support. Thank you for the emotional support, for being that extra set of footprints in the sand when I couldn't walk, and for not giving up on me when I wanted to give up on myself, I love you. To my sweet baby boy, Daniel, mommy loves you with all of my heart. When I was facing my darkest days, a picture of you would always brighten it. To my brother, Chevin, and my sister, Chela, thank you for believing in me and giving me strength. To my mother, for always knowing the exact words I needed to hear to go throughout my day. You have been such as inspiration on my life, and I couldn't have made it without you. And finally to my extended family who always took out tide to send cards and other words of encouragement, thank you.

I would have never gotten this far in life without the many people who mentored me and served as valuable role models. A big thank you goes to my VT-PREP family for giving me the opportunity to attend VT. A specific thanks to Drs. Huderson, Sutton, and Vaughan. I am proud to say that I have now joined your club, thanks for paving the way. I will miss the camaraderie, free food, restaurant loitering, venting sessions, conference trips and girl talks but I know that the best times are yet to come. Also, I would like to thank my undergraduate mentor. Dr. Lisa

Webb, who encouraged me to go to graduate school and showed me what true woman in science looks like.

To the past members of the Mahaney lab: Vidhya, Lesley, John, Cara Marie, Marla, and Danielle. Thank you for all the assistance you have given at some point and time on this project. I will never forget the crazy lab conversations, inside jokes, makeshift birthday hats, playing with dry ice shipments, blasting obscene music, the inappropriate penguin poster, and all other general forms of buffoonery. You made my time in the lab more enjoyable and helped keep my sanity.

To the beautiful and devastating ladies of the Blacksburg Alumnae Chapter of Delta Sigma Theta Sorority, Inc. thank you for all extending the hand of sisterhood and allowing me to be a part of your lives. Each member has touched my life in a special way and I want to thank you all for your genuine spirits and never ending encouragement. Special thanks go to my linesisters from Fall '09. Ladies, we have been through hell and back and I couldn't have made it without you. Thank you for showing me the woman that I really am, and being a listening ear even if you couldn't relate.

To my other support system that helped me keep my life in order amongst the chaos. Nikki and Steve, I can never thank you enough for watching Daniel free of charge so that I could run errands or take a time out. Sarah Ohar, thank you for keeping me calm and taking such wonderful care of my baby when I was in the lab. Daniel learned so much from you and you have impacted his life in such a positive way.

Last but certainly not least, I would like to extend a heartfelt thanks to my advisor, James Mahaney and to the rest of my committee members. Dr. Mahaney, thank you for giving me the opportunity to work in your laboratory and make a contribution to science. I know that we did not always see eye to eye, but thank you for always having my best interest at heart and seeing me through to the end, I will never forget that. To my committee members, thank you for all of your guidance and wisdom. I truly appreciate the time that each of you committed to myself and this project.

TABLE OF CONTENTS

LIST OF FIGURES

LIST OF TABLES

LIST OF ABBRIVIATIONS

AcMNPV	**autographa californica nuclear polyhedrosis virus**
Amp	**Ampicillin**
AS	**angeli's salt**
ATP	**adenosine triphosphate**
BP	**base pairs**
BSA	**bovine serum albumin**
CamK-II	**camodulin kinase-II**
cAMP	**cyclic adenosine monophosphate**
$CaCl_2$	**calcium chloride**
CHF	**congestive heart failure**
CSR	**cardiac sarcoplasmic reticulum**
DTNB	**5,5'-dithiobis-(2-nitrobenzoic acid**
DTT	**Dithiothreitol**
EC	**excitation-contraction**
ER	**endoplasmic reticulum**
GST	**glutathione-*S*-transferase**
HNO	**Nitroxyl**
HRP	**horseradish peroxidase**
kDa	**Kilodalton**
MOI	**multiplicity of infection**
MW	**molecular weight**
OD	**optical density**
PAGE	**polyacrylamide gel electrophoresis**
PBS	**phosphate buffered saline**
PCR	**polymerase chain reaction**
PKA	**protein kinase A**
Pfu	**plaque forming unit**
PLN	**Phospholamban**
PVDF	**polyvinylidine fluoride**
RyR	**ryanodine receptor**
RPM	**revolutions per minute**
SDS	**sodium dodecyl sulfate**
SERCA	**sarco(endo)plasmic reticulum calcium ATPase**
SR	**sarcoplasmic reticulum**
WT	**Wildtype**

CHAPTER I

INTRODUCTION

General heart physiology

The heart is one of the most important organs in the entire human body. This involuntary muscular organ is responsible for pumping life-sustaining blood via a 60,000 mile long network of vessels. The organ works ceaselessly, beating an average 100,000 times a day to keep the body supplied with fresh oxygen and nutrients. The human heart is divided into four main chambers: two upper chambers, called atria, and two lower chambers, called ventricles. In essence, the heart acts as a double pump. The function of the right side of the heart is to collect deoxygenated blood in the right atrium from the body and deposit it into the right ventricle to pump into the lungs. The left side of the heart receives the oxygenated blood from the lungs through the left atrium where the blood moves to the left ventricle which pumps the blood out to the body. The rhythmic beat of your muscular heart is controlled by a cascade of biological processes that begins with a cardiac action potential and ends with myocyte contraction and relaxation. This fundamental physiological control is called excitation-contraction (EC) coupling (*1*).

Normal E-C Coupling – The calcium transient

Cardiac EC coupling forms the biophysical underpinnings of the heart beat and is intimately related to calcium homeostasis (*2*). The regulation and maintenance of Ca^{2+} homeostasis within the cardiomyocyte is a crucial process as it enables the chambers of the heart to contract and relax. A diagram showing the key proteins involved in normal EC coupling can be seen in Figure 1-1. At the beginning, the calcium transient is initiated in response to an action potential generated by the atrioventricular node in which extracellular Ca^{2+} enters the cell through depolarized-activated L-type Ca^{2+} channels (*1, 3, 4*). The influx of Ca^{2+} instigates the release of stored Ca^{2+} from the sarcoplasmic reticulum (SR) via the spatially proximate ryanodine receptors (RyR2), a term called calcium induced calcium release. The combination of Ca^{2+} influx and release from the SR raises the free intracellular Ca^{2+} concentration, allowing Ca^{2+} to bind to troponin C which then activates the actin-myosin contractile machinery. Unlike

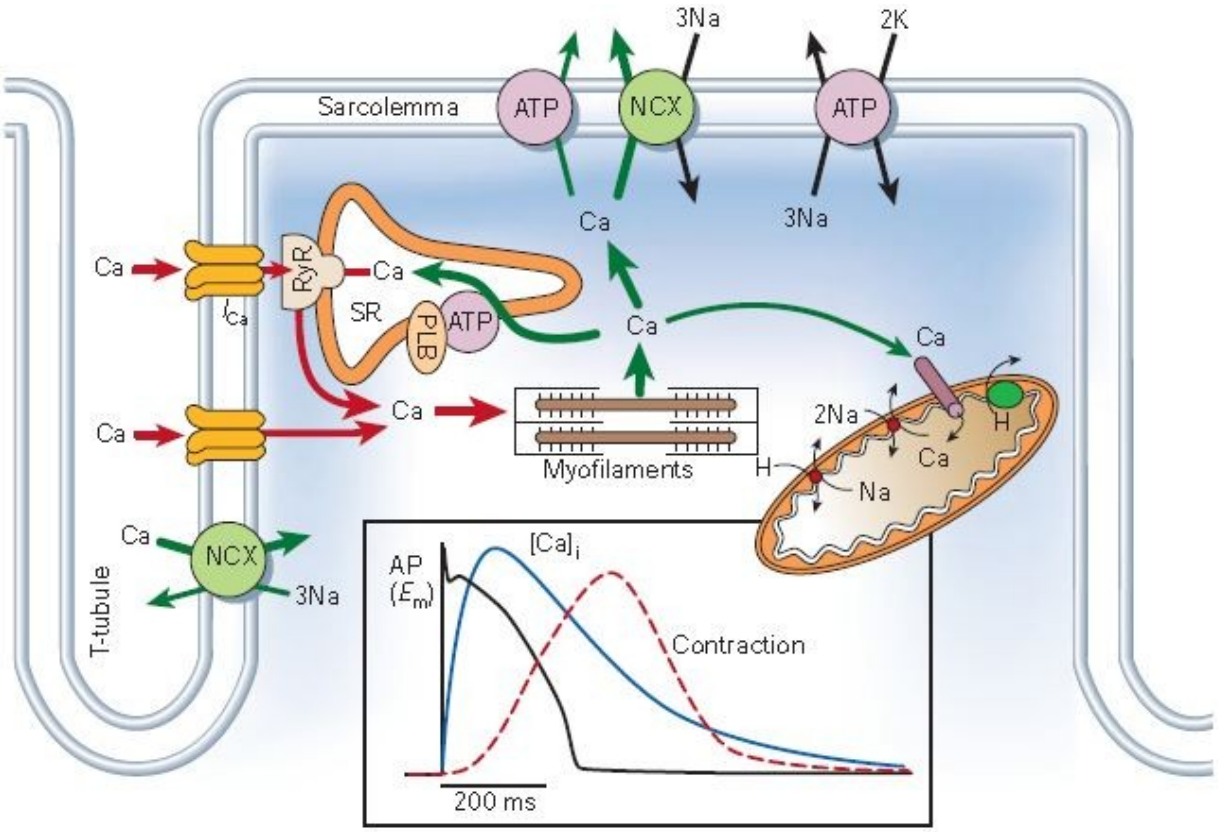

Figure 1-1. Ca^{2+} transport in ventricular myocytes.
Inset shows the time course of an action potential, Ca^{2+} transient and contraction measured in a rabbit ventricular myocyte at 37°C. This figure was taken directly from Bers, D. M. (2002). "Cardiac excitation-contraction coupling." Nature **415**: 198-205. Fair use determination attached.

different muscle types that depend completely on Ca^{2+} SR storage, the extracellular calcium is needed in order for the heart to have a more forceful contraction. Relaxation results from a closure of release channels, and removal of Ca^{2+} from the sarcoplasm. There are four ways in which Ca^{2+} can be transported out of the cytosol: SR Ca^{2+}-ATPase, sacrolemmal Na^{+}/Ca^{2+} exchange, sarcolemmal Ca^{2+}-ATPase or the mitochondrial Ca^{2+} uniport. The majority (~75%) of Ca^{2+} leaves through the SR Ca^{2+}-ATPase (SERCA) (*3-5*).

Calcium homeostasis can also be regulated by β-adrenergic receptor signaling. Sympathetic stimulation of the heart via β-adrenergic signaling increases contractility (inotropy) and relaxation rate (lusitropy). β-adrenergic receptor agonist stimulation activates a GTP-binding protein that stimulates adenylyl cyclase to produce cAMP, which in turn activates protein kinase A (PKA). PKA then phosphorylates several proteins related to EC coupling, including phospholamban (PLN), L-type calcium channels, ryanodine receptors, and myosin binding protein (*2*). The lusitropic and inotropic effect of PKA is mediated by phosphorylation of PLN and the ryanodine receptors respectively (*6*).

The sarcolemma (muscle cell plasma membrane) is one of the main components of EC coupling as this is the site where calcium enters and leaves the cell through a distribution of various channels and pumps. One of the main structural specializations of the sarcolemma is the formation of membranous tubules (transverse or t-tubules) that transverse the sarcoplasm. These t-tubules help to bring the extracellular environment in close proximity to the cell for quick depolarization. As depicted in Figure 1-1, the sarcolemma (t-tubules) are surrounded by the sarcoplasmic reticulum. The sarcoplasmic reticulum is the enlargement of smooth endoplasmic reticulum that consists of terminal and longitudinal components. The terminal cisternae are adjacent to the walls of the sarcolemma formed t-tubules to form a dyadic cleft with the face of the cleft composed of mostly Ryanodine receptors (RyR). The longitudinal SR consists of primarily the SR proteins, SERCA2a, and the associated regulatory phosphoprotein, phospholamban (PLN).

Because SERCA2a and PLN play a central role in myocardiac contractility, the molecular mechanisms of regulation have been the subject of intense investigation for many decades (*7*). As stated above, SERCA2a actively transports Ca^{2+} into the SR thus regulating Ca^{2+} concentration, SR Ca^{2+} load, and the rate of cardiac contraction and relaxation of the heart. As a major regulator of intracellular Ca^{2+} homeostasis, any changes in expression and activity

levels of either SERCA2a and or PLN has shown to lead to decreased SR Ca^{2+} content and a variety of pathological conditions including cardiac diseases (*7-11*). The Mahaney lab focuses our efforts on understanding the interaction of SERCA2a and PLN, therefore these proteins will be discussed in further detail, including their role in cardiac dysfunction.

SERCA

There are three separate genes that encode the SERCA family of calcium pumps SERCA1 found in fast twitch skeletal muscles, SERCA2 (a/b) found in smooth and cardiac muscle, and SERCA3 a ubiquitous form (*12*). These isoforms have approximately the same number of amino acids (~110kDa) and have 75-85% sequence identity with the majority of variability occurring at the C-terminus (*13*). Because it is relatively straightforward to purify, the fast twitch Ca^{2+} pump, SERCA1, was the first pump to be studied in detail and thus is the most understood. In addition, SERCA1 is also the only P-type ion ATPase for which a detailed 3D structure is known. In 2000, high resolution structures of several confirmations of SERCA1 were published by Toyoshima and Nomura (*14*). From these studies, it has been confirmed that the SERCA Ca^{2+} pump consists of a single polypeptide chain folded into four major domains (Figure 1-2). There is a transmembrane domain (M), comprised of 10 transmembrane helices and the two calcium binding sites, three cytosolic domains; the actuator domain (A), the phosphorylation domain (P) and the nucleotide domain (N) (*14, 15*). The links between the A and M domains and the N and P domains are thought to be flexible to allow for the large scale movements needed for the catalytic cycle conformational changes (*16*).

The catalytic cycle of SERCA pumps are based on the transformation between two major conformational states, designated as E1 and E2 (*5, 17*) (Figure 1-3). In the E1 confirmation, the two transmembrane Ca^{2+} binding sites face the cytoplasm and are of high affinity for calcium. In the E2 confirmation, the Ca^{2+} binding sites face the luminal side of the membrane and there is a low affinity for calcium. The first step in the cycle consists of the binding of either cytosolic ATP or 2 Ca^{2+} ions to the E1 conformation. This creates the $2Ca^{2+}$-E1-ATP formation which then undergoes phosphorylation to form $2Ca^{2+}$-E1-P. Next, there is a major conformational change to a lower energy $2Ca^{2+}$-E2-P form whereby the Ca^{2+} binding sites are converted to a low-affinity state and reorient themselves towards the luminal side of the membrane. The cycle

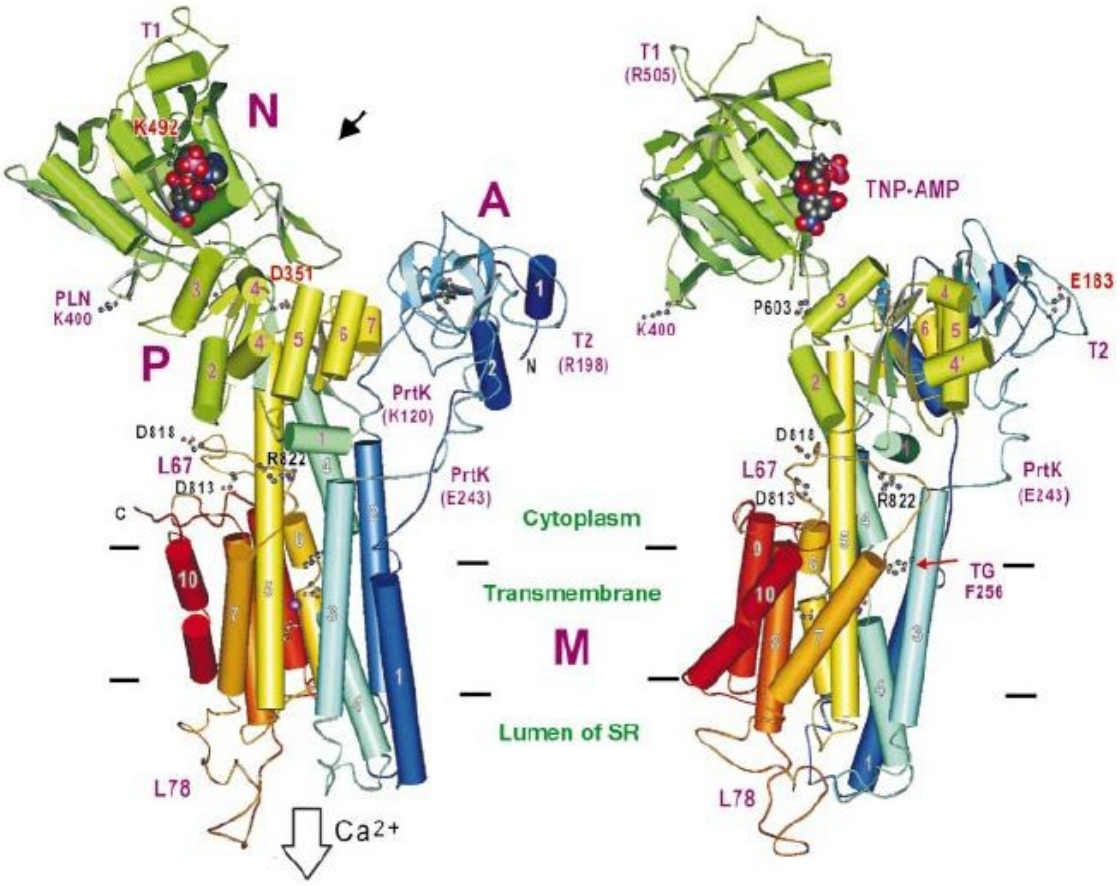

Figure 1-2. Architecture of the sarcoplasmic reticulum Ca^{2+}-ATPase. α-helices are represented by cylinders and β-strands by arrows. Color changes gradually from the N terminus (blue) to the C terminus (red). Three cytoplasmic domains are labeled (A, N and P). Transmembrane helices (M1-M10) and those in domains A and P are numbered. The model is orientated so that transmembrane helix M5 is parallel to the plane of the paper. Reprinted by permission from Macmillian Publishers Ltd: Nature (Toyoshima et. al."Crystal structure of the calcium pump of sarcoplasmic reticulum at 2.6 Å resolution" 405(6787), 647-655), copyright (2000).

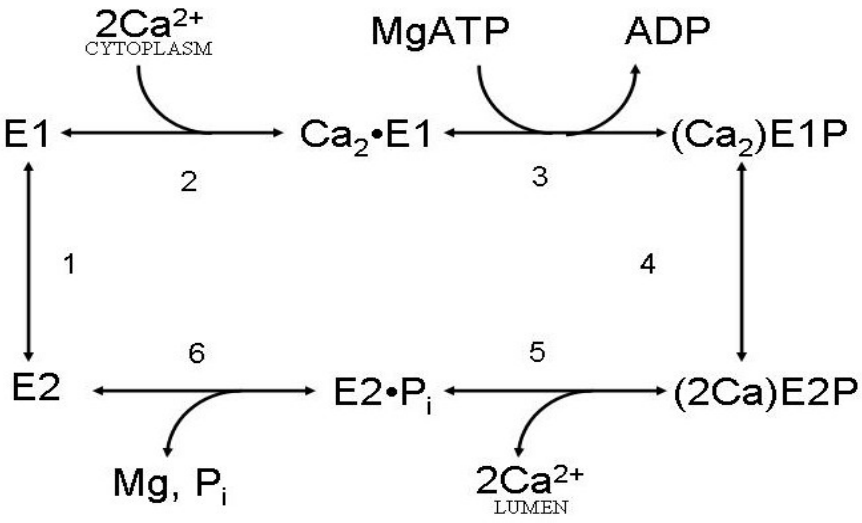

Figure 1-3. The Ca^{2+}-ATPase catalytic cycle
The numbers (1-6) in the diagram indicate the step in the process. The cytoplasm and lumen are labeled within the image to orient the cycle to the membrane.

ends with the release of Ca^{2+} and phosphate and a major conformation change back to the E1 state.

SERCA2a (997 amino acids), a splice variant of the SERCA2 gene, is the main isoform in the SR of cardiac muscle and the major enzyme responsible for regulating Ca^{2+} cycling. Similar to the other SERCA pumps, the cardiac isoform is a Ca^{2+} pump powered by ATP hydrolysis. The main function of SERCA2a is to actively transfer Ca^{2+} from the cytosol of the cardiomyocyte into the lumen of the sarcoendoplasmic reticulum to stimulate cardiac relaxation (*14*). This process is under the reversible regulation of phospholamban.

Phospholamban

In cardiac muscle, SERCA2a is regulated by the small integral membrane phosphoprotein phospholamban (PLN) (*15, 18*) thereby making PLN a key regulator of Ca^{2+} pump kinetics and cardiac contractility (*18*). PLN is a 52-amino acid amphipathic protein of 6.1 kDa with a hydrophilic N-terminus and a hydrophobic C-terminus. The 52 amino acids are organized into three physical and functional domains. Domain Ia (residues 1-20) and domain Ib (residues 21-30) comprise the cytosolic domain and is mostly α-helical and carries a net positive charge. Domain II is the transmembrane domain (residues 31-52) which is made up of solely uncharged residues and is α-helical in conformation as well (*19*). PLN is highly conserved in most species and can be found in slow twitch skeletal, cardiac muscle and some smooth muscle. However, PLN is not present in fast twitch skeletal muscle because of the absence of the β-adrenergic signaling pathway.

The complete primary sequence was discovered by Fuji et. al. in 1989 by amino acid sequencing and cDNA cloning revealing a monomer of ~6 kDa (*20*). Further studies in lipid bilayers revealed that PLN exists mainly as a homopentamer in a dynamic equilibrium with the monomer form (*21*). By performing alanine-scanning mutagenesis, the quaternary structure of PLN was determined to be a coiled-coil stabilized by a heptad repeat of leucine and isoleucine (leucine-isoleucine zipper) within the transmembrane domain (*18, 21-23*) (Figure 1-4 "A"). In addition to the leucine-isoleucine zipper, Karim et. al demonstrated the importance of the three transmembrane cysteine residues (positions 36, 41, 46) to the pentameric stability of PLN. Of particular importance is the cysteine at residue 41 as their work showed that PLN quaternary structure is intolerant of bulky amino acid (i.e. Phe or Ser) changes at this position (*20, 22*).

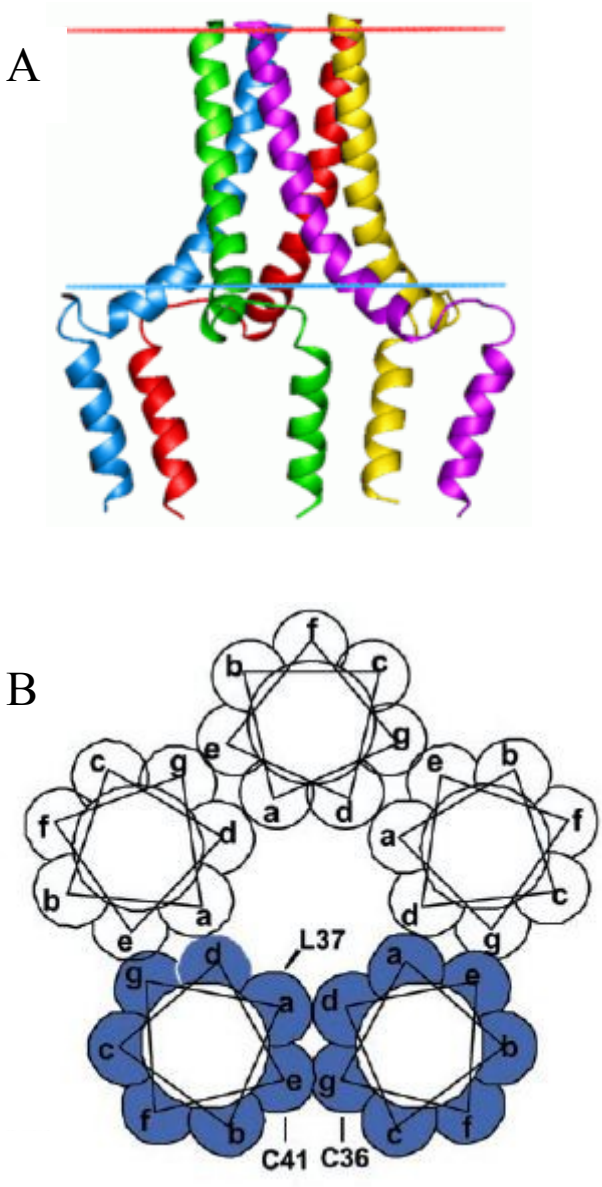

Figure 1-4. PLN pentameric structure and helical wheel representation. (A) PDB rendering of PLN pentameric structure based on 1fjk. The red line marks the luminal side of the ER while the blue line marks the cytoplasmic side. (B) Helical wheel model of PLN. This figure was taken directly from Karim, C. B., Paterlini, M. G., Reddy, L. G., Hunter, G. W., Barany, G., and Thomas, D. D. (2001) Role of cysteine residues in structural stability and function of a transmembrane helix bundle, *Journal of Biological Chemistry 276*, 38814-38819. (accessed on May 25, 2012). Used with permission of ASMB, letter attached.

Determination of a high-resolution structure of PLN transmembrane domain by X-ray crystallography or NMR is handicapped by the hydrophobic nature of the peptide, thus the current understanding of PLN structure is based on several reported models and theories. Figure 1-4 "B" shows the most recent helical wheel model of PLN. In this model, the leucine and isoleucine residues occupy positions *a* and *d*. Cys-36 and Cys-41 are at positions *g* and *e*, respectively, whereas Cys-46 faces the lipid environment at position *c*. The pentameric structure of PLN appears to occlude the sulfhydryl side chain of cysteine 41 supporting the work reported by Karim et. al. showing the addition of bulky side chains prevents the assembly of PLN pentameric structure by disrupting the transmembrane domain hydrophobic packing (*24*).

Although the majority of PLN exists in the pentamer, previous studies show only the monomeric form of PLN regulates SERCA2a (*18, 21*). Most of the PLN transmembrane helix residues contribute to the interaction with SERCA (*23*); at positions that are important in Ca^{2+} binding (*19, 25-27*). The cytosolic domain of PLN also interacts with the stalk and nucleotide-binding domain of SERCA thereby blocking long-range Ca^{2+}-dependent conformational changes needed to activate the enzyme to for ATP-dependent Ca^{2+} cycling (*19, 28*). Figure 1-5 depicts the current theory on PLN:SERCA2a regulation.

It is well accepted that PLN has the greatest affinity for the E2 state, or calcium free state, of SERCA2a. Dephosphorylated PLN binding to SERCA2a stabilizes this state, which thereby inhibits the transition to the E1 calcium bound state (*29*). This inhibition of SERCA2a by PLN leads to a decrease in apparent Ca^{2+} affinity without an effect on the maximal velocity (V_{max}) or calcium binding cooperativity (*2*). Phosphorylation of PLN alters the PLN-SERCA2a interaction, relieving the Ca^{2+}-ATPase inhibition and enhancing relaxation and contractility rates (*18, 30, 31*). During β-adrenergic stimulation of the heart, PLN is phosphorylated by protein kinase A (PKA) at Ser^{16} and by Ca^{2+}/calmodulin-dependent protein kinase at Thr^{17}. Experimentally, the effects of PLN phosphorylation can be mimicked using the anti-PLN monoclonal antibody, 2D12, which uncouples PLN from SERCA2a.

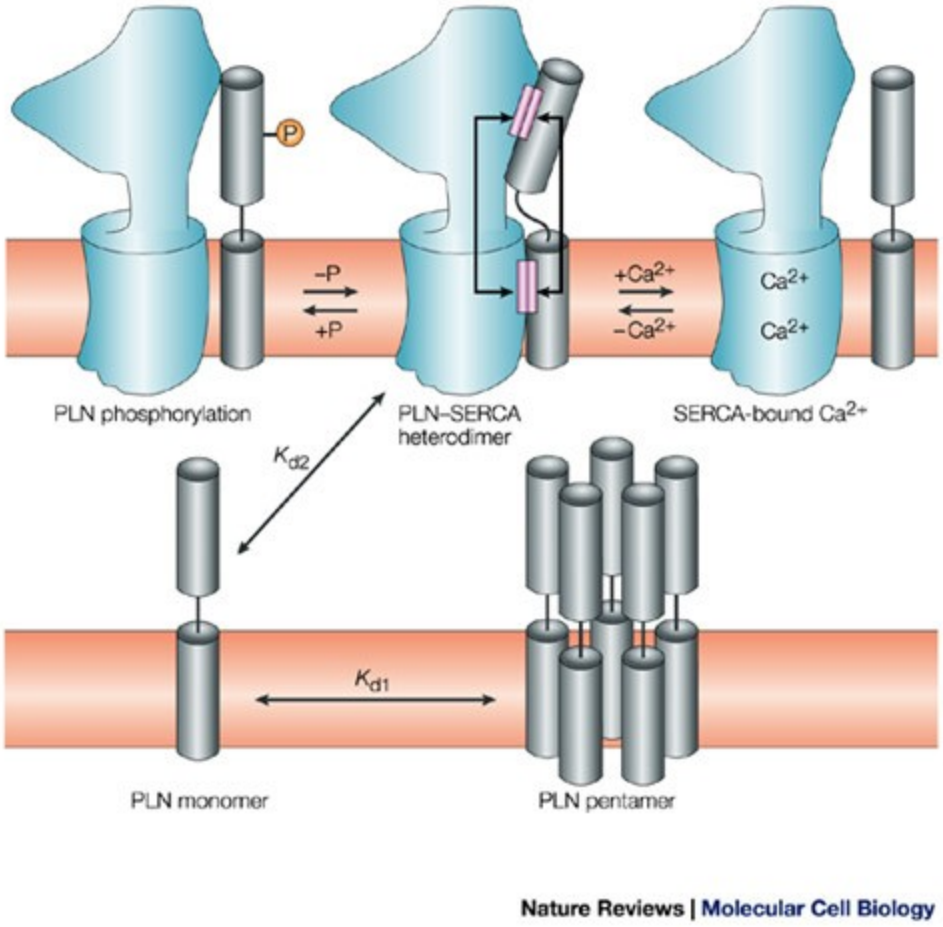

Figure 1-5. Regulatory features of the PLN-SERCA interaction. Two steps can be dissected in the reversible inhibition of sarco(endo)plasmic reticulum Ca2+-ATPase (SERCA) activity by phospholamban (PLN): first, the association/dissociation of pentameric PLN (Kd1), and second, the association/dissociation of monomeric PLN and SERCA (Kd2). The phosphorylation of PLN and Ca^{2+} binding to SERCA are driving forces for the dissociation of the PLN–SERCA complex, thereby activating SERCA. Phosphorylation of PLN dissociates functional interactions, but is less effective than Ca^{2+} binding to SERCA in breaking up physical interactions. Reprinted by permission from Macmillian Publishers Ltd: Nature Reviews (MacLennan and Kranias ." Phospholamban: A crucial regulator of cardiac contractility" 405(6787), 647-655), copyright (2003).

Pathological E-C coupling

Abnormal changes in any of the key proteins that are involved with EC coupling and calcium homeostasis usually causes major problems with myocardial functionality. There are many different heart failure model studies that disagree about whether certain factors such as SERCA expression are increased, decreased, or unchanged (*32-34*). In general heart failure is characterized by myocyte loss or impaired function of viable myocardium which usually reflects alterations in signaling pathways that modulate EC coupling (*35, 36*). Many studies have measured cardiac SERCA expression and function and show a general decrease in function across the board. On the other hand, PLN has not been found to be altered in heart failure, thus becoming over regulatory leading to a decreased Ca^{2+} affinity of SR Ca^{2+} transport (*2*). There is other data that suggests the phosphorylation state of PLN may be reduced in heart failure which would further reduce Ca^{2+} sensitivity of SERCA2a and slow Ca^{2+} transport back into the SR (*37*). Despite the discrepancy between heart failure models, there is a general agreement that alterations of key proteins involved in EC coupling can contribute to heart failure.

The term heart failure as defined by the American Heart Association is a chronic, progressive condition in which the heart muscle is unable to pump enough blood through the heart to meet the body's needs for blood and oxygen. This term is often used interchangeably with many other types of heart diseases that display impaired cardiac function. One of the most common types of heart failure, which generates from altered EC coupling proteins, is congestive heart failure (CHF).

Congestive Heart Failure

Congestive heart failure (CHF) resulting from cardiomyopathy is a serious condition and a principal cause of death and disability in children and adults. As blood flow out of the heart slows, blood returning to the heart through the veins backs up, causing congestion in the body's tissues. There are many causes that can encourage the development of CHF which range from lifestyle choices, environment, diabetes, and obesity. Recent studies suggest that overregulation by PLN is a contributing factor to CHF (*5, 8, 11, 12, 38, 39*). The most common cause of CHF is dilated cardiomyopathy which affects 40 people in every 100,000. The true incidence of CHF is probably underestimated as many cases go untreated. CHF is the leading cause of heart transplantation with an associated healthcare cost of $200 million per year in the United States

(*35*). Statistics from the American Heart Association (2008) show that at age forty, a person's lifetime risk of developing CHF is 1 in 5 (*40*).

The clinical course of CHF, despite the underlying cause, is progressive with roughly 50% of individuals reported to die within 5 years of diagnosis without a transplant (*35*). Longer survival can be accomplished through drug therapies such as angiotensin-converting enzyme inhibitors and beta blockers. Yet, despite advances in current drug therapies, the prognosis patients with CHF remains poor (*41*). Treatment of CHF with positive inotropic (contractility enhancing) agents led to therapies that initially improved the condition but increased the mortality rate (*42, 43*). Thus, there has been a large imitative to find effective and safe pharmacological agents.

Nitroxyl (HNO)

This proposal focuses on nitroxyl (HNO) a novel class of drugs that have shown new pharmaceutical properties for combating CHF. Nitroxyl (HNO) is the one electron reduction product of nitric oxide (NO) and exists in a protonated form at physiological pH (*41*). Since the 1980s, nitric oxide chemistry has been investigated extensively and found to have key roles in mammalian physiological and pathophysiological processes (*44*). The chemistry and pharmacological relevance of nitrogen oxides such as NO, NO_2, and $ONOO^-$ have been well established in the literature and found to have biological relevance. However, understanding of the chemistry and biological relevance of the one-electron reduced species, nitroxyl (HNO), remains in its infancy.

For an up to date review on the pharmacology of nitroxyl see references (*44-48*). In summary, nitroxyl is found to be a weak acid (pKa >11) with an atypical acid-base equilibrium because of the different electron spin states of HNO/NO^-. HNO is in a singlet state (all electrons are paired) while NO^- is in a triplet state (2 unpaired electrons in different orbitals) making deprotonation uncommon. Endogenous production of HNO has been refuted by the low (-0.4V) reduction potential of NO to HNO. Within a cell, the most prevalent reaction from HNO at nM concentrations is a dimerization into hyponitrous acid followed by decomposition into nitrous oxide and water. The existence of this reaction makes working with HNO problematic without a HNO donor. There are several avalible HNO donors including Piloty's acid, nitrosocarbonyls, cyanamide, and acyloxynitroso compounds. For the purpose of this research, we plan to use the

most common HNO donor Angeli's Salt (sodium trioxodinitrate) (Figure 1-6 "A"). At pH >4 Angeli's Salt (AS) spontaneously decomposes to generate 1 equivalent of HNO and NO_2^-. At a pH < 4, AS converts to a NO donor. Studies using AS should account for potential nitrite effects.

In terms of HNO kinetics, it has been shown that HNO has a high reactivity with a large variety of biological species. The HNO reaction depends on one of two things: (1) the concentration of the target and (2) the reaction rate of HNO with those targets. It was postulated that the fate of HNO in a cell would be the high concentration of glutathione (GSH). In contrast, it was determined that high levels of HNO can deplete a cell of almost all GSH. But, in some yeast models, low levels of HNO selectively modify thiols without altering GSH concentration. From these studies, it was determined that only certain thiols may be selectively active towards HNO. Nagasawa and co-workers (*49*) showed the earliest demonstration of the thiophilic reactivity of HNO (Figure 1-6 "B"). The initial formation of N-hydroxysulfinamide occurs via an attack of the nucleophilic sulfur atom on the electrophilic nitrogen atom of HNO. The N-hydroxysulfinamide can further react with an excess thiol to give either an intra- or inter-molecular disulfide bond and hydroxylamine. Other major biological targets of HNO include metalloproteins (i.e. ferric hemes, copper) (*46*) (weak association) and metal-oxygen species (oxymyoglobin) resulting in the oxidation of iron(*50*). Several additional studies have demonstrated the potential biological importance of HNO being a vasorelaxant (*51*) and an inhibitor of aldehyde dehydrogenase (*49*).

HNO- A Pharmacological agent for CHF

Much of the recent excitement regarding HNO biology and chemistry results from Paolocci and co-workers (*6*) in failing hearts. They reported that HNO has the unique ability to increase left ventricular contractility and simultaneously lower cardiac preload (pressure stretching the heart ventricle) and diastolic pressure (relaxation) without increasing arterial resistance (*6, 45, 52*). It has also been shown that HNO is able to improve heart function by directly enhancing calcium cycling (*53*) by stimulating the ryanodine receptor (Ca^{2+} induced Ca^{2+} release channel) and the sarco(endo)plasmic reticulum Ca^{2+} ATPase independent of the β-adrenergic pathway. Yet, despite the fact that HNO improves overall cardiac function, the chemistry and molecular mechanism by which HNO works in cardiac SR proteins is not well

A

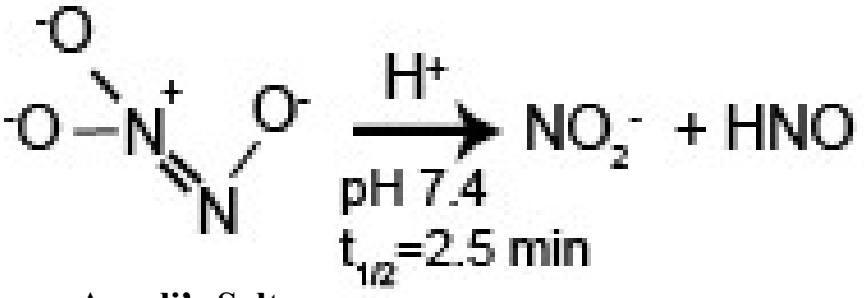

Angeli's Salt

B

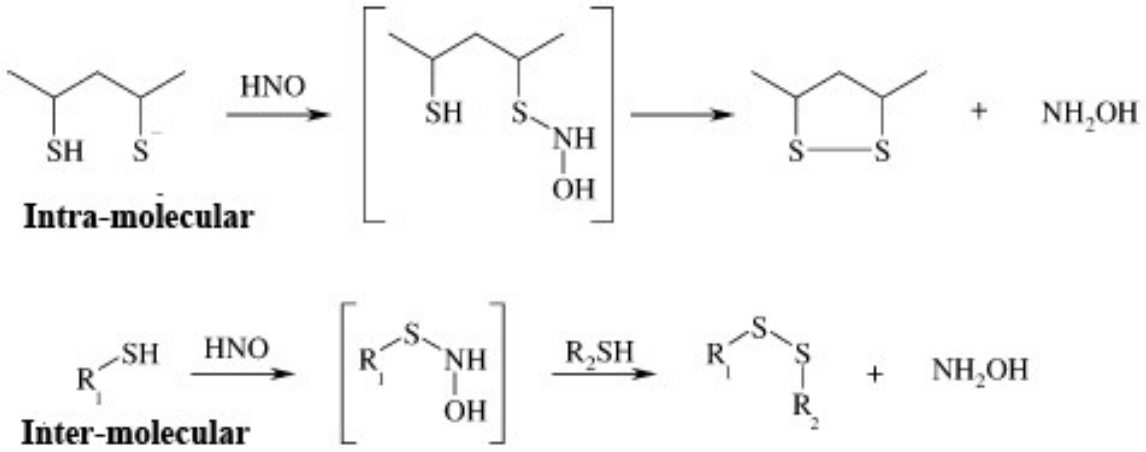

Figure 1-6. Angeli's Salt decomposition and HNO reactivity.

understood. Thus, it is important to evaluate the effects of HNO on Ca^{2+} transport in order to evaluate it as a therapy for CHF.

PLN is important in HNO stimulation of SERCA2a

Within the hydrophobic amino acids that comprise the transmembrane region of PLN, there are three proximal cysteine residues at positions 36, 41, and 46 (see Figure 1-7). Karim et. al. (*18, 24*) reported that these residues contribute to PLN pentamer formation, and particularly cys-41, but the these residues do not appear to be important for PLN inhibitory function. Froehlich et. al (*54*) reported that HNO stimulates SERCA2a in the presence of wild-type PLN, but not in the absence of PLN. Furthermore, treating SERCA2a + PLN containing membranes with dithiothreitol (DTT) after HNO reversed the HNO-dependent stimulation. Finally, when coexpressed with a null-cysteine PLN mutant, HNO had no effect on SERCA2a activity. These results strongly support the hypothesis that activation of SERCA2a by HNO is PLN-dependent and that the cysteine residues in the transmembrane domain of PLN play a critical role in SERCA2a activation. The fact that HNO-induced activation of SERCA2a can be reversed by DTT (*54*) suggests that disulfide bond formation may be important in activating Ca^{2+} uptake. HNO is a potent thiol oxidant, with the ability to modify a cysteine residue to a sulfinamide, but will readily form disulfide bonds in the presence of a proximal cysteine (*44, 45*) (Figure 1-6). SDS-PAGE and immunoblot analyses (*54*) have not shown a significant amount of PLN inter-molecular cross-links (i.e., dimers, trimers, tetramers, high MW aggregates) upon treatment with HNO. This suggests the possibility that HNO promotes the formation of "forbidden" intra-molecular disulfide bonds within PLN. As described by Wouters et al. (*55*), these disulfide bonds are considered "redox switches" that can reversibly distort the local structure of a helix. If so, such a disulfide bond would therefore disrupt the contact interaction between PLN and SERCA2a. If true, this would be a novel finding for the role of redox signaling on the regulation of SERCA2a by PLN, apart from the potential role of HNO as a therapeutic agent for controlling SERCA2a function. An alternate possibility is that HNO uncouples PLN from SERCA2a by acting directly on SERCA2a sulfhydryls. This effort is being investigated in the Mahaney laboratory. Since the experimental evidence strongly points towards PLN as a primary target for HNO action, this project will focus on PLN cysteine modification by HNO, and move toward SERCA2a modification as dictated by the ongoing results in the overall study.

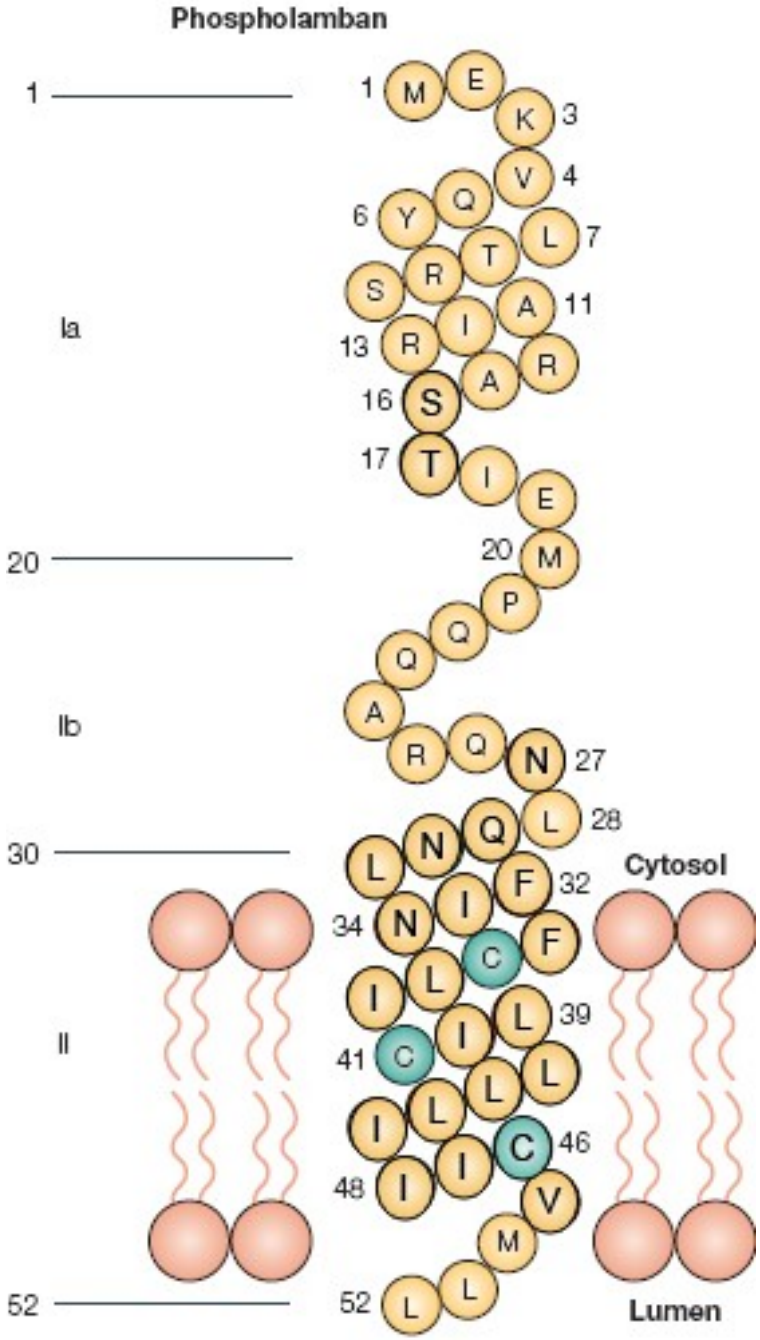

Figure 1-7. Illustration of PLN highlighting transmembrane cysteines. Adapted and reprinted by permission from Macmillian Publishers Ltd: Nature Reviews (MacLennan and Kranias ." Phospholamban: A crucial regulator of cardiac contractility" 405(6787), 647-655), copyright (2003).

Research Significance and Objectives

The goal of this project is to understand the effects of nitroxyl (HNO) on the principal cardiac Ca^{2+} cycling protein, the Ca^{2+}-ATPase (SERCA2a), and its regulation by phospholamban (PLN). Clinical studies have shown HNO improves cardiac function by stimulating Ca^{2+} cycling in cardiomyocytes (*6, 46, 53, 56*), but the mechanism by which it works is still unknown. Previous studies in the Mahaney lab show that HNO increases SERCA2a activity in the presence of PLN, but HNO has little or no effect on SERCA2a activity in the absence of PLN (*54*), suggesting a central role for PLN in HNO stimulation. It is therefore important to ask if HNO modifies PLN in a way that affects its ability to regulate the Ca^{2+} pump. HNO is a potent thiol oxidant, which converts sulfhydryls to hydroxysulfinamides that readily interact with a second thiol to form a disulfide bond and hydroxylamines (*44, 45*). There are three proximal cysteines (positions 36, 41, 46) in the transmembrane domain of PLN. We hypothesize that HNO, a thiol oxidant, modifies one or more of the three PLN cysteine residues (C36, C41, C46) affecting the regulatory potency of PLN toward SERCA2a. However, it is important to first determine which PLN cysteine residue(s) is (are) modified by HNO in its mechanism of action. To answer this question (which is fundamental for testing the overall hypothesis) we constructed PLN cysteine mutants, expressed, and conducted a combination of biochemical, kinetic and SDS-PAGE/immunoblotting studies on HNO treated SERCA2a in the presence and absence of PLN cysteine mutants. We used our baculovirus insect cell expression system to express the PLN cysteine mutants individually and co-expressed with SERCA2a. Studies using native skeletal SR vesicles were included as well as expressed wild-type PLN and null cysteine PLN for comparison. We used Angeli's Salt ($Na_2N_2O_3$, sodium trioxodinitrate) as an HNO donor (*57, 58*). Our studies followed these specific aims:

Aim 1: Generate a series of PLN cysteine mutants containing a single or double cysteine mutation at positions 36, 41, 46.

Starting with null cysteine PLN (A36/A41/A46 PLN), cysteines were added one at a time to create three single PLN cysteine mutations: 36C, 41C, and 46C via site-directed mutagenesis. In addition, three double cysteine PLN mutations: 36/41C, 36/46C, and 41/46C were created using the same methodology. PLN cysteine mutants were expressed individually and co-expressed with SERCA2a using the baculovirus insect cell system. The coexpressed SERCA2a

and PLN samples were tested to determine cysteine mutant PLN regulatory potency toward SERCA2a.

Aim 2: Correlate the effects of HNO on PLN cysteine modification with HNO-dependent SERCA2a activation.

[Ca^{2+}]-dependent activity assays were used to determine how the modification of individual cysteines in PLN affected PLN-dependent stimulation of ATPase activity. Immunoblotting was be used to test for HNO-dependent disulfide bond cross links between PLN cysteine mutants and/or PLN-SERCA2a cross links.

HNO has great potential as a novel therapeutic agent in the treatment of congestive heart failure. It is therefore essential to understand the biochemical and molecular effects of HNO on cardiac muscle cell proteins, in order to properly consider it as a therapy for CHF. By focusing on the effects of HNO on the PLN-SERCA2a interaction, we hope to demonstrate a physical methodology whereby the same approach could be applied to other key regulatory proteins involved in calcium cycling such as the ryanodine receptor, dihydropyrodine receptor, or troponin C, and other Ca^{2+} handling proteins. The results of this study provide important new insight into the mechanism of action of HNO on the regulatory interaction of PLN with SERCA2a as a potential CHF therapeutic agent.

CHAPTER II

MATERIALS AND METHODOLOGY

General Instrumentation

Unless otherwise noted, all laboratory reagents were purchased from Fisher Scientific (Pittsburgh, PA) or Sigma-Aldrich (St. Louis, MO). Light absorption was measured with a Beckman Coulter DU® 800 Spectrophotometer (Atlanta, GA) or Molecular Devices Spectra Max M5 (Sunnyvale, CA), depending on the protocol. Fluorescence was measured using the Molecular Devices Spectra Max M5 Multi-Mode Microplate Reader (Sunnyvale, CA). The pH of solutions was determined using an Accumet Basic AR15 pH meter from Fisher Scientific. PCR amplifications were performed using a DNA thermocycler from Perkin-Elmer Cetus (Norwalk, CT) or Eppendorf Mastercycler® ep (Hamburg, Germany), depending on availability. Bacterial and cell cultures were harvested by centrifugation on a Beckman Coulter Allegra™ X-12R or Avanti™ J-30I centrifuge equipped with a SX4750A ARIES™ rotor in the Allegra™ X-12R or either the JA30.5 or JLA16.2.5 rotor in the Avanti™ J-301. All rotors were supplied by Beckman Coulter. Cells were lysed with a Polytron® PT-MR 3100 homogenizer (Bohemia, NY) with a PT-DA 3012/2EC probe or alternatively, a Sonic Dismembrator, Model F60, equipped with a high voltage ultrasonic convertor from Fisher Scientific. All acrylamide gel electrophoresis was performed with Bio-Rad (Hercules, CA) equipment. Depending on the application, either the mini Trans-Blot® Cell or Protean II xi Cell was used powered by the PowerPac Basic or PowerPac HC respectively. This equipment was used for SDS-PAGE and western blotting. For preparative electrophoresis, Bio-Rad Model 491 Prep Cell was used powered by the PowerPac Universal. Agarose gel electrophoresis was performed on Bio-Rad Mini-Sub® Cell GT. Microcentrifuge tubes and pipet tips were from Fisher Scientific and VWR (San Diego, CA) or Molecular BioProducts (San Diego, CA), respectively.

Materials

Materials for molecular biology, enzyme expression and characterization

All custom oligonucleotide primers were synthesized by Integrated DNA Technologies (Coralville, IA). QuickChange XL Site-Directed Mutagenesis Kit and *Pfu* Turbo DNA Polymerase were supplied by Stratagene (La Jolla, CA). ACCUZYME™ mix, a PCR master mix from Bioline (London, UK) was used for regular PCR reactions. The Bac-to-Bac® Baculovirus Expression System which included DH10Bac™ *E.coli* and Cellfectin® was obtained from Invitrogen. Within this system, proteins of interest were cloned into the pFastBac™1 vector. JM109 Competent *E. coli* cells were purchased from Stratagene. Insect cells were maintained using both NUNC™ Brand disposable flasks (part of Thermo Fisher Scientific) and Kimax® Baffled Culture Flasks. AgarPlaque Plus Agarose (now BD BaculoGold™) from BD Biosciences (San Diego, CA) was purchased for plaque assays. S.O.C media (Super Optimal broth with Catabolite repression) was from Invitrogen (Carlsbad, CA). QIAprep™ Spin Miniprep kit and QIAfilter™ Plasmid Midi kit were supplied from QIAGEN (Valencia, CA). DNA sequencing was performed at The Georgia Genomics Facility (Athens, GA) or the Core Laboratory Facility in the Virginia Bioinformatics Institute (Blacksburg, VA). To determine viral titers, a rapid titer kit was used from Clontech (Mountain View, CA). Bovine Serum Albumin was from Fisher. Fetal Bovine Serum was purchased from Atlanta Biologicals (Lawrenceville, GA). PVDF (polyvinylidine fluoride) and Nitrocellulose membranes for protein transfer were purchased from Bio-Rad. Anti-Phospholamban (2D12) and Anti-SERCA2a (2A7-A1) mouse monoclonal antibodies were from Affinity BioReagents (Rockford, IL). Goat anti-mouse HRP (Horseradish peroxidase) conjugate was from Bio-rad. JM109 ultracompotent *E.coli* cells were from Invitrogen. Insect cell lines Sf21 and Sf9 (*Spodoptera frugiperda)* and High 5 (*Trichoplusia ni*) were obtained from Invitrogen. The culture media and reagents to maintain the insect cell culture was purchased from Invitrogen (Carlsbad, CA) using the GIBCO® product line.

General Methods

Solutions and procedures for growth of cells

The growth and maintenance of the Sf9, Sf21 and High Five™ insect cells lines were prepared as described in the Invitrogen™ User manual *Growth and Maintenance of Insect Cells Lines (8 June 2009)*. All handling of the insect cells lines were done under sterile conditions in a laminar flow hood. Cultures of either cell line were initiated from a frozen stock into the appropriate cell culture media. High Five™ cells were thawed into Express Five® SFM and Sf9/21 cells in Grace's Insect Medium, Unsupplemented. A table outlining the steps to initiate and culture cells from a frozen stock can be seen below.

Step	Action
1	Remove cells from liquid nitrogen or dry ice.
2	Thaw cells into desired medium.
3	Let cells attach for 30-45 minutes.
4	Remove medium (with DMSO) and add fresh medium.
5	Grow to confluency and passage.
6	Subculture until cells are doubling every 18-24 hours and are 95% viable.
7	Freeze down several vials of low passage cells as backup.

The initiation of all cell lines began in as an adherent culture using NUNC™ flasks. Both adherent and suspension cultures were maintained of all cell lines at various times using the respective medium for each line. Adherent cells were maintained in $25cm^2$ and $75cm^2$ flasks within an incubator set at 27°C. Once these cells reached confluency, a technique referred to as sloughing, was used to subculture the cells in a 1:5 dilution to maintain log phase growth. This technique involves streaming medium over the attached monolayer using a sterile Pasteur pipette. Invitrogen recommends this technique as it dislodges the monolayer with the least manipulation and mechanical force. Full details describing the technique can be seen in the manual. The adherent cell lines must be established before beginning a suspension culture. Suspension cultures were maintained using Kimax® baffled culture flasks placed in a 27°C shaker at 70-80 RPM. Suspension cultures were passaged back before they reached a density of 2.0 to 2.5 x 10^6cells/ml and dilute back to 0.7 to 1.0 x 10^6cell/ml to maintain log phase growth. Pluronic® F-68 was added to the suspension medium in a final concentration of 0.1% in Sf9 and Sf21 cells as a surfactant to decrease shearing. Suspension cultures could be maintained in a volume up to a 2000 ml baffled flask. To increase the flask size, enough culture volume was

transferred at 2 x 10^6cells/ml to seed the larger flask with at least 1 x 10^6cells/ml. For general insect cell maintenance, fresh cell culture medium was always equilibrated to room temperature before use. A cell log was kept to monitor the density and viability of each culture using a hemacytometer. Every month, each of the cells lines were renewed as the viability of the cells drastically decreases after this time period. If any of the cultures were found to become contaminated or the one month period has come, a new culture is initiated. For the growth of *Escherichia coli (E.coli)* cells, Luria-Bertani (LB) liquid medium and LB agar plates as well as antibiotic solutions were prepared as described in the appendices of *Molecular Cloning: A Laboratory Manual* (Sambrook, Fritsch et al. 1989) unless otherwise specified.

Site-directed mutagenesis

Mutant variants of phospholamban were generated using the QuikChange® XL Site-Directed Mutagenesis kit according to the manufacturer's protocol. In synopsis, 6 sets of mutagenic primers (5' – 3' and 3' – 5') were designed using the QuikChange Primer Design website by Agilent Technologies (http://www.genomics.agilent.com). The template plasmid was a null cysteine (cys→ala) PLN cDNA in the double stranded expression vector, pFastBac™1 (already provided). The mutagenic primers created point mutations to revert the Ala at positions 36, 41, and 46 back to a cysteine one at a time and two at a time. (A36C, A41C, A46C, A36/41C, A36/46C, A41/46C) Mutagenic primers, 125 ng each, were added to 5 µl of 10X reaction buffer, 5 µl (2ng/µl) dsDNA template, 1 µl dNTP mix, 3 µl of QuikSolution, and sterile double deionized water was added to a final volume of 50 µl. Next, 1 µl of *Pfu*Turbo DNA polymerase (2.5 U/µl) was added to the mixture in thin-walled PCR tubes and incubated in a thermal cycler as follows. An initial denaturing step of 1 minute at 95°C was followed by 18 cycles of a) 50 sec at 95°C b) 50 sec at 60°C, c) 5 min at 68°C. The last step was a continuation of the extension period at 68°C for 7 minutes. Following temperature cycling, the reaction tubes were kept at 4°C until further use. To digest the parent strand of DNA, which was the methylated strands lacking the desired mutation, 1 µl of the *Dpn* I restriction enzyme (10 U/µl) was added to each reaction tube and incubated for 1 hour at 37°C. The mutant vector was then transformed into XL10-Gold® Ultracompetent *E. coli* cells (gentotype: $Tet^R\Delta$ (*mcrA*)183 Δ(*mcrCB-hsdSMR-mrr*)173 *endA1 supE44 thi-1 recA1 gyrA96 relA1 lac* Hte [F' *proAB*

lacI^{q}*Z*ΔM15 Tn10(Tet^{R}) Amy Cam^{R}]) for amplification and repair of nicked plasmids per manufacturer's instructions.

Plasmid isolation and sequence verification

Each XL10-Gold® transformation was plated on LB agar plates containing 10µg/ml ampicillin for selection of the pFastBac™1 1 vector. The transformation plates were incubated at 37°C for > 16 hours. The expected colony number is between 10 and 1000 colonies. Selected colonies were used to inoculate, via a sterile inoculating loop, 5 ml of LB media containing 10 µg/ml Amp for the mutated pFastBac™1 vector. Following an overnight incubation in a shaking incubator at 37°C 225 rpm, plasmid DNA was isolated from each culture using a QIAprep™ Spin Miniprep kit as directed by the manufacturer. On occasion, the starter 5 ml LB cultures would be used to create a larger 100 mL culture to isolate a higher number of plasmids using the QIAfilter™ Plasmid Midi kit. The plasmid DNA was eluted with 50 µl of double deionized water. A portion of the eluate which contained at least 3 µg of isolated plasmid was submitted to the Georgia Genomics Facility or to the Virginia Bioinformatics Institute's (VBI) Core Laboratory Facility for sequencing of the DNA mutagenic insert. Instead of using commercial primers, template specific sequencing primers were designed and given to the sequencing facilities. These primers flanked the regions just outside of the mutagenic sequence. Only plasmids with the intended mutations were kept for further use.

Baculovirus Expression System

The Bac-to-Bac® Baculovirus Expression System (Invitrogen) was used to generate recombinant baculovirus. Baculoviruses are the most prominent viruses known to affect the insect population, particularly insects of the order Lepidoptera. The baculovirus isolate that was used to express phospholamban mutants and SERCA2a was *Autographa californica* multiple nuclear polyhedrosis virus (AcMNPV). The major difference between the naturally occurring *in vivo* infection and the recombinant *in vitro* infection is that the naturally occurring polyhedrin gene within the wild-type baculovirus genome is replaced with a recombinant cDNA. During the very late phase of infection, the inserted heterologous genes are placed under the transcriptional control of the strong polyhedrin promoter. Thus, recombinant product is expressed in place of the naturally occurring polyhedrin gene. Because the baculovirus

expression system is eukaryotic, phospholamban was processed, modified, and targeted to the appropriate sarcoplasmic reticulum. Baculoviruses have emerged as an accepted system for overproducing recombinant proteins in eukaryotic cells for several reasons. Primarily, the baculovirus system is eukaryotic which allows for the protein modification, processing, and transport systems in higher eukaryotic cells unlike bacterial expression systems. Also, the majority of overproduced protein remains soluble in insect cells, in contrast to the insoluble proteins from bacteria. Lastly, since the viral genome is large, it has the capability to accommodate large segments of foreign DNA. Currently, the most widely used baculovirus expression system utilizes a lytic virus known as *Autographa californica* nuclear polyheedrosis virus (AcMNPV). This virus is a large double-stranded DNA virus that infects arthropods. (*59*) This method was developed by researchers at Monsanto, and is based on the site specific transposition of an expression cassette into a baculovirus shuttle vector or bacmid and propagated in *E.coli (60)*. The DH10Bac cells contain a baculovirus shuttle vector (bacmid) with a mini-attTn7 site to allow for transposition between the mutant PLN pFastBac™1 into the bacmid. At the time the recombinant viruses were created, the Bac-to-Bac® Baculovirus Expression System Manual Version D (6 April 2004) was followed.

Generation of recombinant bacmid

The resulting pFastBac™1 which contains the mutagenic PLN DNA sequence from site-directed mutagenesis are now considered the recombinant pFastBac donor plasmid. These recombinant plasmids were transformed into Max Efficiency® DH10Bac™ competent E. coli cells (genotype: F^- *mcr*A Δ(*mrr-hsd*RMS-*mcr*BC) ϕ80*lac*ZΔM15 ΔlacX74 *rec*A1 *ara*D139 Δ(*ara,leu*)7697 *gal*U *gal*K λ- *rps*L *nup*G/bMON14272/pMON7124) as directed by the manufacturer. A 5 µl aliquot of the purified pFastBac construct was added to 100 µl of DH10Bac competent cells and the mixture incubated on ice for 30 minutes. Afterwards, the cells were "heat-shocked" (incubated in a controlled water bath) at 42°C for 45 seconds then immediately put back on ice. Next, 900 µl of S.O.C. media was added to the cells and the mixture incubated at 37°C with horizontal shaking at 225 rpm for 4 hours. A 10-fold serial dilution of the resulting culture was prepared with S.O.C medium and 100 µl of each dilution was spread on LB agar containing 50µg/ml kanamycin, 7µg/ml gentamicin, 10µg/ml tetracycline, 100µg/ml Bluo-gal, and 40µg/ml IPTG and the plates incubated for 48 hours at

37°C. White colonies (≥10) were picked and restreaked on a fresh LB agar plate containing 50µg/ml kanamycin, 7µg/ml gentamicin, 10µg/ml tetracycline, 100µg/ml Bluo-gal, and 40µg/ml IPTG to verify phenotype. Plates were incubated overnight at 37°C. Liquid LB medium (5 ml) containing 50µg/ml kanamycin, 7µg/ml gentamicin, 10µg/ml tetracycline was inoculated, via a sterile inoculation loop, from a single colony with a confirmed white phenotype. After an overnight incubation (~8 hours) at 37°C, the 5 ml starter culture was diluted 1/1000 (200 µl starter in 100 ml LB) in fresh LB medium containing the selective antibodies listed above. The culture was placed in a 37°C incubator for 12- 16 hours shaking at ~300 rpm. Afterwards, the *E. coli* cells were harvested by centrifugation at 6,000 x g for 15 min at 4°C and the QIAfilter™ Plasmid Midi kit was used to isolate and purify the recombinant bacmid. Alternatively, the pellet was kept at -20°C until ready. To verify transposition, the isolated bacmids were analyzed by PCR. For each reaction, 12.5 µl of ACCUZYME was combined with 1.25 µl of both M13 forward and reverse primers, 1µl bacmid DNA (0.1 µg/µl), and brought to 25 µl with 10.25 µl with ddH_2O. Reactions were performed in a thermal cycler programmed as follows: an initial denaturation step of 3 min at 93°C followed by 30 cycles of a) 45sec at 94°C b) 45 sec at 55°C c) 5 min at 72°C for extension. The reaction was concluded with a 7 minute incubation at 72°C for further elongation. PCR products were analyzed using agarose gel electrophoresis loaded with a 1kb DNA ladder from Promega (Madison, WI). If transposition had occurred the expected product was ~2,470 bp while the bacmid alone would have shown ~300 bp.

Generation of recombinant baculovirus

Once a confirmed recombinant bacmid that contains the gene of interest is isolated and purified, it is ready to transfect insect cells to produce a recombinant baculovirus. Sf21 cells were used to create the baculoviral stocks following the manufacturer's protocol with minor adjustments for optimization. In summary, all transformations began with a 6-well (35 mm) plate that contained 9 x 10^5 cells in 2 ml Unsupplemented Grace's Insect Cell Culture Medium, containing 50 U/ml penicillin streptomycin per well.. The cells used were plated from the current viable Sf21 suspension culture. During the one hour cell attachment period at 27°C, the bacmid DNA:Cellfectin® complexes were made. Cellfectin reagent is a 1:1.5 (M/M) liposome formulation of the cationic lipid N,N,N,N -- Tetramethyl – N,N,N,N – tetrapalmitylspermine (TM-TPS) and dioleoyl phosphatidylethanolamine (DOPE). Bacmid samples were diluted to

500 ng/µl in 1X TE buffer. Two microliters of each bacmid samples was mixed with 100 µl of unsupplemented Grace's medium. This was added to a dilution of 6 µl Cellfectin® reagent in 100 µl of unsupplemented Grace's medium. The combined diluted bacmid:Cellfectin® mix was incubated for 30 min at room temperature. Meanwhile, the attached cells were washed one time with 2 ml unsupplemented Grace's medium. After the wash media was removed, the DNA:lipid complexes were added to each well containing cells and incubated at 27°C for 5 hours. After 5 hours, the DNA:lipid complexes were removed and 2 ml of complete growth media was added to the cells. The plate was returned to the 27°C incubator for a minimum of 72 hours or until signs of viral infection were seen.

Isolating P_0 viral stock and amplifying to P_1 and beyond

Budded viruses should be released into the medium 72 hours after infection. Beginning at this time point, the cells were checked daily for visual signs of infection. Typical characteristics of infected cells include cell lysis, detachment, granular appearance, and cessation of cell growth. For this reason, each transfection reaction always had a control well for comparison. Once the cells have shown signs of transfection, the medium containing virus was collected from each well and transferred to a sterile 15 ml conical. Cells were centrifuged at 500 x g for 5 minutes in which afterwards the clarified supernatant was transferred to a clean 15 ml conical and stored at 4^oC. This was considered the P_0 stock of each virus. The titer of the P_0 stock was assumed to be 1×10^6 pfu/ml. From this assumption, new Sf21 cells plated in NUNC 25 cm^2 flasks were infected with the P_0 virus stock at an MOI of 0.1. MOI refers to the number of virus particles per cell. The flasks were placed in a 27°C incubator until signs of infection were seen (72+ hours) and then harvested by centrifugation as described above. This stock became the P_1 passage of each virus. At this point, the titer of each virus was determined by one of two methods described below. After the titer was determined, further passages of each virus were done in succession (P_2, P_3, P_4, etc) in the same manner using an MOI of 0.1 to infect new Sf21 cells. This was done to obtain higher titers needed for the expression studies. After each passage, the titer was determined. Much of this work was done by Lesly De Arras who was a laboratory technician at the time this was performed.

Determination of viral titer

The concentration of infectious viruses in each samples, or titer, was determined using the widely accepted viral plaque assay. All steps in the viral plaque assay were performed in a sterile ventilated hood. To perform the plaque assay, 10 fold dilutions of each virus stock (P_1 and above) were prepared as indicated in the chart below.

Dilution	Instructions
10^{-2}	Add 5 µl virus to 495 µl medium
10^{-4}	Add 5 µl virus to 495 µl medium
10^{-5}	Add 150 µl virus to 1.35 ml medium
10^{-6}	Add 300 µl virus to 2.7 ml medium
10^{-7}	Add 250 µl virus to 2.25 ml medium
10^{-8}	Add 150 µl virus to 1.35ml medium

Cells were plated at a density of ~3 x 10^6 Sf21 cells into 60 mm NUNC petri dishes (8 plates needed per virus) with a total volume of 4 ml and allow to attach. The plates were labeled with a corresponding dilution factor starting with 1 plate for 10^{-5}, 10^{-8} and control, 2 plates for 10^{-6} and 10^{-7}, and 1 plate for 0.5 x 10^{-6}. Once the cells had attached, all but 1 ml of medium from each plate was removed using a sterile aspirator. One milliliter of each viral dilution (0.5 ml for 0.5 x 10^{-6} plate) was added to the appropriate plate in a slow circular motion, a drop at a time. All of the plates were incubated at room temperature for 1 hour. During the one hour incubation period, plaquing medium (mixture of culture medium and agarose) was prepared. An appropriate amount of AgarPlaque Plus agarose was autoclaved and mixed with room temperature Grace's culture medium right before use. All viral medium was aspirated off the plates and 4 ml of the plaquing medium was added. This step was done quickly as to avoid desiccation of the cell monolayer. The agar was allowed to harden and each plate was wrapped in parafilm to prevent evaporation. All plates were incubated at 27°C for 6 days for the plaques to develop. A neutral red overlay was added to facilitate the counting of plaques by staining. To 10 ml of medium 1 mg of neutral red was added and mixed with an appropriate volume of autoclaved AgarPlaque Plus agarose. Three milliliters of the red agar was added to each plate and the plaques were counted visually with the help of a light box. The following formula was used to calculate the titer, or plaque forming units per ml of each viral stock.

titer (pfu/ml) = number of plaques x dilution factor x (1/ ml of inoculum per well)

A quicker method to determine viral titers was used when available. The BacPAK™ Baculovirus Rapid Titer Kit from Clontech Laboratories is specially suited for AcMNPV-based baculovirus systems. The kit utilizes a standard immunoassay for viral envelope glycoprotein (gp64) to identify virally infected cells in two days instead of the 6-7 days for a plaque to form. Titers were determined by antibody detection of the glycoprotein antigens. Because this method is not dependent on the ability of the virus to replicate in infected cells only on the ability to infect and express a virally-encoded protein, hence titers are expressed in IFU/ml or infectious units per ml. The protocol was followed per manufacturer's instructions using the choice of the paraformaldehyde instead of formyl buffered acetone at step 1 while the additional reagents needed where purchased from Sigma-Aldrich (St. Louis, MO) and used as specified.

Expression of recombinant protein and the creation of microsomes

Protein expression and isolation of phospholamban using the baculovirus system has been optimized from established protocols (*61*) All expression of recombinant proteins, including wild-type SERCA2a and cysteine mutant PLN, were expressed in High Five™ cells grown in suspension 1 x 10^6cells/ml (log-phase) in recommended GIBCO® Express Five® SFM culture media supplemented with 10 U/ml Heparin. For expression of SERCA2a alone, an MOI of 10 was used whereas for co-expressions of SERCA2a and PLN, an MOI of 15 was used for SERCA and 5 for PLN. The appropriate amount of virus was added to pelleted cells using the mentioned MOI and known viral titers. The virus was allowed to incubate with the cells for 1 hour before diluting back to original suspension volume. Afterwards, the baffled flask(s) were placed back into the 27°C incubator with shaking at ~40 rpm for 48 hours to allow viral replication. After 48 hours, virus-infected cells in a 300 ml suspension (500 x 10^6 cells) were transferred to a 500 ml conical centrifuge tube and pelleted at 600 x g for 15 minutes at 4°C in the Allegra™ X-12R centrifuge. The resulting supernatant was decanted into a waste container and the pellet was washed twice with 150 ml of ice-cold PBS containing 137 mM NaCl, 2.7 mM KCl, 4.5 mM Na_2HPO_4, and 1.4 mM KH_2PO_4 (pH 7.4) by centrifugation for 15 minutes at 600 x g (4°C) with the same centrifuge as before. The washed cells were then resuspended in 30 ml of Buffer 1 (10mM $NaHCO_3$, 0.2 mM $CaCl_2$) then 30 ml of Buffer II (60 mM $MgCl_2$, 0.5M

Sucrose, 60 mM Histidine, 0.3M KCl, pH 7.2) was added to resuspended cells. The following protease inhibitors were added to this suspension in 60 µl aliquots: 2 µg/ml Leupeptin, 0.1 mM Pefabloc, 1 µg/ml Pepstatin A, and 10 µg/ml Aprotinin. The suspended cells plus inhibitors were homogenized for 90 seconds using the Polytron® PT-MR 3100 homogenizer at 18,000 rpm. During this step, the cells were placed on ice to prevent with denaturation. Before homogenization, the probe was washed at full speed with ice cold ddH_2O to help the probe not transfer heat. The homogenized cells were allowed to rest for about 15 minutes on ice to allow the foam to dissipate. After resting, the homogenate mixture was distributed equally into two JA30.5 centrifuge tubes avoiding as much foam as possible. The mixture was centrifuged at 3,000 x g for 20 minutes at 4°C to remove any large debris in the Avanti™ J-30I refrigerated centrifuge. The supernatant was collected and 15 ml of 3 M KCl was added. This mixture was them poured into new clean JA30.5 centrifuge tubes and centrifuged for 20 minutes at 9,000 rpm, 4°C. The supernatant was collected and the High-Five insect cell microsomes were pelleted by centrifugation for 40 minutes at 26,000 rpm, 4°C in a Beckman Ti45 rotor. The pellets were resuspended in 1-2 ml of 10 mM Imidazole, 250 mM sucrose (pH 7.2) and stored in 0.25 mg aliquots at -80°C.

Determination of protein concentration

Protein concentrations were determined with the method of Biuret assay (*62*), using bovine serum albumin as a standard (Sigma). A protein standard curve was generated by detecting the absorbance at 540 nm produced from a linear gradient of 0 -340 µg of BSA. This standard curve was used to determine the unknown concentration of total microsomal protein. The percentage of the total protein concentration for SERCA2a or phospholamban expressed in microsomes developed from a baculovirus has been previously determined by (*63*). In a SERCA2a only microsomal preparation, SERCA2a makes up 8.3% of total protein whereas in a co-expressed sample, SERCA2a comprises 3% and Phospholamban 0.26% (1:1.6 mole ratio). Although the total protein concentration determined by the biruet assay is greater than SERCA2a, this figure was used to calculate ATPase activity. The average yield per 600 ml of infection was 30 mg of microsomal protein.

Expression and Purification of Phospholamban from E. coli

In addition to using the baculovirus method, phospholamban was expressed and purified from *E. coli* cells. Using this method allows us to study the effect of the mutant PLN in a pure environment without the background noise of the other ATPases when using the baculovirus system. Detergent micelles are able to show the same kinetic profile as microsomes which allow us to direct compare the results from wither preparation method. There are certain questions that could only be answered using this purified system because of the plethora of native cysteines in a cell environment which would prohibit DTNB, and mass spec work. This was done using an established method and protocol from Diana Bigelow's laboratory (*64*). From previous work done by the Bigelow lab, the PLN gene from genomic DNA of a porcine heart was amplified by PCR and inserted in the pGEX-2T plasmid expression vector from Pharmacia (Piscataway, NJ). In this vector, there is a tac promoter that is chemically inducible, and the gene product is fused to glutathione *S*-transferase which allows for purification of PLN by conventional strategies to isolate soluble proteins. Site-directed mutagenesis was employed to create a null cysteine variant of PLN in the pGEX-2T vector. The null cysteine PLN pGEX-2T vector was graciously supplied to the lab for further experimentation. From the supplied null cysteine PLN pGEX-2T construct, site-directed mutagenesis was employed using the QuikChange® XL Site-Directed Mutagenesis kit to create the single and double cysteine mutants as described previously using a newly designed set of primers that were specific to the vector.

Expression of GST-PLN fusion protein

Cultures of JM109 *E. coli* cells (genotype: e14$^-$(McrA$^-$) *recA1 endA1 gyrA96 thi-1 hsdR17 ($r_K^- m_K^+$) supE44 relA1 Δ(lac-proAB)* [F' *traD36 proAB lacI^{q}ZΔM15*] were grown in sterile LB with shaking at 37°C. JM109 cells were transformed with mutant cysteine PLN in pGEX-2T vectors using the heat shock method described previously in the baculovirus system. Transformed JM109 cultures were grown with shaking at 37°C with 100 μg/ml Ampicillin in 2000 ml flasks containing 500 ml LB. Isopropyl β-D-thiogalacto-pyranoside was added at a final concentration of 0.5 mM when the culture reached an OD_{600} of 0.3-0.4 (log-phase growth). In addition, we also used BL21 (DE3) pLysS-T1^R Competent Cells (genotype: F$^-$ *ompT hsdS$_B$*(r_B^- m_B^-) *gal dcm λ*(DE3) *ton*A pLysS (Cm^R)) to express GST-PLN fusion proteins via

transformation with pGEX-2T vector. The growth, transformation, and expression of these cells were followed per manufacture protocol (Sigma-Aldrich).

Solubilization of GST-PLN fusion protein

After 5 hours, cells were harvested from cultures by centrifugation at 2,000 x g for 10 minutes. The cells are washed once by resuspending in 50 ml TBS and centrifuged at 12,000 x g for 10 minutes. Afterwards, 30 ml cell lysis buffer (200 µg/ml Lysozyme (Sigma) in 20 mM Tris, pH 7.5) was added to resuspend the cells and left to incubate at room temperature for 15- 30 minutes. Subsequently, the suspension was sonicated using 5 second bursts using a probe sonicator (-----) at 5 output control for 10 minutes or until the solution was no longer viscous. The non-soluble proteins were harvested by centrifugation at 15,000 x g for 15 minutes. The resulting pellet was solubilized in 20 ml of 1% (w/v) Sarkosyl (Sigma) in 20 mM Tris, pH 7.5 and left at room temperature for 30 minutes, shaking gently. The solubilized proteins were centrifuged at 15,000 x g for 15 minutes to remove nonsolubilized material. The resulting supernatant was saved that contained the GST-PLN and kept at -20°C for later use.

Preparative gel electrophoresis

Purification of the GST-PLN fusion protein was achieved by preparative electrophoresis using the Bio-Rad Model 491 Prep Cell. Preparative electrophoresis refers to a procedure that is able to purify at least a few milligrams of protein at a time as distinguished from analytical electrophoresis at the microgram level. Up to 50 mg of total protein from the saved supernatant was loaded onto a discontinuous SDS-PAGE column gel (37 mm) with a 4% stacking gel and a 9% resolving gel. Electrophoresis was performed at a constant 12 W using the Bio-Rad PowerPac Universal for 10 hours. Proteins were eluted from the preparative gel with elution buffer consisting of 10 mM Tris (pH 8.5), 2 mM β – mercaptoethanol. The eluted proteins travelled through supplied tubing connected to a peristaltic pump which led to an automated fraction collector (Bio-Rad Model 2110) set to collect 50 drops per tube. Column fractions were analyzed for protein content with Coomassie blue staining on 9% SDS slab gels in addition to immunoblots with anti-PLN antibody (2D12). Fractions that contained GST-PLN (33-kDa) were pooled and thrombin, a protease, digestion was performed by adding thrombin (from human plasma) in a ratio of 35 U/mg GST-PLN. The digestion takes ~40 hours at room temperature.

The products of thrombin cleavage were lyophilized and resuspended in 8-10 ml SDS-boiling buffer (10 mM Tris, pH 6.8, 4% SDS, 200 mM DTT, 0.2% bromophenol blue, 20% glycerol). Heat mixture in boiling water bath for 15 minutes and let cool to room temperature before loading onto a discontinuous SDS-PAGE column gel (28 mm) with a 4% stacking gel and a 12% resolving gel. Electrophoresis was performed at a constant 8 W for 8 hours. PLN was eluted and collected from the preparative column gel with elution buffer as described above. Column fractions containing only PLN, confirmed by Western immunoblotting were pooled and lyophilized.

Characterization of mutant PLN microsomes

SDS-PAGE

The amount of expressed SERCA2a and PLN in the insect cell microsomes is quantified by gel electrophoresis and immunoblotting using methods developed by Porzio et al. (*51*). Insect cell microsomes were solubilized at 37°C for 5 minutes in a dissociation medium that contained 137 mM Tris-HCl (pH 6.8), 4.4% SDS, 22% glycerol, and 0.0025% bromophenol blue before electrophoresis. SDS-PAGE was conducted in a Bio-Rad Mini Protean II System using either a hand-poured continuous 12% polyacrylamide gels or manufactured gradient (10-20%) polyacrylamide gels (BIO-RAD). Each gel was run at the constant voltage specified by the manufacturer until the dye front reached the bottom of the cassette. Precision-Plus (Kaleidoscope) prestained molecular weight markers (BioRad) were used as standards.

Western blotting to transfer proteins

The proteins within the SDS-PAGE gels were transferred to a membrane for further analysis using a wet-transfer electrophoretic procedure according to the instructions provided by the manufacturer. After SDS-PAGE, described above, the gel was equilibrated in transfer buffer (25 mM Tris, 192 mM glycine) for 10-15 minutes along with a nitrocellulose or PVDF membrane (Bio-rad). PVDF membranes were activated by soaking in 100% methanol before adding to the transfer buffer. The Bio-Rad Trans-Blot Cell cassette transfer apparatus was setup according to the manufacturer's user guide. Electrophoresis was performed at a constant 90 V for 25-30 minutes at 4°C using a Bio-Rad PowerPac Basic power supply.

Immunological detection of proteins

The immobilized proteins transferred onto a polyvinylidene difluoride (PVDF) or nitrocellulose membrane were exposed to monoclonal antibodies that were conjugated to enzymes that were detectable through a colorimetric assay. After the electrophoretic transfer, the membranes were placed in a try containing 10 ml of 2% BSA used as a blocking buffer. Each of the primary antibodies were prepared in the 2% BSA in a 1:5,000 dilution and added to the membranes. The membranes were probed with anti-SERCA2a mouse monoclonal antibody 2A7-A1 for detection of SERCA2a or with anti-phospholamban mouse monoclonal antibody 2D12 for the detection of phospholamban. Following the one hour incubation on a horizontal shaker, the antibodies were decanted and saved at 4°C. The membranes were washed with 2 x 10 ml TBS buffer and 2 x 10 mL TBA plus 0.1% (v/v) Tween-20. After washing, a 10 ml solution containing the Goat-Anti-mouse HRP conjugate (1:2,500) in 2% BSA was added to the membranes. The membranes were incubated with the secondary antibody for 30 minutes at room temperature with horizontal shaking. After decanting and storing the secondary antibody, the membranes were washed with TBS in the same manner as described above. HRP Color development buffer (Bio-Rad) was mixed according to the manufacturer and added to the membranes until bands of purple appeared indicating the location of the secondary antibody and therefore SERCA2a and/or PLN. Rinsing the membrane with ddH_2O terminated the colorimetric reaction.

ATPase Characterization Methods

Malachite green assay for inorganic phosphate detection

The ATP hydrolysis activity of SERCA2a in insect cell microsomes is measured colorimetrically using an inorganic phosphate liberation assay (*65*) adapted from the procedure of Lanzetta et. al (*49*). The enzyme is suspended (0.05 mg/ml) in a buffer containing 100mM KCl, 3mM $MgCl_2$, 1mM EGTA and varying amounts of [$CaCl_2$] in increments of 0.1 mM providing buffered $[Ca^{2+}]_{free}$ levels between 30nM and 2.4μM. At time zero, 5mM MgATP is added to start the reaction. At serial times after the ATP initiation, a 50 μL aliquot is removed from the incubation tube and added to a culture tube containing 1.6 ml of malachite green ammonium-molybdate reagent. The reaction was quenched with 200μL sodium citrate to

stabilize color development. After about 30 minutes of color stabilization, the absorbance is read at 660 nm (see reaction equation below).

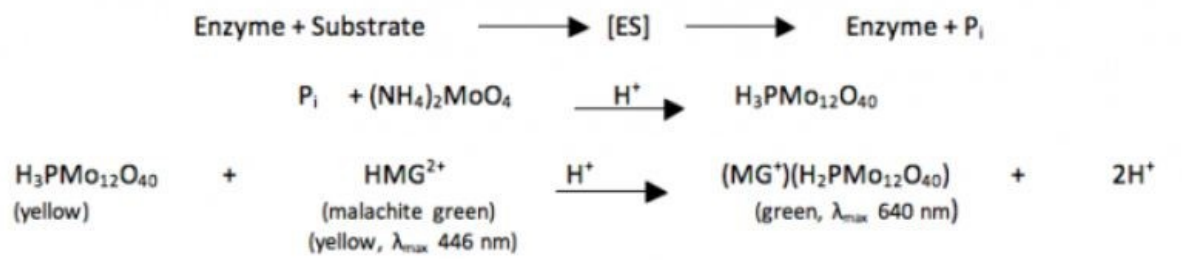

Malachite-green ammonium molybdate phosphate reaction.

A phosphate standard curve was also generated by adding predetermined amounts of phosphate to the malachite green ammonium-molybdate reagent. The standard curve allowed us to convert the absorbance readings at each $[Ca^{2+}]_{free}$ level to µmol P_i. The specific activity of SERCA2a at each $[Ca^{2+}]_{free}$ level was calculated by the total phosphate produced per unit time per mg of protein. On average, each ATPase assay was done using 0.0025 mg of microsomal protein with 30 minute duration. The resulting $[Ca^{2+}]$-dependent activity curve is sigmoidal because of the cooperative binding of calcium. All ATPase data was analyzed using OriginPro version 8.5.1. To obtain the fit, we used the pre-set non-linear curve DoseResp function which creates a dose-response curve with variable Hill slope given by a parameter 'p'. This function uses the following formula:

$$y = A1 + \frac{A2 - A1}{1 + 10^{(LOGx0 - x)p}}$$

From this data, we were able to extrapolate the maximum enzyme activity (V_{max}) and apparent Ca^{2+} affinity ($K_{0.5}$), two of the key parameters affected by PLN regulation.

The malachite green phosphate assay was used to assess SERCA2a activity after various treatments. In order to assess if co-expressed SERCA2a + PLN microsomes display proper coupling and PLN regulation, microsomes were treated with an anti-PLN antibody 2D12 to physically uncouple PLN from SERCA2a. A 500 µl aliquot of 0.2 mg/ml microsomal protein was treated with 10 µl of 2D12 (Pierce) for 10 minutes on ice. Following 2D12 treatment, the subsequent steps in the phosphate assay are identical.

To assess the effect of HNO on SERCA2a and PLN, we used the HNO donor Angeli's Salt to treat the insect cell microsomes. The white Angeli's Salt powder (MW 121 g/mol) was weighed in a micro centrifuge tube to the amount of 2.0-5.0 mg, and ice cold 10 mM NaOH was added to make a 100mM stock solution. At this point, serial dilutions of Angeli's Salt in 10mM NaOH were made to suit the experiment with a cautious effort to keep all stock concentrations on ice. The microsomes were treated by adding 1 µl of AS to a microcentrifuge tube containing 100 µl of 0.2 mg/ml protein. This reaction was left at room temperature for 15 minutes. If a larger volume of protein was treated, a 1:100 dilution of AS to microsomal protein was always followed. After AS treatment, SERCA2a ATPase activity was measured following the phosphate assay described above.

CHAPTER III

CREATION OF PHOSPHOLAMBAN CYSTEINE MUTANTS

Preliminary Research

Cloning null cysteine PLN ORF into pFASTBac1

Wild type PLN contains three native cysteines residues at positions 36, 41, and 46. The goal of this research was to understand the role of each PLN cysteine residue in the mechanism of action of HNO on SERCA2a. To do this we decided to start with a null cysteine PLN construct, where the native cysteine residues were replaced with alanine residues. Our strategy was to create PLN constructs with individual cysteines at each of the three positions, and double cysteine constructs containing a cysteine at two of the native positions. Experiments using these PLN cysteine mutants would be combined with similar studies using the wild-type and null cysteine PLN. Null cysteine canine PLN cDNA in a pAcSG2 baculovirus transfer vector (Pharmingen) was a gift from Rasvan Cornea, PhD (University of Minnesota) to the Mahaney laboratory. Dr. Mahaney enzymatically removed the PLN null cysteine cDNA from the pAcSG2 vector and subcloned it into to the multiple cloning region of the pFastBac1™ baculovirus transfer vector (Invitrogen), for use within the Bac-to-Bac insect cell expression system used in the laboratory. Although Invitrogen offers a wide array of baculovirus expression vectors, this particular vector was chosen because it does not express a fusion protein to allow for purification. The prominent features of the pFastBac1 baculovirus vector are depicted in Figure 3-1.

Dr. Mahaney used Gene Runner v3.0 to design unique oligonucleotides for site-directed mutagenesis experiments with the purpose of adding back a single cysteine via point mutations at each of the three transmembrane positions to the null cysteine (alanine) PLN background.

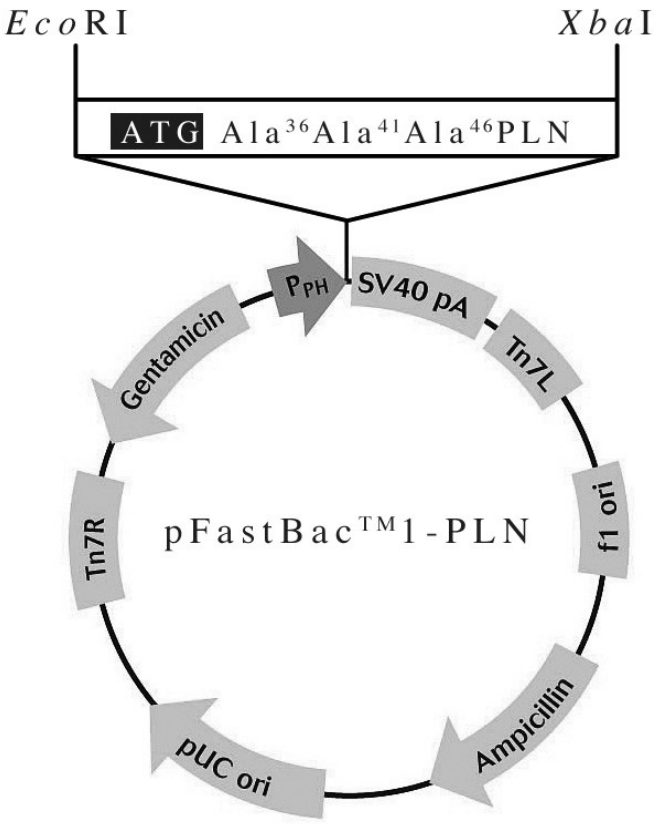

Figure 3-1. pFASTBac™1 Vector Map.
Depiction of pFastBac1™ vector with key features: polyhedrin promoter site (P_{PH}), SV40 polyadenylation signal, and the Tn7L and Tn7R mini Tn7 elements that permit transposition of the gene of interest into the baculovirus genome. The complete sequence of this vector is available from the website: www.invitrogen.com.

There were also plans to create double cysteine mutations in which two of the alanines would be changed back to the original cysteine. Site-directed mutagenesis experiments were performed as described in Chapter II. After sequencing the resulting PCR products, none of the designed primers were able to introduce the point mutations back into the cDNA, thus a new approach was planned.

Baculovirus expression system

Creating point cysteine mutations in pFASTBac1

Starting from the null cysteine PLN ORF in pFastBac1, mutagenic oligonucleotides were designed using the Stratagene QuikChange Primer Design Program. A total of five sets of forward and reverse primers were designed for each cysteine mutation, three creating a single cysteine point mutation with the last two creating double cysteine point mutations. Although our goal was to create six PLN cysteine mutants, three single and three double, the number of base pairs between the codons for positions 36 and 46 were too far apart to create a single mutagenic primer. Therefore, to create this mutation, a two step mutagenesis was completed where position 46 was mutated first and the designed mutagenic primer for position 36 was used to add the second cysteine. All primers required for site-directed mutagenesis of PLN amino acid residues are listed in Appendix A. As described in Chapter II, we used the PCR-based mutagenesis method Quikchange (Aligent Technologies). The resulting cDNA constructs were individually transformed into competent XL Gold *E.coli* cells (Aligent Technologies) to amplify the cDNA, which was isolated and purified. The average DNA concentration recovered 0.4-0.7 μg/μl. All reactions were sequenced to verify successful point mutations using the mutagenic sequencing primer (5'-ATAACCATCTCGCAAATA-3'). Since the mutations were created in a null cysteine (alanine) PLN background, the nomenclature for each of the PLN mutant are as follows: 36C, 41C, 46C, 36/41C, 41/46C, and 36/46C, see Table 3-1.

Construct	Nomenclature
$Cys^{36}Cys^{41}Cys^{46}$	Wild Type (WT)
$Ala^{36}Ala^{41}Ala^{46}$	Null Cys PLN
$Cys^{36}Ala^{41}Ala^{46}$	36C
$Ala^{36}Cys^{41}Ala^{46}$	41C
$Ala^{36}Ala^{41}Cys^{46}$	46C
$Cys^{36}Cys^{41}Ala^{46}$	36C/41C
$Cys^{36}Ala^{41}Cys^{46}$	36C/46C
$Ala^{36}Cys^{41}Cys^{46}$	41C/46C

Table 3-1. Nomenclature of PLN cysteine mutations

Generation of recombinant bacmid DNA

Once the gene of interest was cloned into the pFastBac1 donor plasmid and the site-directed mutagenesis was completed and verified via sequencing, the result was a recombinant donor plasmid for each PLN cysteine mutation. The transformation of each PLN cDNA construct into DH10Bac *E.coli* cells was the next step to creating bacmid DNA. The heat shock method was used to combine the cysteine mutant donor plasmid and the *E.coli* cells as described in Chapter II. The DH10Bac cells contain a baculovirus shuttle vector (bacmid) with a mini-attTn7 site to allow for cDNA transposition between the mutant PLN pFastBac™1 donor plasmid into the bacmid. At this point, the *E. coli* containing the recombinant bacmid was plated on LB agar including selective antibiotics, Bluo-gal and IPTG for positive selection of transformed and transposed *E. coli.* A single colony with the confirmed phenotype was selected for each PLN cysteine mutant and liquid LB medium was inoculated to create a starter culture for each. The *E. coli* cells were grown and harvested in a large enough quantity isolate and purify the recombinant bacmid as described in Chapter II. Average bacmid DNA concentrations ranged from 0.2-0.5 μg/μl. To verify transposition, the isolated bacmids were analyzed by PCR using M13 oligonucleotide primers which hybridized to the bacmid adjacent to the cDNA recombination site and subjected to subsequent agarose gel electrophoresis. The PCR results for each mutant can be seen in Figure 3-2. If transposition occurred correctly the expected PCR product was expected to be ~2,470 bp, while the bacmid alone would have produced a PCR product of ~300 bp. Each of the PLN cysteine mutant bacmids displayed the expected product band.

Creation of recombinant baculovirus

Recombinant baculoviruses are widely used to express heterologous genes in cultured insect cells, particularly insects of the order Lepidoptera. The purified bacmid DNA containing each of the site-specific transposed cysteine mutant variants of phospholamban cDNA was used to transfect *Spodoptera frugiperda* (Sf9) cells. Per the Invitrogen manual, transfected cells were kept in a 27^{o}C humidified incubator and signs of viral infection were visually inspected daily. Beginning at 72 hours post infection the virally-infected insect cells appeared lysed and showed signs of clearing in the monolayer using an inverted phase microscope at 250-400X magnification. Once the transfected cells showed these signs of late stage infection, the cell

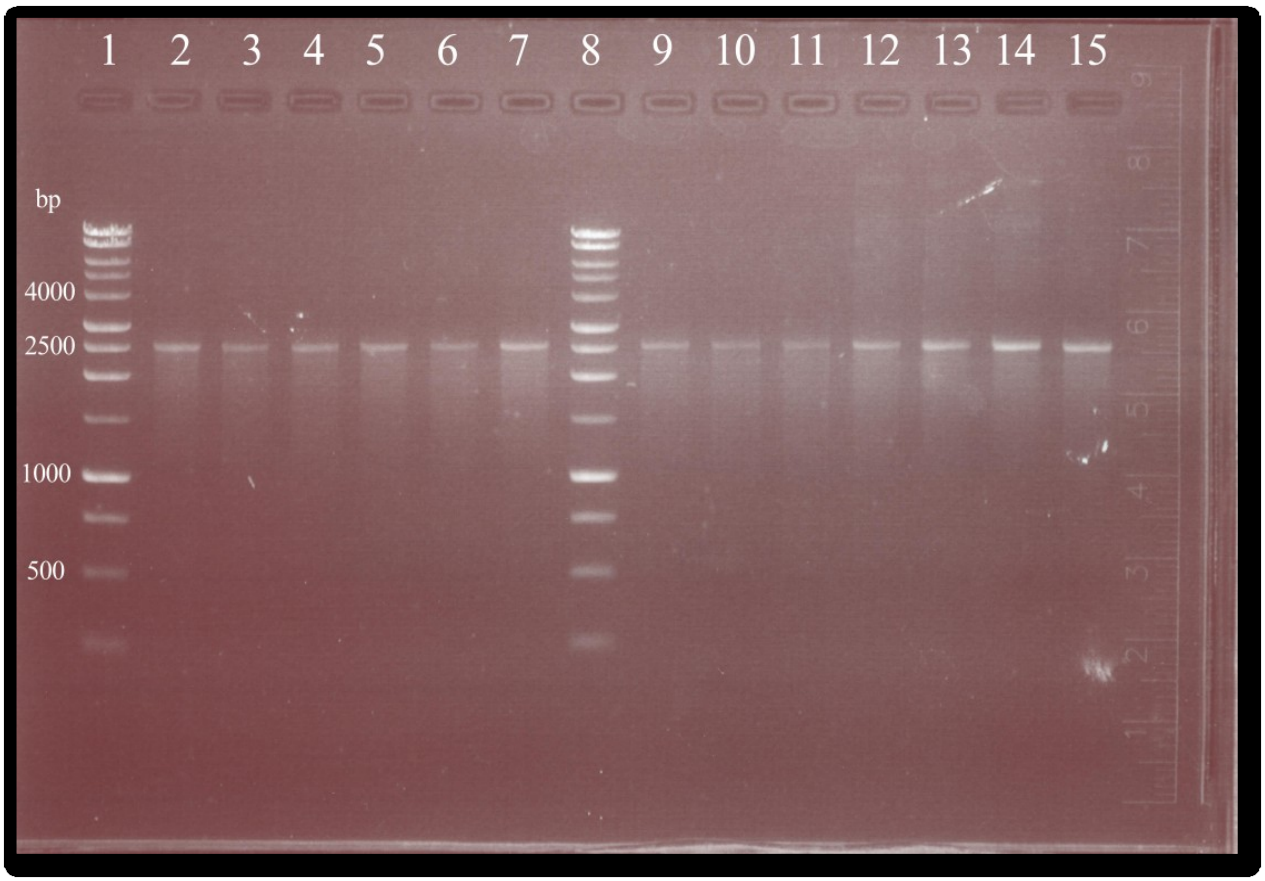

Figure 3-2. Confirmation of PLN cDNA incorporation into recombinant baculovirus. Recombinant bacmid PCR products were separated on 1% agarose gel, and stained with EtBr. Lane assignments 1 and 8 contain a 1kb DNA ladder (Promega), 2-5 A36C PLN, 6-7 A41C PLN, 9-11 A46C PLN, 12 A36/41C PLN, 13 A36/46C PLN, and 14-15 A41/46C PLN. All PLN cysteine mutant samples showed a band around 2500 bp which coincided with the expected PCR product size of ~2,470bp.

medium was collected and processed as described in Chapter II. This was now considered the P1 (e.g., Passage 1) viral stock. A P1 viral stock was made for each of the six phospholamban cysteine mutants along with stocks for null cysteine phospholamban, and wild-type phospholamban. At this point, each of the viral stocks was amplified by infecting additional insect cells, and the resulting viral titer was determined for each baculovirus by plaque assay or rapid titer assay (Clontech). Table 3-2 shows a representative titer of each virus that determined via the rapid titer method. The titer of the initial viral stock generally ranged from 1×10^6 to 1×10^7 plaque forming units (pfu)/ml. Amplification of the virus allowed for production of a P2 (e.g., Passage 2) viral stock with a titer ranging from 1×10^7 to 1×10^8 pfu/ml. Optimal protein expression requires a virus stock solution with a titer of at least 1×10^8 pfu/ml. It is for that reason that all viruses were amplified at least once while many were amplified up to five times to create a P5 (e.g., Passage 5) stock. As the passage number increased with each mutation, the titer values sis show signs of decrease but not enough to affect infection. Over the course of the research project, all virus stocks were kept in sterile pyrex jars at 4^oC for a maximum of 6 months.

In addition to expressing the PLN cysteine mutant proteins alone for individual study, our goal was to coexpress the PLN constructs with the Ca^{2+}-pump (SERCA2a) to determine how HNO treatment modifies the regulation of SERCA2a by phospholamban. For this purpose, we used a wild-type SERCA2a baculovirus construct that was previously developed in the laboratory (Waggoner, 2003).

Mutation	pfu/ 10^{-3} dilution	pfu/ 10^{-4} dilution	pfu/ 10^{-5} dilution	pfu/ml
A36C	136	14	2	6.0×10^{7}
A41C	298	35	3	1.0×10^{8}
A46C	120	13	1	5.0×10^{7}
A36/41C	*	*	20	8.0×10^{8}
A36/46C	*	*	50	2.0×10^{9}
A41/46C	*	*	60	3.0×10^{9}

Table 3-2. Representative viral titers (pfu/ml) for the PLN cysteine mutant recombinant baculoviruses, determined using the rapid titer assay. These titers represent one viral prep from each mutation. (*) indicates the number of plaques in the culture well were too high to accurately count.

Protein expression using High Five™ cells

Protein expression and isolation of SERCA2a and phospholamban using the baculovirus system has been optimized from established protocols (*61*). All expression of recombinant proteins, including wild-type SERCA2a and cysteine mutant PLN were expressed in High Five™ cells. Because the baculovirus system is eukaryotic, both phospholamban and SERCA2a were processed and modified with all naturally occurring post translational modifications and trafficked to the endoplasmic reticulum (*66*). Each of the cysteine mutants were expressed alone and coexpressed with wild-type SERCA2a. The final conditions for protein expression are detailed in Chapter II.

Confirmation of expressed PLN cysteine mutants via SDS-PAGE

Determination of a proteins molecular weight (MW) migration via polyacrylamide gel electrophoresis (PAGE) in the presence of sodium dodecyl sulfate (SDS) is a universally accepted method in biomedical research. Original results with SDS-PAGE have showed that the subunit structure of PLN can include five major electrophoretic mobility forms after complete dissociation of the holoprotein (*67*). When PLN is not dissociated via boiling, a major monomer and homopentamer form can be detected. The apparent MW's for both the pentamer and monomer form of PLN deviate from the formula MW with gel shifts (i.e. migration on PAGE that does not correspond to formula MW). The pentamer has been established to migrate 17% faster than the formula MW while the monomer migrates 48% slower than the formula MW (*68*). The formula molecular weight for both the pentamer and monomer units of PLN are 30 and 6.1 respectively, yet the literature acknowledges the apparent MW on SDS-PAGE as 29 and 9 respectively (*67*).

Each of the cysteine mutants of phospholamban were expressed alone in order to study the effects of HNO on the pentamer- monomer equilibrium and to test for the formation of disulfide bonds upon nitroxyl treatment. The presence and expression level of phospholamban in the microsomes was determined using SDS-PAGE and subsequent immunoblotting. PLN expressed in insect cell microsomes were detected using an anti-PLN primary antibody (2D12) (Figure 3-3).

Similar to results in the literature, microsomal WT-PLN migrates as both a pentamer and monomeric species with a higher percentage of the protein existing in the pentameric form. In

contrast, 36C PLN and 46C PLN seem to only show monomeric species of the protein with no other higher molecular weight oligomers seen. The 41C PLN sample shows similar characteristics to wild-type PLN in that both a pentameric and monomeric form of the protein are clearly apparent; however the equilibrium is clearly shifted toward the monomeric form. In all cases, for the single cysteine PLN mutants, the levels of protein expression appeared to be much less that the wild-type.

The current model in the literature shows the pentameric form of PLN held together by a leucine-isoleucine zipper with additional stabilization from the cysteine at position 41 (*18*). In this model originally proposed by Simmerman et. al. (*22*), the cysteines at position 36 and 41 are adjacent to the leu-ile zipper structure (see Figure 1-?); such that a bulky mutation (i.e. Phe, or Ser) at either site would more than likely perturb pentamer formation. Since each of our PLN mutations only contained a simple alanine in place of the cysteine; there was no indication that the ability to form a pentameric oligomer would be disturbed via steric hindrance. Therefore the previous results showing an absence of pentamer formation in the 36C and 46C PLN mutants led to further experimentation to prove or disprove the ability of these samples to form a pentamer.

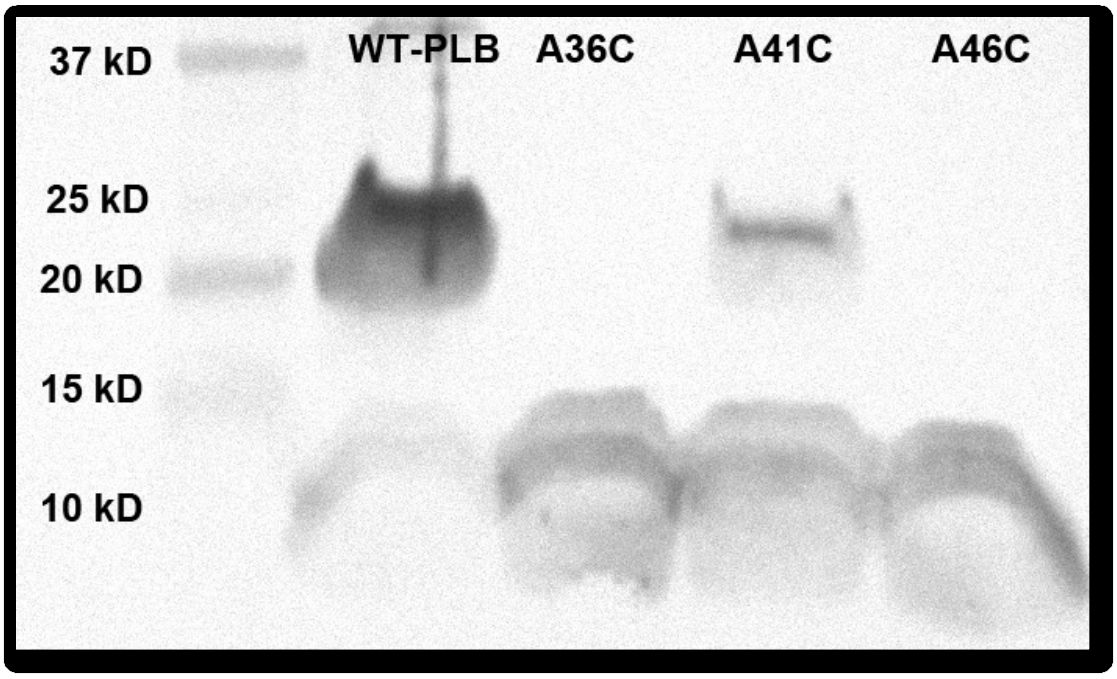

Figure 3-3. Immunoblot of single cysteine PLN. 0.12 mg of each insect cell microsomal sample was loaded onto a 12% denaturing polyacrylamide gel and separated as described in chapter III. The gel dissociation media contained 6.5% SDS final. Proteins were electrophoretically transferred to a PVDF membrane treated with primary antibody 2D12, and detected using a Protein A-HRP color reagent system. The lanes are labeled within the figure.

Effect of SDS concentration on SDS-PAGE results

After we conducted an in depth literature search on phospholamban penatmeric stability, the level of SDS in the sample loading buffer came into question. In 2009, Rath et. al investigated SDS binding capacity within membrane proteins to further elucidate atypical membrane protein SDS-PAGE migration(*68*). They found that membrane proteins are capable of differential solvation by SDS that may result in replacing protein-detergent contacts with protein-protein contacts, implying detergent binding and folding are intimately linked. In the polyacrylamide gel electrophoresis system used to analyze the PLN cysteine mutants, the source of SDS comes from the gel loading buffer. As the original loading buffer which contained 6.5% SDS as a final concentration did not allow for the formation of pentamers, we decided to test a range of lower concentrations to see if pentamer formation was possible.

At 6.6% SDS, the pentamer-monomer migration pattern of wild-type PLN and 41C PLN samples did not seem affected. The non effect on the atypical migration pattern of WT-PLN would be expected as all important amino acids are still intact. There has also been previous work showing the importance of the cysteine at position 41 for pentamer stability (*18*). Since the cysteine at this position is unreactive because of the occlusion of the sulfhydryl group, the higher concentration of SDS does not seem to be able to affect the pentamer-monomer equilibrium. Yet, once the concentration of SDS was lowered to at least 2.2% final both 36C and 46C PLN showed the capability of forming the pentamer, see Figure 3-4.

It is plausible that without the cysteine at position 41 stabilizing the pentamer formation, the higher SDS treatment in these samples resulted in more of a protein-detergent interaction impeding the oligomeric formation. Lowering the concentration of SDS in the loading buffer may have allowed for these PLN mutant samples to have protein-protein contacts, instead of protein-detergent contacts. With this new found information, all subsequent gel electrophoresis experiments used the following 2X sample buffer composition of: 137mM Tris-HCl (pH 6.8), 4.4% SDS, 22% glycerol, and trace bromophenol blue. This change allowed us to study the full effect of HNO on the pentamer- monomer relationship between all PLN mutant samples and WT-PLN.

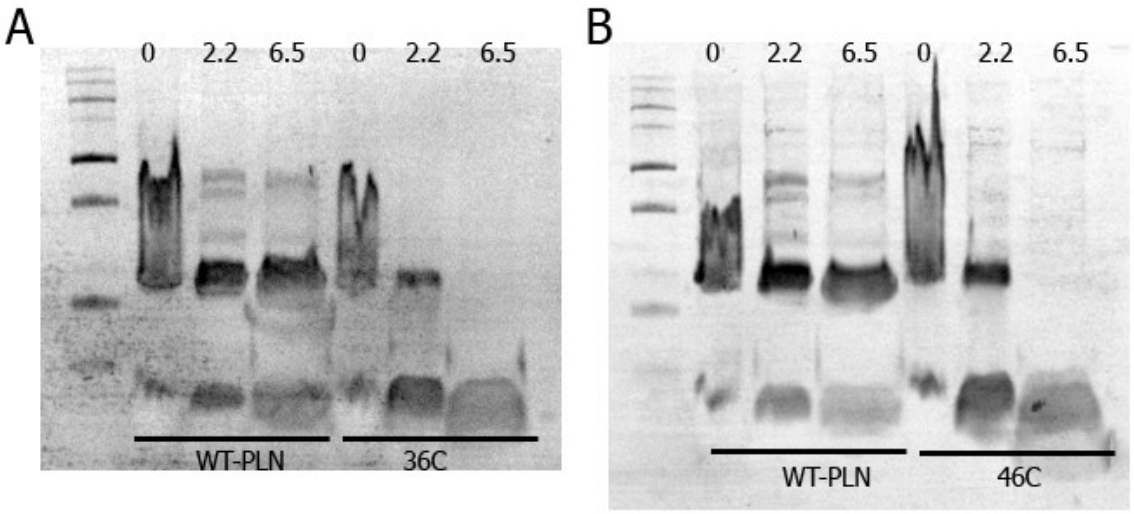

Figure 3-4. Effect of electrophoresis SDS concentration on PLN pentamer formation. Anti-phospholamban immunoblots show WT-PLN has the ability to form pentamers at low (2.2%) and high (6.5%) SDS. But 36C PLN (A) and 46C PLN (B) are only able to form pentamers at a lower amount of SDS. Similar to WT-PLN, 41C PLN (not shown) has the ability to form pentamers at both SDS concentrations.

SDS-PAGE analysis on all expressed PLN mutant samples

Once the electrophoresis conditions were optimized, each of the microsomal protein preparations was analyzed for their pentamer –monomer equilibrium as compared to wild-type PLN. Figure 3-5 shows an immunoblot in which a representative preparation for each PLN cysteine mutation was subjected to PAGE and immunoblotting as described in Chapter II, and detected with the anti-PLN antibody 2D12. The only similarity shared amongst all expressed mutants, regardless of the cysteine position, was the presence of both the pentameric and monomeric form of PLN. Microsomes expressing 41C, 36/41C, and 36/46C PLN display a pentamer-monomer pattern similar to WT-PLN. These samples show the pentamer-monomer equilibrium shifted more towards the pentameric form as evidenced by the much darker pentamer bands detected with PLN antibody. This pattern was expected in the WT-PLN sample, as previous literature has shown that only a small percentage of PLN is in the active monomeric form (*21, 69*). In contrast, microsomal samples 36C and 46C showed the opposite trend where the monomeric form of PLN shows a greater expression. This is evident by the robust color development at the expected monomeric molecular weight and a faint band seen at the molecular weight corresponding to the pentameric form of PLN. Quite the opposite, 41/46C PLN migrates as more of the pentamer form than the monomeric form. All these data reconfirm the importance of a cysteine at position 41 for pentameric stability. It seems that to ensure the formation of a pentamer, PLN must have at least two cysteines present (ie. 36/46C PLN, WT-PLN) or have at least a cysteine at position 41.

The literature has shown that introducing a mutation at a key leucine or isoleucine residue within the transmembrane domain of PLN results in monomeric super inhibitors as compared to the WT-PLN (*70*). The rationale is that the more monomeric or active form of PLN is available to bind to the Ca^{2+}-pump the more PLN has an opportunity to inhibit enzymatic activity. Thinking forward to the Ca^{2+}-ATPase activity experimentation with the cysteine mutations, we would expect to see 36C and 46C PLN show a higher inhibitory effect as compared to the WT-PLN since there is apparently more monomeric PLN available. We can look at the ΔpK_{Ca} in the next section to see if this theory corroborates with previous literature theory.

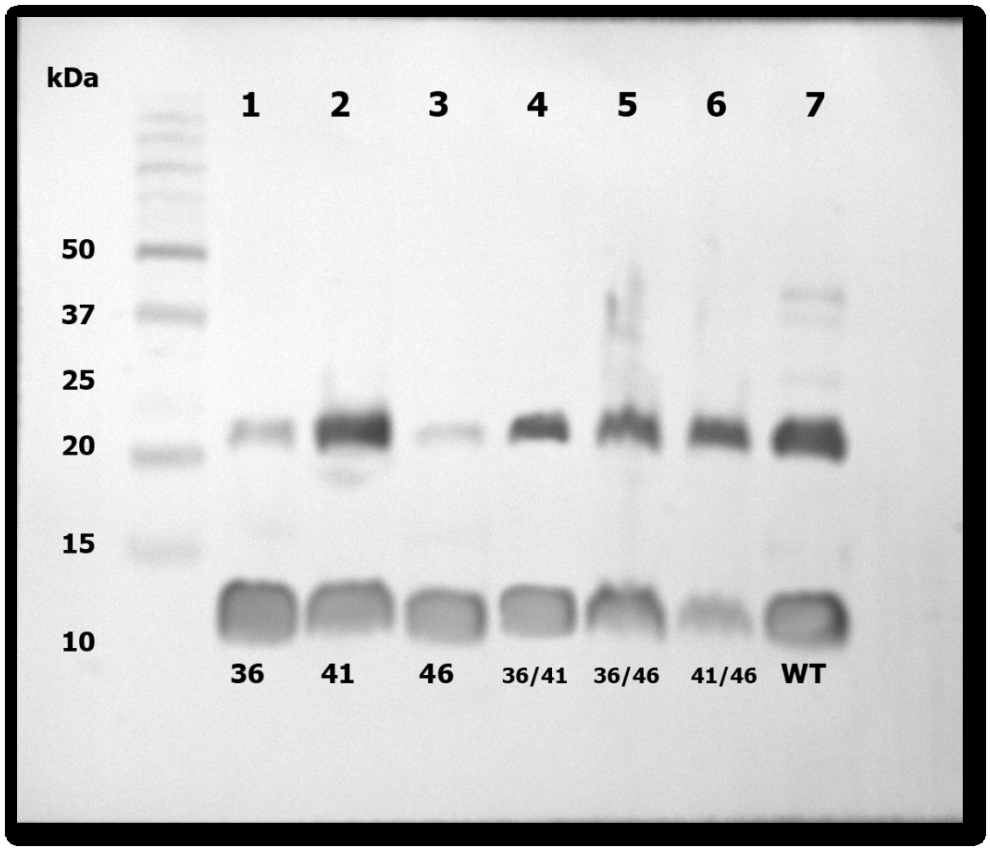

Figure 3-5. Effect of PLN cysteine mutation on the PLN pentamer-monomer equilibrium. All of the PLN cysteine mutations show a migration pattern similar to the WT-PLN displaying both the pentameric and monomeric units. It can be seen that the cysteine at position 41 plays a significant role in PLN pentamer stability as this mutant shows the highest pentamer formation in comparison to microsome samples containing a cysteine at positions 36 and 46. 0.2mg of each insect cell microsomal sample was loaded onto a 12% denaturing polyacrylamide gel and separated as described in chapter III. Proteins were electrophoretically transferred to a PVDF membrane treated with primary antibody 2D12 and detected using a Protein A-HRP color reagent system. The lanes are labeled within the figure.

Co-expression of cysteine mutants with SERCA2a

Karim (*18*) and MacLennan (*19*) have indicated that the three cysteine residues have no direct role in the mechanism of Ca^{2+}-ATPase regulation by PLN. However, if bulky side chains (like Phe) are substituted for the cysteines, and especially cysteine 41 (*22*), then PLN regulation of Ca^{2+}-ATPase is diminished. This suggests that AS/HNO modification of one or more PLN thiols, particularly cysteine 41, may affect PLN regulation of the Ca^{2+} pump. In order to elucidate effects of phospholamban cysteine modification on the regulatory potency of PLN on the sarco(endo)plasmic reticulum Ca^{2+}-ATPase, we co expressed the Ca^{2+} pump with each of the PLN cysteine mutants.

The baculovirus expression system allowed for the creation of co-expressed proteins in which two separate viruses were added simultaneously to co-infect a batch of insect cells. The end result should theoretically be a microsome that contains a functionally coupled SERCA2a and PLN (*65*). As described in Chapter II, there is a body of literature that has optimized the MOI factors needed for each virus in order to obtain the correct stoichiometry between SERCA2a and PLN to mimic the native myocyte. Although the optimum MOIs determined for each individual protein was a good starting point for co-infection, conditions still had to be optimized to our laboratory.

After several co-expression attempts using the established procedure developed by Waggoner (*65*), it became evident that each PLN mutant and SERCA2a co-expression had to be individually optimized as certain conditions would work for some co-expressions and not others. More than 50% of all co-expression attempts ended in malfunction as either one of the two proteins did not express, or if expressed, SERCA2a was not functionally active, and/or PLN was not coupled with the enzyme as determined by an enzyme assay. These protein samples were not usable in data collection. The following are some of the parameters that were altered to optimize the protein preparatory protocol: multiplicity of infection factor for each virus, length of viral incubation, type of insect cell used (High Five or Sf21), duration of viral infection, speed of cell homogenization, the order in which viruses were added to the cells, and the length and force of centrifugation spins.

With the completion of each co-expression protein harvest, the presence of each PLN and SERCA2a was determined by an immunoblot with primary antibodies raised against each protein, 2D12 and 2A7-A1 respectively. Once it was determined if each protein was present, an

Ca^{2+} dependent ATPase functional assay (details in Chapter II) assessed whether or not SERCA2a was active and if PLN was functionally coupled with SERCA2a. After multiple attempts, only 1-2 successful co-expressions were created with the single and double cysteine PLN mutants and SERCA.

Immunoblot analysis of PLN and SERCA2a co-expression

Using primary antibodies raised against PLN and SERCA2a, we were able to detect the presence of both SERCA2a and PLN in a single microsome but also to examine if there were changes in the migrational pattern of either protein resulting from protein-protein interactions. The data shows when SERCA2a is coexpressed with the single cysteine PLN mutants, there is a change in PLN pentamer-monomer dynamics (see Figure 3-6). As shown in the literature wild-type PLN shows an identical pentamer-monomer relationship regardless of the presence of SERCA2a (*71*). In our microsomes, even though the WT-PLN co-expression displays the expected pentameric and monomeric PLN bands (~30kDa and 7 kDa respectively) as seen in lanes 1 and 2, notice that in the presence of SERCA there is a smaller monomer band and a slightly darker pentamer. PLN mutant 36C (lanes 3 and 4) shows only a monomeric PLN unit when co-expressed with SERCA2a contrary to the expression of both the pentamer and monomer forms being identified when the mutant is expressed alone. Both the expected pentamer and monomeric band are present in PLN mutant 41C (lanes 5 and 6) when expressed alone and/or with SERCA2a. Although the data shows a clear decrease in the expression level of 41C PLN when co-expressed with SERCA2a, when expressed individually, 41C PLN shows a high expression level similar to WT-PLN. In regards 46C PLN (lanes 7 and 8), there was no difference seen in the migration pattern with the addition of SERCA2a. In both cases, individually expressed and co-expressed, 46C PLN showed only the monomeric form of the protein. This result is different from previous immunoblots with 46C PLN showing the capability to form a pentameric unit when the SDS concentration is lowered.

A repeat of this same experiment using different microsomes expressing the sample proteins showed a completely different result (see Figure 3-7). Here, there is evidence that each of the single cysteine mutants show a pentamer and monomer form of PLN co-expressed with SERCA2a. There is no obvious difference between the three samples (lanes 2-4) in regards to the expression level of either protein. However, there is a clear preference for the monomeric

form of PLN. We were also able to show the co-expression pattern of SERCA2a and PLN amongst the double cysteine mutants (lanes 5-7). Each of these samples showed the expected band ~110kDa for SERCA2a and both the pentamer and monomeric bands at the correct molecular weight for PLN. The difference between these results can be attributed to variation amongst individual protein preps. We acknowledge that each microsomal protein preparation was completed at various times often with different batches of cells and different viral passages. It is for this reason that multiple experiments were done with each protein prep and the results were always referenced back to look for similarities and common trends.

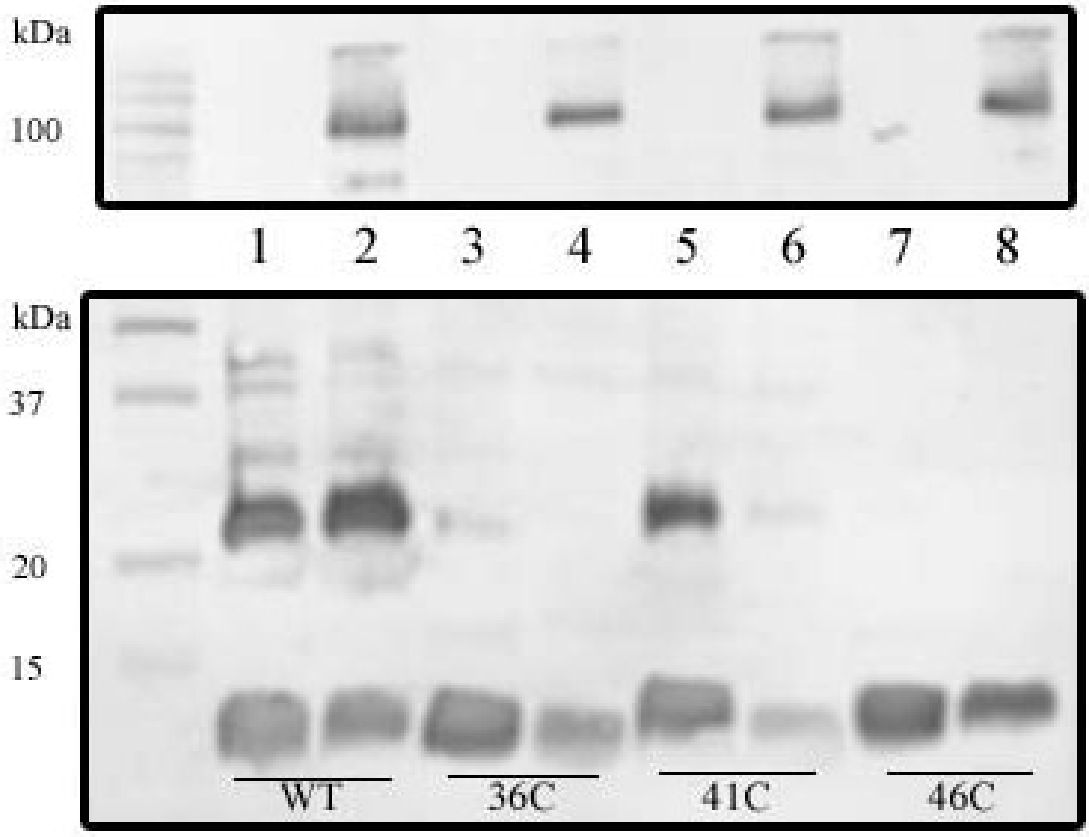

Figure 3-6. Effect of SERCA2a+PLN co-expression on PLN migration pattern. The presence of SERCA2a in the coexpressed microsomes altered the oligomeric dynamics of PLN in cysteine mutant samples. In lanes 1 and 2, it is clear that WT-PLN migrates as both a pentamer and monomer despite the presence of SERCA2a. 41C PLN showed pentameric units when expressed alone but not with SERCA2a, whereas 36C-PLN showed only a trace of pentamer. 46C PLN shows no difference in migration pattern despite coexpression. 0.2mg of each insect cell microsomal sample was loaded onto a 12% denaturing polyacrylamide gel and separated as described in chapter III. Proteins were electrophoretically transferred to a nitrocellulose membrane treated with primary antibodies 2D12 (PLN) or 2A7-A1 (S2a) and detected using a Protein A-HRP color reagent system. The lanes are labeled within the figure.

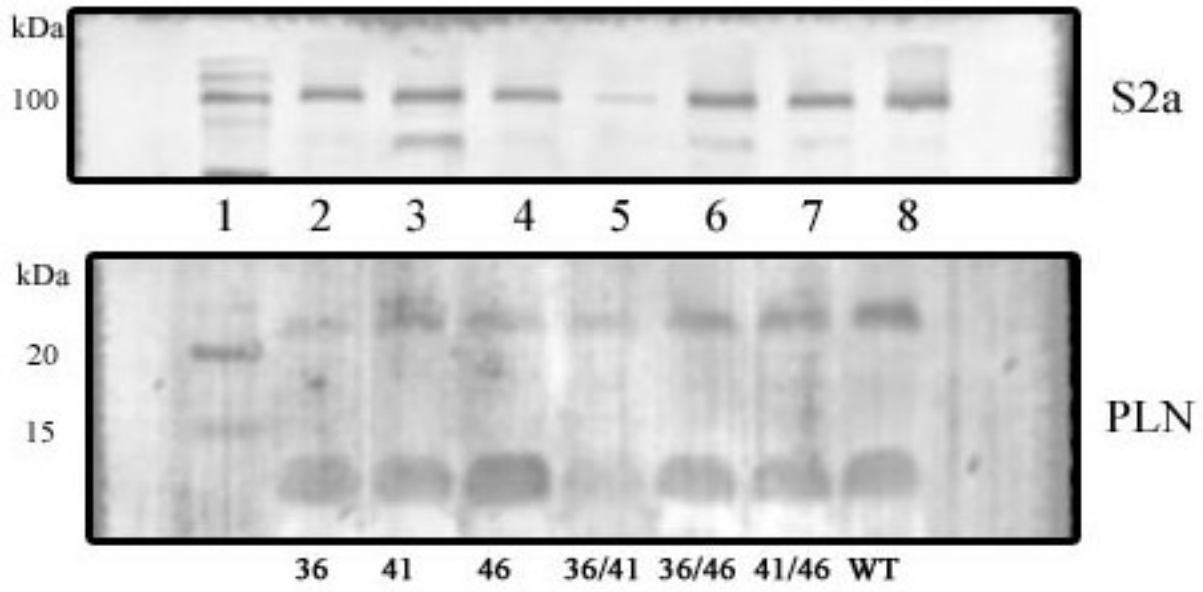

Figure 3-7. Effect of SERCA2a+PLN co-expression on PLN migration pattern. In comparison to Figure 4-6, WT-PLN (lane 8) and all three single cysteine PLN mutants (lanes 2-4) migrate as both a pentamer and monomer when coexpressed with SERCA2a. This pattern of stable SERCA2a and pentamer/monomer PLN expression is also seen in the double cysteine PLN mutants (lanes 5-7). 0.2mg of each insect cell microsomal sample was loaded onto a 12% denaturing polyacrylamide gel and separated as described in chapter III. Proteins were electrophoretically transferred to a nitrocellulose membrane treated with primary antibodies 2D12 (PLN) or 2A7-A1(S2a) and detected using a Protein A-HRP color reagent system. The lanes are labeled within the figure.

Functional characterization of co-expressed PLN cysteine mutants with S2a

After it was determined which microsomes expressed both PLN and SERCA2a via immunoblot analysis, a functional characterization of the PLN:SERCA2a complex was completed. ATP hydrolysis activity of SERCA2a in insect cell microsomes was measured colorimetrically by an inorganic phosphate liberation assay (details can be found in Chapter II). Using a phosphate standard curve, the absorbance readings at each $[Ca^{2+}]_{free}$ level were converted to μmol free inorganic phosphate. Since the initial protein concentration is known, the specific activity of SERCA2a can be calculated. The resulting $[Ca^{2+}]$-dependent activity of SERCA2a displays a sigmoidal curve because of the cooperative binding of calcium. All activity data was fit using the Hill equation, which reports the maximum enzyme activity (V_{max}) and apparent Ca^{2+} affinity ($K_{0.5}$), two of the key parameters affected by PLN regulation. To determine if the coexpressed mutant PLN was actively coupled to SERCA2a, the activity assay was done after the addition of an anti-PLN antibody, 2D12. The addition of this antibody creates a "no-PLN" control in which PLN responds in a similar fashion to native phosphorylation thereby relieving inhibition. This should result in a shift of the Ca^{2+}-ATPase activity curve, as evidence by a decrease in the $K_{0.5}$ value. Thus, SERCA2a displays an increase in the apparent $[Ca^{2+}]$ sensitivity due to relief of PLN.

The relief of PLN inhibition upon the addition of 2D12 as shown in ATPase activity assay data (Figure 3-8) confirms effective coupling of each single cysteine mutant PLN and SERCA2a microsome. In all cases, upon the addition of 2D12, the inhibitory function of PLN is relived by a confirmed shift in apparent SERCA2a Ca^{2+} affinity as defined by $\Delta pK_{Ca.}$ SERCA2a plus 36C PLN shows a decrease in the $K_{0.5}$ by 56% while SERCA plus 41C and 46C PLN show a decrease in $K_{0.5}$ by 23% and 45% respectively. It has been accepted that in native cardiomyocytes or native cardiac SR vesicles, relief in PLN inhibition by PKA or CAM-KII phosphorylation is shown by a decrease in the calcium $K_{0.5}$ by about 50% (*65*). Additionally, it has also been shown that insect cell microsomes and cardiac SR have nearly identical Ca-ATPase kinetics behavior as affected by PLN (*65*). Therefore, it is with this knowledge that we accept these co-expressions as adequate for further analysis to study the effects of HNO on PLN and SERCA2a. If HNO modifies PLN in a way that affects physical coupling, HNO treatment may have the same effect as treatment with 2D12. Note that even though all samples confirm successfully coupling of PLN and SERCA2a, 36C and 46C PLN have a significantly larger

percent ΔpK_{Ca} than 41C PLN. This may mean that the 36C and 46C PLN are more easily dissociated from SERCA than 41C PLN. Nevertheless, this demonstrates that the substitution of cysteines in PLN does not prevent PLN from regulating the Ca^{2+}-ATPase. These results are consistent with previous findings that there supporting previously reported data (*24*).

Although the goal of this project was to create microsomes expressing single cysteine or double cysteine PLN mutants with SERCA2a, we are unable to report any functional data on any of the double cysteine PLN co-expressions at this time. We have been unable to create a microsomal sample that expressed both PLN and SERCA2a with the proper activity profile. This inactivity was determined via the same inorganic phosphate liberation assay used for the single cysteine mutant co-expressions. With the absence of Ca^{2+}-ATPase activity, it was unfeasible to test whether PLN functionally regulated SERCA2a within the microsomal sample. A minimum of three separate attempts were made for each co-expression to make viable microsomes after which the initiative was put on hold. Because these samples are imperative to fully understanding the mechanism of HNO on the PLN cysteines, current members of the lab are working on successfully creating these samples.

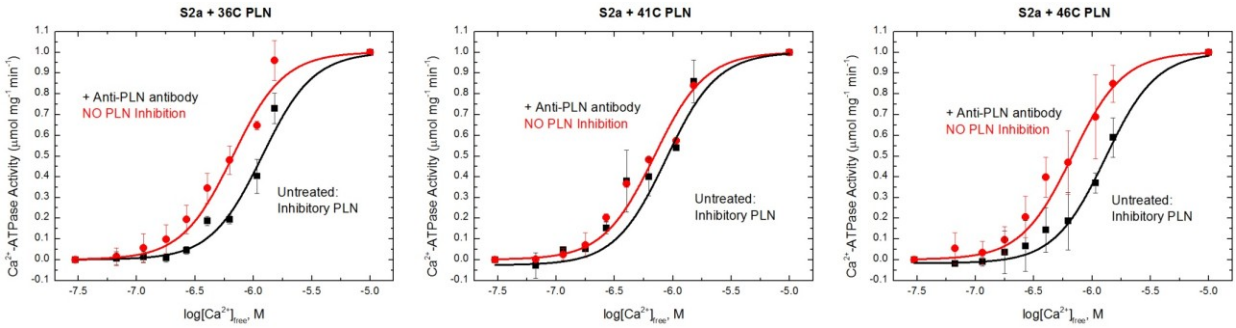

Microsomal Ca-ATPase $K_{0.5}$ (μM) values			
Sample Type	Control	2D12	ΔpK_{Ca}
S2a + WT-PLN	0.60±0.03	0.30±0.04	0.30±0.03
S2a+36C	1.2±0.05	0.65±0.03	0.50±0.04
S2a+41C	0.74±0.04	0.63±0.05	0.11±0.04
S2a+46C	1.4±0.05	0.62±0.06	0.76±0.05

Figure 3-8. Kinetics of S2a+ single cysteine PLN. The conditions for incubating the microsomes with 2D12 (anti-PLN antibody) and assaying ATPase activity of SERCA2a are given in Chapter III. The relief of PLN inhibition upon the addition of 2D12 as shown in ATPase activity assay data confirms effective coupling of each single cysteine mutant PLN and SERCA2a within the microsome. All data sets have been normalized to their relative V_{max} values to facilitate a direct comparison of the $[Ca^{2+}]$-dependence of each sample. Best fit parameters are given in the table below with (±) denoting standard deviation error.

Discussion- Baculovirus expression system

Starting in a null cysteine background, the proposed six PLN cysteine mutations [36C, 41C, 46C, 36/41C, 36/46C, 41/46C] were created and expressed individually and coexpressed with SERCA2a using the baculovirus expression system. Although we reached our goal of creating each of the six individual microsomal preparations, the total percentage of successful SERCA2a + PLN co-expressed preparations was low. The average co-expression microsomal prep, regardless of the PLN mutation, would produce one of the two proteins or express an inactive SERCA2a. A successful co-expression was defined by testing the microsomes for overall SERCA2a activity, functional regulation of SERCA2a by PLN, and expected migration patterns for both proteins. If the microsomal prep produced both PLN and SERCA2a as evidenced by an immunoblot using their appropriate antibodies, yet PLN was not functionally coupled to SERCA2a or SERCA2a displayed no activity, this was considered an unsuccessful prep.

The baculovirus expression system has been used for many years as a standard in labs to create recombinant proteins with relatively easy success (*72, 73*). The Mahaney lab is no exception, and has had success in the past (1999-2003) creating active SERCA2a and PLN co-expressed microsomes using the protocol established though this laboratory (*65*). However, starting in ~2007 we began to encounter some difficulty in recreating previously successful preps. After referencing the Invitrogen insect cell growth manuals, speaking with technical service representatives, and consulting other faculty members that use the system, we determined there are several possibilities to why we encountered such difficulty.

The first important aspect in successfully using the baculoviral expression system is viral competency. Using a low passage, high titer virus (preferably plaque-purified) is instrumental to creating functional and active recombinant proteins. After time, we realized that our current viral stocks may have been passaged too many times to maintain adequate virility. New viruses were made using "master" stocks (P5/P6) of either PLN or SERCA2a which had been kept at $4^{o}C$ for upwards of six months. Although the titers of these new viral preps were usually in usable range of 5×10^{7} to 1×10^{8} pfu/ml, it is possible that the key virility factors had deteriorated over time thus prohibiting successful recombinant protein expression. In an effort to maintain a healthy stock of all SERCA2a and PLN viruses, the lab is currently in the process discarding all old viruses and bringing up new stocks from viral plaques. There are some

promising new viruses in which we plan to use in the creation of co-expressed SERCA2a and double cysteine PLN mutants.

Secondly, an Invitrogen technical service representative brought to our attention a possibility of viral competition. The insect cells used in the baculovirus expression system have multiple viral receptors on the cell surface, effectively allowing more than one virus to enter and infect the cell simultaneously. Apparently, in some cases, one virus can be naturally stronger than the other not allowing the second virus to enter the cell. This phenomenon could explain why we always were able to detect PLN within the microsome but only 30% of the attempts showed SERCA2a. In an effort to avert this problem, both viral stocks were pre-mixed before infecting the cells instead adding each virus one at a time as suggested in Unit 16.11.11 of the Current Protocols Molecular Biology (*74*). Unfortunately, this technique did not increase the likelihood of success. The next step was to conduct a full scale investigation into the MOI used for each virus to determine if the viral competition could be ablated. In the end, we found the original MOI factors reported by Waggoner et. al. (*65*) to be suffice and we created microsomes that expressed both SERCA2a and each of the double cysteine PLN mutations (Figure 3-7).

Because none of the above co-expressed microsomes displayed any SERCA2a activity we now believe that the loss of important virility factors in the SERCA2a virus is the primary factor that has contributed to the stagnant pace of creating successful co-expressions. There is no evidence that the mutations within PLN effects viral competency as the same issues have impacted the creation of SERCA2a + WT-PLN microsomes also. In addition to the above speculations, there are other factors that may have impacted co-expression. It may be necessary to also adjust lysis and homogenization conditions to maintain protein integrity. In general, larger proteins tend to be more unstable, and the incubation time for maximal expression is not always the optimal time for maximal intact protein. Shorter infection times that lead to less protein tend to give more intact and active complexes (*74*). Taking all of these setbacks into account, we naturally began to question the use of the baculovirus expression system and look for alternative methods to study the effect of HNO on SERCA2a and PLN. The literature has shown the use of reconstituted membranes (*75-77*) and a more direct analysis using purified proteins to study SERCA2a and PLN regulation is effective in obtaining accurate and reproducible results. The following section begins the discussion of the pGEX2T system in which we attempted to employ these methodologies.

pGEX2T expression system

Although the baculovirus expression system is a widely accepted technique used to create large quantities of active recombinant proteins, the presence of the native insect proteins must be taken into account during data analysis. Within the scope of this project, there are limitations to using this system to fully understand the effects of HNO on only PLN and/or SERCA2a as HNO has the ability to interact with other proteins in the system. It is for this reason that the pGEX2T-*E.coli* PLN expression system was employed to generate large amounts of purified WT and mutant PLN, for individual study and for co-reconstitution with SERCA2a. Purified mutant PLN sample allows for exploration of disulfide bond or cysteine modification upon HNO treatment, in the absence of the other cysteine containing proteins.

A pGEX2T plasmid vector already containing a null cysteine PLN sequence was graciously given to the laboratory from Dr. Diana Bigelow (University of Washington) in 2005. Figure 3-9 shows the pGEX2T vector map with the PLN insert and other important construct features. Dog null cysteine cDNA was cloned into the expression vector in frame with the GST gene to create a GST-PLN fusion protein. This *E. coli* expression system takes advantage of GST being a large soluble protein which allows to easy purification of the small hydrophobic protein PLN attached as a fusion. To verify that there were no abnormalities within the plasmid, the vector was sent off for sequencing using the following primer [5'-TGGCAAGCCACGTTTGGTG-3'] to the University of Georgia. Once validity was confirmed, five sets of primers were designed to introduce the three transmembrane cysteines back in the same convention as the baculovirus system [36C, 41C, 46C, 36/41C, 36/46C, 41/46C PLN]. A list of all site-directed mutagenesis primers for the pGEX2T system can be found in Appendix A. After verification of mutagenesis by sequencing, recombinant JM109 *E. coli* was grown in standard Luria-Bertani medium supplemented with ampicillin and inoculated for expression from an overnight culture. When cultures reached an optimal density, expression was induced by adding IPTG and harvested via centrifugation. Sequential lysis, DNA fragmentation, and re-solubilization ended in a supernatant that should be highly enriched in GST-PLN fusion protein. At this point, the highly enriched GST-PLN fusion protein was run on a preparative electrophoresis unit for the first round of electrophoretic purification. Once the dye front had

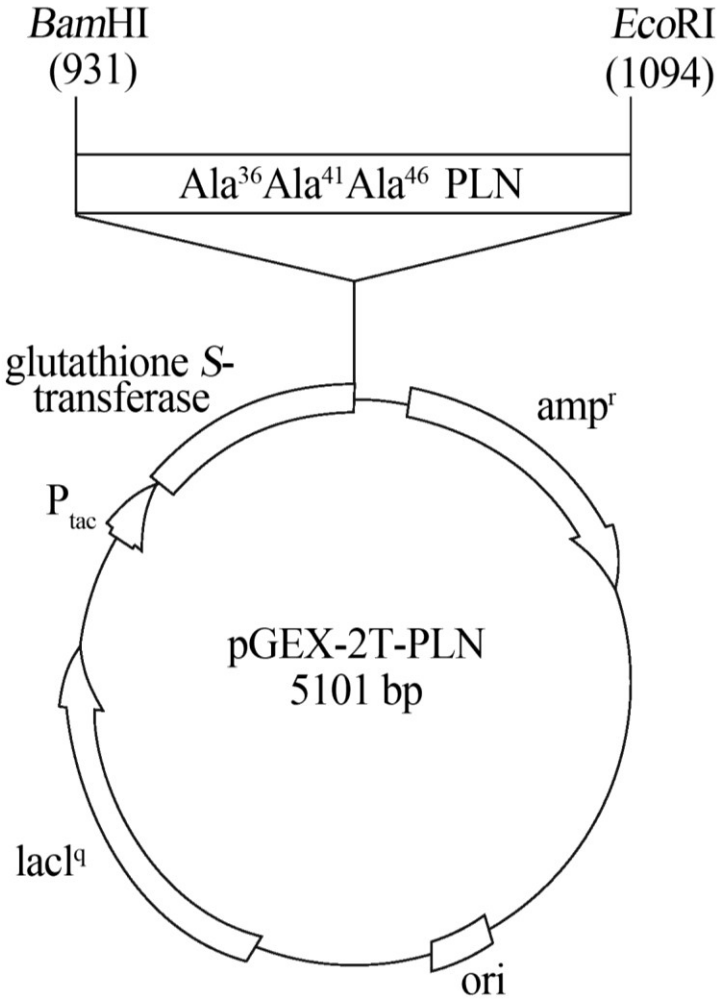

Figure 3-9. **pGEX2T-PLN vector map.** The 153 bp cDNA was cloned between BamHI and EcoRI sites of the expression vector pGEX-2T resulting in plasmid pGEX-2T-PLN

eluted from the gel, an additional 150 fractions of elutate were collected to capture the GST-fusion protein.

To test the new protocol, the initial experiments were done using the transformed 36C PLN cDNA into the pGEX2T vector. After the steps were taken to obtain the supernatant as described above, neither GST nor PLN were detected within the collected fraction range which was indicated on the protocol (~50-75 fractions after the dyefront). Specific protein content was determined by immunoblot analysis using GST and PLN primary antibodies while a biuret assay was used to quickly select fractions that contained a large amount of total protein. Once all 150 fractions were analyzed, it was clear that the migration and elution of the assumed GST-PLN fusion protein was different from what was expected as PLN detection was found within the dye front fractions. Alas, there was no evidence of the GST-PLN fusion construct as SDS-PAGE and subsequent immunoblotting with 2D12, the primary PLN antibody, showed PLN migrating at 7 kDa which is the molecular weight for monomeric PLN. The expectation was to see PLN migrate with GST at ~55 kDa confirming the GST-PLN fusion construct. When we examined the insoluble protein fractions we realized that the GST-PLN fusion protein accounted for none of the proteins found. The pGEX2T vector provides a specific protease factor recognition site which allows the specific removal of GST from a fusion protein. Since most of the soluble protein in the collected fractions was only PLN and not the GST-PLN fusion protein the addition of thrombin did not change the amount of soluble PLN protein contained in the fractions. Unfortunately, none of the PLN confirmed fractions showed a detectable signal with the anti-PLN antibody when run on a denaturing polyacrylamide gel and transferred to a nitrocellulose membrane. We speculated that the amount of PLN detected was just a background amount and the addition of IPTG did not induce the majority of the constructs.

Since the pGEX2T-PLN transformed JM109 cells did not successfully produce a GST-PLN fusion protein, we decided to try a different *E.coli* strain, BL21, a gift from Dr. Pablo Sobrado. A control experiment where pGEX2T-36C PLN transformed BL21 cells were not induced by IPTG was setup alongside experimental transformed BL21 cells in which IPTG was added according to protocol. Using this line of cells, both GST and PLN were detected via an immunoblot after the first preparative electrophoresis within a range of collected fractions (Figure 3-10). The control (non-induced) cells were expected to not show any viable detection of either GST or PLN as the expression of GST is controlled by lactose promoter. Contrary to

the experimental design, the control cells expressed both GST and PLN. In comparison to the experimental GST-36C PLN, there is a noticeable decrease in the expression of GST when IPTG was not added to the control. The 2D12 immunoblot shows a comparable PLN expression between both control and GST-36C PLN experimental group. It can thus be concluded that PLN is constitutively expressed in the cell with or without the induction by IPTG. Even though the experimental group shows positive for GST and PLN, there was not a formation of a GST-fusion protein. The GST moiety is 26kDa; therefore the expected MW for the GST-PLN fusion protein should be ~32 kDa. Via SDS-PAGE and subsequent immunoblotting with 2D12, PLN did not migrate at 32 kDa but migrated at the expected molecular weight for PLN (~6 kDa). Similar to the JM109 experiments, there was no detection of GST-PLN fusion proteins. We tried varying expression conditions with the change of *E. coli* strains and varied the conditions for inductions. None of these conditions yielded a significant increase in the GST-PLN fusion protein. Eventually, the effort to create a purified mutant PLN was placed on hold until the protocol was optimized.

Discussion – pGEX2T expression system

The preparation of glutathione-*S*-transferase (GST) fusion proteins as a tool for the synthesis of recombinant proteins in bacteria has been widely used as a tool in biochemical research. One of the main reasons for the use of these systems is the ease in which the GST-fusion protein can be affinity-purified without denaturation. Our lab was gifted a pGEX2T vector (IPTG-inducible GST fusion expression vector) where the null cysteine PLN cDNA was already cloned (Figure 3-9). Many bacterial strains could be have been used with this vector, but we decided to first use JM109 cells which are commonly used for cloning. The failure to induce protein expression in the JM109 cells more than likely resulted in poor optimization of the induction. In addition to the troubleshooting techniques tried, we could have titrated the amount of IPTG added, altered the time during log-phase growth at which the IPTG was added, lowered the temperature of bacterial growth, or induced for longer or shorter periods of time (*78*). Nevertheless, after consulting a faculty expert in bacterial protein purification, we were encouraged to try a different strain of *E. coli* that was better suited for our purpose.

The gifted BL21 *E. coli* was a commercial available bacterial strain designed for protein expression with a protease-deficient genetic background. Although the expectation to generate a

high yield of GST-36C PLN fusion protein was not met, the use of the BL21 cells did allow for expression of both GST and PLN as determined by a quick immunoblot on the supernatant. Because both proteins were detected, but not together, there is a possibility that the GST-PLN fusion protein was formed in the cell but cleaved by endogenous proteases before further processing. Although the BL21 cell genotype is supposed to be protease deficient, the addition of protease inhibitors to the protocol would help to eliminate any premature cleavage. There is also a possibility that majority of the GST-PLN fusion protein was in the insoluble fraction. As insolubility was not an originally foreseen issue, the insoluble fraction was not tested, but will be in future trials. In addition to the aforementioned techniques to increase fusion protein expression, we will also consider optimization of the lysis and sonication steps.

One of the main reasons for using the pGEX-2T vector to express and purify PLN in *E.coli* was the possession of a standardized and verified protocol (*64*) from the lab of Diana Bigelow. While we were not able to reproduce this protocol, there are other options available that will support our goal to create purified PLN. The use of GST fusion proteins was originally developed for gene expression in *E. coli*, but has recently become widely used in the baculovirus expression system (*79, 80*). To express the protein as a GST fusion, the pAcGHLT-A, -B, and –C vectors are commercially available (Pharmingen). This vector produces an N-terminal GST fusion protein which can be purified by selectively binding the protein of interest on immobilized glutathione and then eluting the protein by competition with a solution of reduced glutathione. Since our lab is well equipped to handle the baculovirus expression system, this switch might be advantageous. Another option within the baculovirus expression system is to express the protein as a poly-histidine fusion protein. There are several available vectors: pAcHLT (Pharmingen), pFASTBacHT (Invitrogen), and pBac-2cp (Novagen). The use of either option will effectively move the project forward in the event that the *E. coli* system does not work.

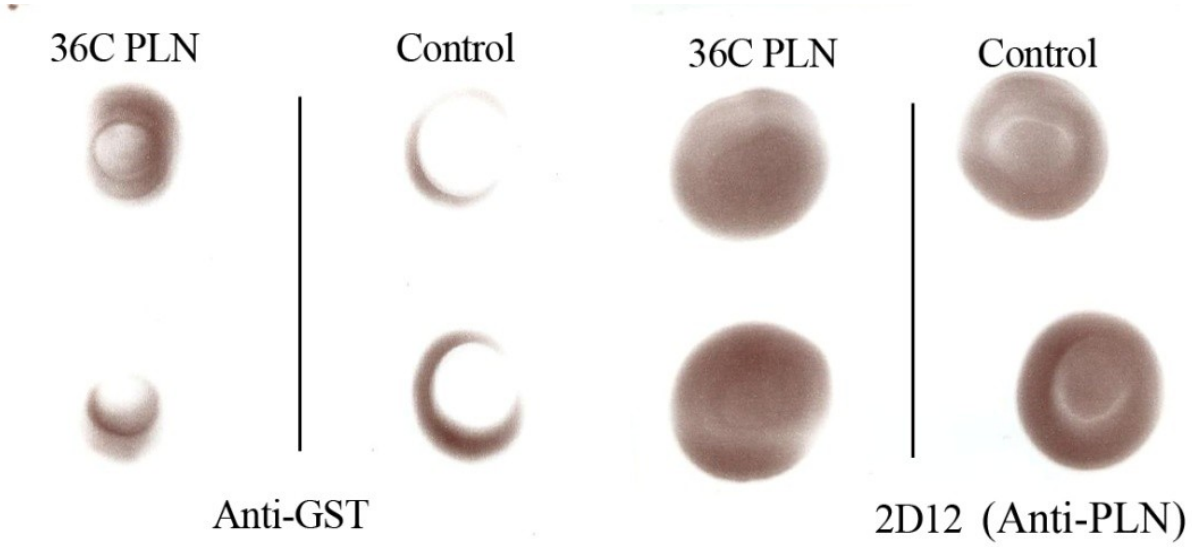

Figure 3-10. Immunoblot-BL21 *E. coli* cells testing for GST-36C PLN fusion. BL21 cells were transfected with a pGEX2T vector that contained 36C PLN in the multiple cloning site. Following standard protocol, two flasks of the transfected BL21 cells were brought up to 2L volume. The control cells were not induced via the addition of IPTG while the 36C PLN experimental cells were induced. Figure shows the results of 2 immunoblots in which 10μL of each final supernatant were placed in duplicate on a nitrocellulose membrane and both GST and PLN were detected using their respective antibodies. Despite the lack of IPTG, the control cells express both GST and PLN. The BL21 cells transfected with pGEX2t-36C PLN also showed both GST and PLN expression.

CHAPTER IV

FUNCTIONAL CHARACTERIZATION OF THE EFFECT OF NITROXYL ON PLN AND SERCA2A IN INSECT CELL MICROSOMES

Effect of PLN mutants on Ca^{2+}-ATPase activity as a function of HNO

The functional effects of HNO on the PLN cysteine mutants coexpressed with SERCA2a were studied by measuring the calcium dependence of ATPase activity (Figure 4-1) prior to and following treatment with Angeli's Salt. The mutants tested initially were 36C, 41C, and 46C PLN as active SERCA2a coexpression was not obtained in the 36/41C, 36/46C, and 41/46C PLN microsomes. Recombinant baculoviruses containing the coding region for the cysteine mutant dog PLN or dog SERCA2a were used to co- infect High Five™ insect cells at a predetermined MOI to create a final microsome that contained SERCA2a functionally coupled to PLN that kinetically mimicked the native SR membrane (*81*). For simplicity, only the data from a single microsomal prep is shown in Figure 4-1 as a representative sample for all other preps. As described in Chapter IV, SERCA2a ATPase activity displays a sigmoidal dependence on [Ca^{2+}] which, using the Hill equation (methods), can provide the maximum activity of the sample at saturating Ca^{2+} (V_{max}) and the [Ca^{2+}] required for half-maximal activity ($K_{0.5}$). Wild-type PLN, and each of the three single cysteine PLN variants functionally inhibit SERCA2a by increasing the $K_{0.5}$ for SERCA2a. PLN itself doesn't inhibit V_{max}, only the [Ca^{2+}] dependence of SERCA2a activity (*29*). The effects of HNO on the $K_{0.5\ a}$nd V_{max} are summarized in the Table 4-1. Upon the addition of 0.1 mM Angeli's Salt, there was a significant loss (>50%) of ATPase function in each of the three co-expressed samples (middle panel, ●), compared to the control, untreated samples (middle panel, ■). At saturating calcium, the V_{max} decreased by 75.8% in the SERCA2a + 36C PLN sample and 61.9% in the SERCA2a + 46C PLN sample. The SERCA2a + 41C PLN sample displayed the lowest decrease in V_{max} at 55.6%. Angeli's Salt treatment shifted the $K_{0.5}$ values showing a 0.33 μM change for SERCA2a + 41C and SERCA2a + 46C and a 0.12 μM change for SERCA2a + 36C PLN. Table 4-1 also shows the $K_{0.5}$ and V_{max} data for SERCA2a + WT-PLN and SERCA2a microsomes collected by a previous graduate student, Vidhya Sivakumaran. The same incident of decreased Ca^{2+}-ATPase activity upon in the addition of

Angeli's Salt can be seen in the SERCA2a+WT-PLN sample as well, indicating that the presence of mutations within PLN, themselves, is not the cause of the V_{max} effect.

Waggoner et. al. (2004) (*65*) have shown that SERCA2a expression is depressed in cells that are co-infected with PLN, due to virus competition at cell surface receptors. However, SERCA2a and its regulation by PLN are near exactly the same as SERCA2a + PLN in active cardiac SR membranes (*82*). To remove these expression differences and allow direct comparison of the SERCA2a data with and without PLN, we typically normalize the curves to the maximum SERCA2a activity value. For the present data, we also normalized the + AS treated data to allow its comparison to the untreated data also (Figure 4-1, top panels). We also included activity data from the SERCA2a + PLN samples treated with anti-PLN antibody (but not AS/HNO) to uncouple PLN from SERCA2a, to show SERCA2a activity free of PLN inhibition, for comparison to SERCA2a + PLN samples treated with AS/HNO. Coexpressed SERCA2a + PLN microsomes treated with 2D12 show SERCA with a greater apparent Ca^{2+} affinity (red curves,●), compared to untreated SERCA2a + PLN samples (black curves,■), where the SERCA2a activity curve is shifted to the right relative to that of the 2D12 curve. According to our hypothesis, if HNO modifies PLN in a way that affects physical coupling with SERCA2a, HNO treatment should have the same effect as treatment with 2D12. Incubation with AS at a concentration of 0.1mM (blue curves,▲) shows activity curves that are almost identical to the 2D12 activity curve for the 41C PLN and 46C PLN samples, whereas there was almost no change for the 36C- PLN sample. This implies that PLN cysteines at positions 41 or 46 are important for AS activation of SERCA2a. Moreover, it demonstrates that the cysteine at position 36 is not or not as necessary for HNO activation of the pump.

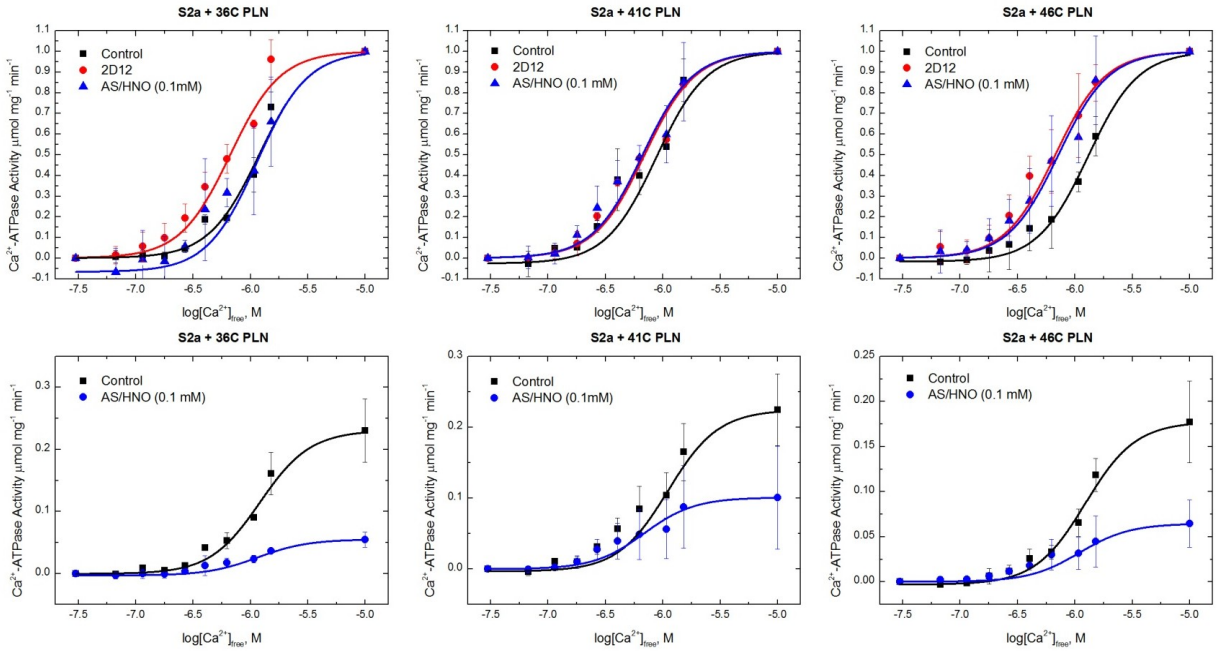

FIGURE 4-1. HNO effect on Ca^{2+}-ATPase Activity of S2a + single cysteine PLN mutants. SERCA2a was coexpressed with each PLN single cysteine mutant using the baculovirus-High Five insect cell expression system and isolated as insect cell microsomes. The SERCA2a ATPase activity of each sample was assayed at 37°C, using 5 mM MgATP and various $[Ca^{2+}]_{free}$ levels between 30nM and 15µM. Samples were preincubated in the absence (control, ■) or the presence of either 2D12 (2D12, ●), or 0.1mM AS/HNO (AS/HNO, ▲) for 15 minutes at room temperature. The bottom panel shows raw SERCA2a ATPase specific activity expressed in terms of mg of SERCA2a, according to the amount of total protein in the High Five cells for each sample. The top panel shows the specific activities normalized to the V_{max} calculated from fitting the raw data to the Hill equation. Errors denote the spread of triplicate determinations for a single experiment using a single preparation of expressed protein. Experimental repeats using difference preparations gave similar results. Best fit parameters are given in Table 5-1.

	V_{max} -AS	V_{max} +AS	$K_{0.5}$ -AS	$K_{0.5}$ +AS
Sample Type	µmol mg SERCA2a^{-1} min^{-1}		(µM)	
SERCA2a alone	0.85±0.06	0.43±0.05	0.34±0.40	0.34±0.30
SERCA2a + WT-PLN	0.68±0.05	0.37±0.03	0.48±0.50	0.18±0.30
SERCA2a + 36C PLN	0.23±0.02	0.05±0.03	1.2±0.07	1.1±0.05
SERCA2a + 41C PLN	0.23±0.03	0.10±0.05	0.96±0.10	0.62±0.09
SERCA2a + 46C PLN	0.18±0.04	0.07±0.02	1.2±0.09	0.92±0.07

Table 4-1. Kinetic parameters for SERCA2a + PLN ATPase activity. The data in Figure 4-1 was fit using the Hill equation, which reports the maximum enzyme activity (V_{max}) and apparent Ca^{2+} affinity ($K_{0.5}$) values seen in this table. (±) denotes standard deviation error. SERCA alone and SERCA + WT-PLN data were obtained from the dissertation of Vidhya Sivakumaran.

Angeli's Salt concentration effects Ca^{2+}-ATPase activity at saturating Ca^{2+}

In the first set of experiments, we measured the effect of 0.1 mM AS on the [Ca^{2+}] dependence of SERCA2a coexpressed with each of the single cysteine PLN mutants in insect cell microsomes (Figure 4-1 and Table 4-1). Although normalization of the ATPase activity data shows that cysteines at positions 41 and 46 are important in HNO activation of SERCA2a, there was also an unexpected V_{max} effect seen in all samples. This data prompted a set of additional ATPase experiments to further examine the effect of HNO on the insect cell microsomes. In rationale, if the data from these studies are to be used to support a potential pharmacological therapy for heart failure patients, it is important to investigate inactivation of the key enzyme using the drug of interest.

Instead of re-testing each of the coexpressed insect cell microsomes, we decided to focus on SERCA2a + 41C PLN. one of the two coexpressions that displayed activation of SERCA2a via HNO. We measured the effect of various Angeli's Salt concentrations on the activity of SERCA2a +41C PLN microsomes via the colorimetric phosphate assay as described in Chapter II (Figure 4-2). Samples were preincubated either without or with (1.0μM, 2.5μM, 10μM, or 0.1mM) Angeli's Salt for 10-15 minutes prior to the initiation of the reaction via 5mg ATP.

As expected, SERCA2a + 41C PLN displayed a sigmoidal dependence on [Ca^{2+}] at each HNO treatment concentration. The $K_{0.5}$ and V_{max} values (Table 4-2) of the 0.1 mM AS curves were nearly identical to those obtained from the [Ca^{2+}]-dependent ATPase activity in the first set of experiments (Table 4-1). The effect of 10μM AS/HNO on SERCA2a +41C PLN microsomes was similar to the 0.1mM AS/HNO treatment in terms of V_{max} and $K_{0.5}$ values (0.10±0.07 μmol mg $SERCA2a^{-1}$ min^{-1} and 0.67±0.01 μM). Once the AS/HNO treatment concentrations began to reach 1.0-2.5 μM range, there was a relief in ATPase activity as evidence by the restoration of the V_{max} values closer to the control (no AS treatment) showing only a 21% decrease in activity. However, once the activity data is normalized, the lower AS/HNO concentrations showed very little to no change in the calcium sensitivity of SERCA2a ($K_{0.5}$ values Table 4-2). SERCA2a + 41C PLN microsomes treated with 10 μM AS shifted the Ca^{2+} activation curve to the left, resulting in a 38% decrease in the $K_{0.5}$ value as compared to the control. As observed, this data suggests that SERCA2a activation by HNO can be achieved using a concentration range of at least 10 μM to 0.1mM AS. In addition, decreasing the AS treatment concentration to below ten

micromolar does allow for the relief of SERCA2a V_{max} inhibition, but is not strong enough to induce SERCA2a activation.

Discussion – Effect of HNO levels on Ca^{2+}-ATPase activity

The general purpose of this study was to investigate more fully whether the activation of the SR Ca^{2+} pump by HNO is mediated by the thiol residues in PLN and to identify which of the 3 cysteine residues are involved. Incubation with AS at concentrations of 0.1 to 0.25 mM was shown to activate Ca^{2+} uptake in cardiac SR vesicles and cardiomyocytes (*53*). Given that we observed SERCA2a enzyme inhibition at those levels of AS we elected to treat our microsomes with μM amounts of AS in an effort to match the previously reported findings. However, once the concentration of AS treatment was below 10μM, there was little inhibition of V_{max}, but there was no significant increase in SERCA2a calcium sensitivity (Figure 4-2). While speculating a reason for this significant difference in data, it was concluded that the variation in cellular microenvironments between the insect cell microsome and the cardiomyocytes was a key factor.

To date, there have been many studies comparing the *in vitro*, *in vivo*, and *ex vivo* effects of HNO donors (for example, refs. (*50, 52, 83, 84*)) in which it has been determined that HNO reactivity can be accessed based on the redox situation of the cellular environment (*46*). Cells and tissues are comprised of heterologous mixtures containing varied concentrations of GSH and other metals. In the cellular compartments such as the cytosol or mitochondria, where there is a rich concentration of GSH (1-10mM), HNO would be expected react with the GSH and have little opportunity to react with other targets. In the cell membrane, where the concentration of GSH is substantially lower, HNO would have a longer lifetime to allow for modification of a target. The *in vivo* systems of myocytes and whole hearts are dramatically different than isolated microsomes as there are other factors such as cellular pathways, proteins, and other structural elements which HNO can interact before reaching the targeted SERCA2a and PLN. Thus, we suspect the reported concentration of AS in these studies (0.1-0.25 mM) did not fully reflect the actual concentration that reached the target proteins. In contrast, the SERCA2a and PLN in our microsomes were exposed to the full 0.1 mM AS. It was clear that further study was needed to find the correct range of AS concentration to use with the microsomes that would elicit the same Ca^{2+} pump response as observed in cardiomyocytes.

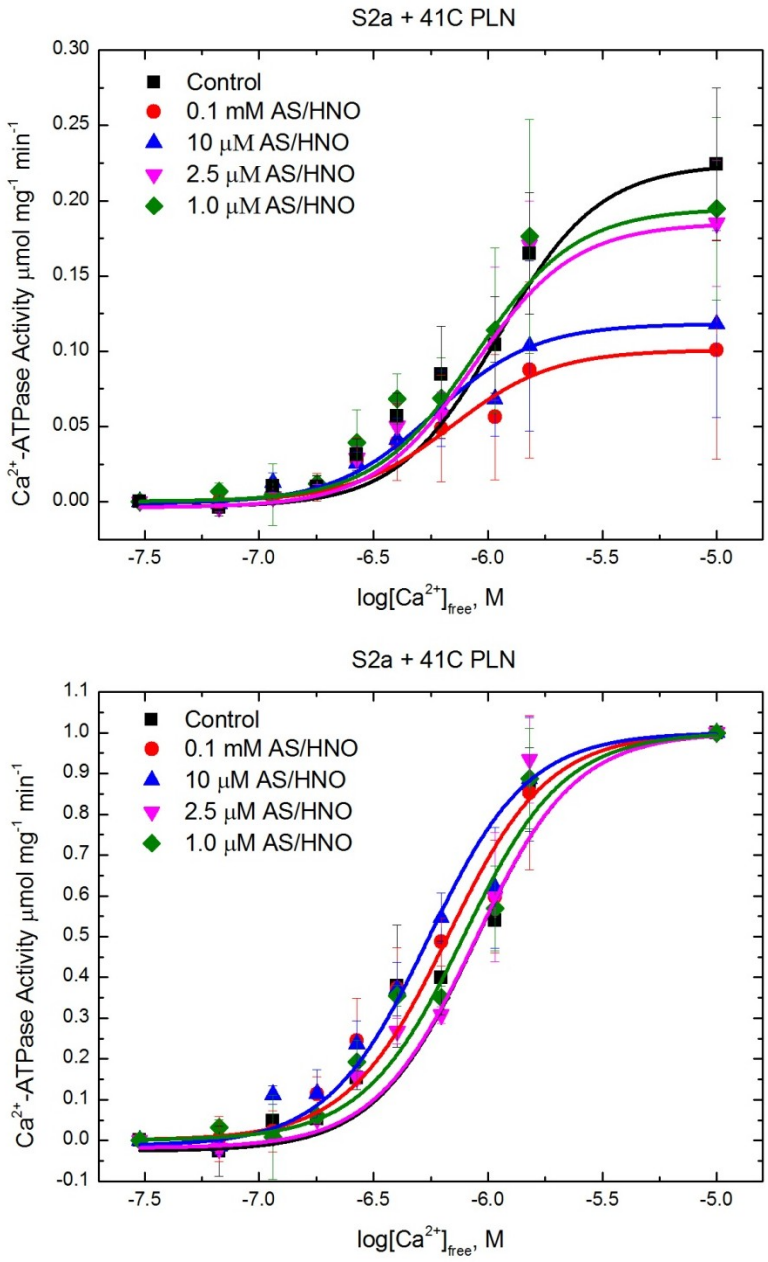

Figure 4-2. SERCA2a+41C PLN ATPase Activity as effected by AS/HNO. SERCA2a was co-expressed with 41C PLN in High Five insect cell microsomes and further treated with various levels of AS as described in Chapter III. The data are plotted as specific ATPase activity (μmol mg^{-1} min^{-1}) versus the log of free calcium (M). Decreasing the [AS] relieved SERCA2a V_{max} inhibition (top panel), but also decreased the apparent shift in the $[Ca^{2+}]$ dependence of SERCA2a activity that followed AS modification of PLN (bottom panel). Error bars denote the standard deviation of triplicate experiments. Experimental repeats using difference preparations gave similar results. The same effect was observed in S2a+46C PLN (not shown).

	V_{max} (μmol mg SERCA2a^{-1} min^{-1})	$K_{0.5}$ (μM)
Raw data		
Control	0.22±0.05	1.1±0.01
1.0 μM	0.19±0.06	0.88±0.01
2.5 μM	0.18±0.04	0.87±0.01
10.0 μM	0.12±0.06	0.58±0.01
0.1 mM	0.10±0.07	0.70±0.02
Normalized data		
Control	-	0.88±0.02
1.0 μM	-	0.78±0.01
2.5 μM	-	0.88±0.02
10.0 μM	-	0.55±0.02
0.1 mM	-	0.67±0.01

Table 4-2. Kinetic parameters for SERCA2a+41C PLN ATPase activity. The data in Figure 4-2 was fit using the Hill equation, which reports the maximum enzyme activity (V_{max}) and apparent Ca^{2+} affinity ($K_{0.5}$) values seen in this table. (±) denotes standard deviation error.

Influence of Angeli's Salt on SDS-PAGE migration pattern of PLN cysteine mutants

As established in Chapter IV, the apparent MWs for both the pentamer and monomer form of PLN deviate from the formula MW with gel shifts. The pentamer has been established to migrate at an apparent MW of 29 kDa and the monomer at 9 kDa (*67*). Under normal conditions, the pentamer and monomer are the major mobility forms that migrate on an SDS-PAGE. However, upon complete dissociation of PLN via boiling or other methods, the other three major electrophoretic mobilites (dimer, trimer, and tetramer) exist between the pentamer and monomer. The use of SDS-PAGE will allow us to gain insight into HNO ability to induce potential chemical changes within PLN. If our hypothesis is correct, HNO (as donated by AS) should potentially form a disulfide bond between two free thiol groups either an intramolecularly (within a monomer) or intramolecularly (between monomers). This change will be evident by the appearance of the intermediate electrophoretic PLN mobilites as determined by SDS-PAGE and subsequent immunoblotting as described in Chapter II.

Insect cell microsomes expressing each single cysteine PLN mutant (36C, 41C, 46C) were pretreated with a final concentration of (0, 1.0, 2.5, or 10 μM) AS for ten minutes and then mixed in a 1:1 ratio with gel loading buffer containing either no DTT (-DTT) or 6 mg/ml DTT (+DTT). 30 micrograms of each sample were electrophoretically separated on a 12% denaturing continuous polyacrylamide gel, then transferred to a PVDF membrane. The PLN migration pattern was detected using an anti-PLN antibody, 2D12 and compared to molecular weight standards. The 9 kDa PLN monomer species visible in Figure 4-3 does not change in any of the cysteine mutants regardless of AS or DTT treatment. Visually scanning up the blot from the monomer, there were no other electrophoretic mobilites detected in any of the single cysteine PLN mutants until the 25 kDa pentamer form is reached. Similar to the monomer form, there was no change in the appearance of the pentamer plus the addition of neither HNO nor DTT treatment. The apparent differences in pentamer abundance between each of the single cysteine PLN was not attributed to AS treatment as these results are similar to Figure 4-5. Residues 41C and 46C are important for stabilization of the pentamer (*24*) which is why there is more of a pentamer band detected compared to 36C PLN.

Additionally, the same experiment was completed with the individually expressed double cysteine PLN microsomes. Here, since there are two available thiol groups within each PLN monomer there is a possibility to form intramolecular disulfide bonds unlike the single cysteine

mutants. In a similar fashion, insect cell microsomes expressing each double cysteine PLN mutant (36/41C, 363/46C, 41/46C) were pretreated with a final concentration of (0, 1.0, 2.5, or 10 μM) AS for ten minutes and then mixed in a 1:1 ratio with gel loading buffer containing either no DTT (-DTT) or 6 mg/ml DTT (+DTT). 30 micrograms of each sample were electrophoretically separated on a 12% denaturing continuous polyacrylamide gel, transferred to a PVDF membrane. The PLN migration pattern was detected using an anti-PLN antibody, 2D12 and compared to molecular weight standards. In the absence of DTT treatment, the presence of a monomer, dimer, and pentamer were observed in each of the three double cysteine PLN mutants (36/41C, 36/46C, 41/46C). Only the dimer mobility disappeared when the microsomes were treated with DTT after the Angeli's Salt. Upon first consideration, we can conclude that the apparent dimer formation in PLN is caused by HNO and it is held together by a disulfide bridge as DTT made the dimer disappear. However, the dimer was also present in the control (no AS treatment) lane, therefore it was not the result of HNO treatment.

Lastly, we investigated the effect of HNO to chemically modify the PLN cysteine mutants in the presence of SERCA2a. Using these coexpressed SERCA2a + PLN microsomes, we were able to answer questions of whether HNO causes disulfide crosslinks to form between SERCA2a and PLN in addition to the original hypothesis that HNO causes disulfide bonds within PLN individually. Co-expressed microsome samples were treated and prepared as in the previous experiments. Once the proteins were separated and transferred to a PVDF membrane, one membrane in each set was incubated in the anti-SERCA2a antibody, 2A7-A1, while the other was incubated in the anti-PLN antibody, 2D12. Although we have established that certain levels of HNO do not cause an effect in PLN mobility within single cysteine mutants (Figure 4-3), in Figure 4-5, we can observe similar mobility patterns. In each of the three coexpressions, there is no change in the migration pattern of SERCA2a between control and AS treatments. The 2D12 blots of SERCA2a +41C PLN and SERCA2a + 36C PLN shows no change in the pentamer and monomer mobility pattern of PLN. Only the monomer form of PLN was detected on the 2D12 blot of SERCA2a + 46C PLN (Figure 4-3, C) despite the appearance of both major electrophoretic species in previous experiments. This could be the result of the low sensitive detection methods or variation between microsomal preps. There was no evidence of PLN-SERCA2a crosslinking as there was no PLN detected at the molecular weight of SERCA2a (not shown).

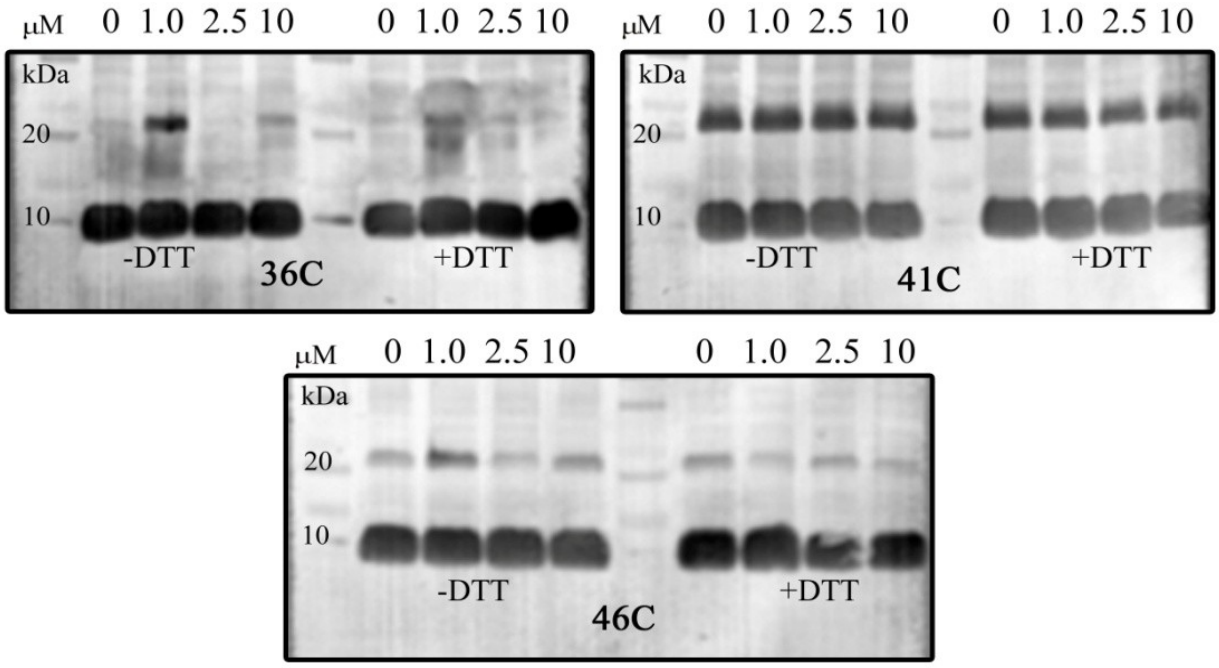

Figure 4-3. Immunoblot- Single cysteine PLN mutants ± AS/HNO. 2.0 mg/ml of High Five™ microsomes containing each of the three single cysteine PLN were treated with AS for 10 minutes at room temperature with a final concentration of (0, 1.0, 2.5, 10 μM), lanes labeled. Following AS treatment, the treated microsomes were mixed in a 1:1 ratio with a gel loading buffer containing either no DTT (-DTT) or 6 mg/ml DTT (+DTT). 30μg of each microsome were electrophoresed on a 12% continuous gel and transferred onto a PVDF membrane. PLN was detected using the anti-PLN monoclonal antibody 2D12. Molecular weight standards are shown in the most left lane in each gel.

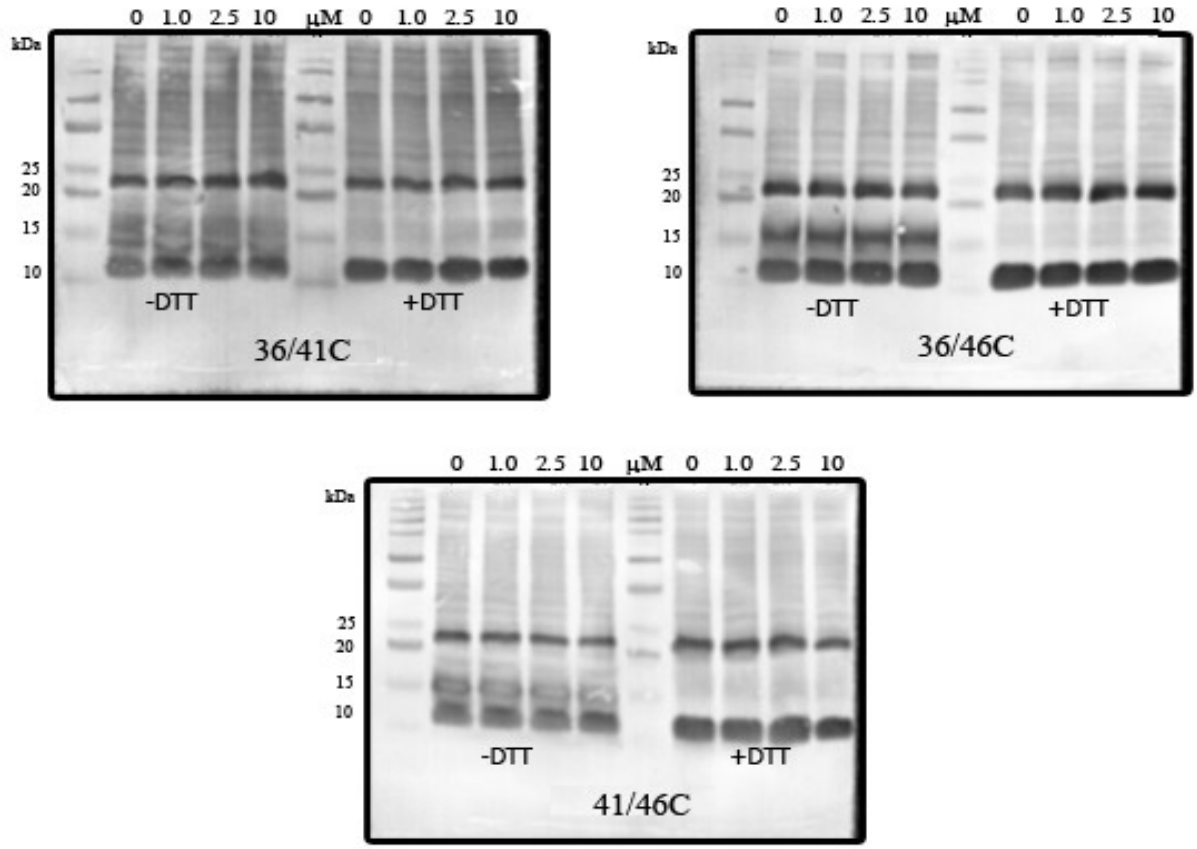

Figure 4-4. Immunoblot- Double cysteine PLN mutants ± AS/ HNO. 2mg/ml of High Five™ cell microsomes containing recombinant double cysteine PLN were treated with AS for 10 minutes at RT with a final concentration of (0, 1.0, 2.5, 10 µM), lanes labeled. After the treatment with AS, the microsomes were mixed in a 1:1 ratio with a gel loading buffer containing either no DTT (-DTT) or 6 mg/ml DTT (+DTT). 30 µgrams of each microsome were electrophoresed on a 12% continuous gel and transferred onto a PVDF membrane. PLN was detected using the anti-PLN monoclonal antibody 2D12. Molecular weight standards are shown in the most left lane in each gel.

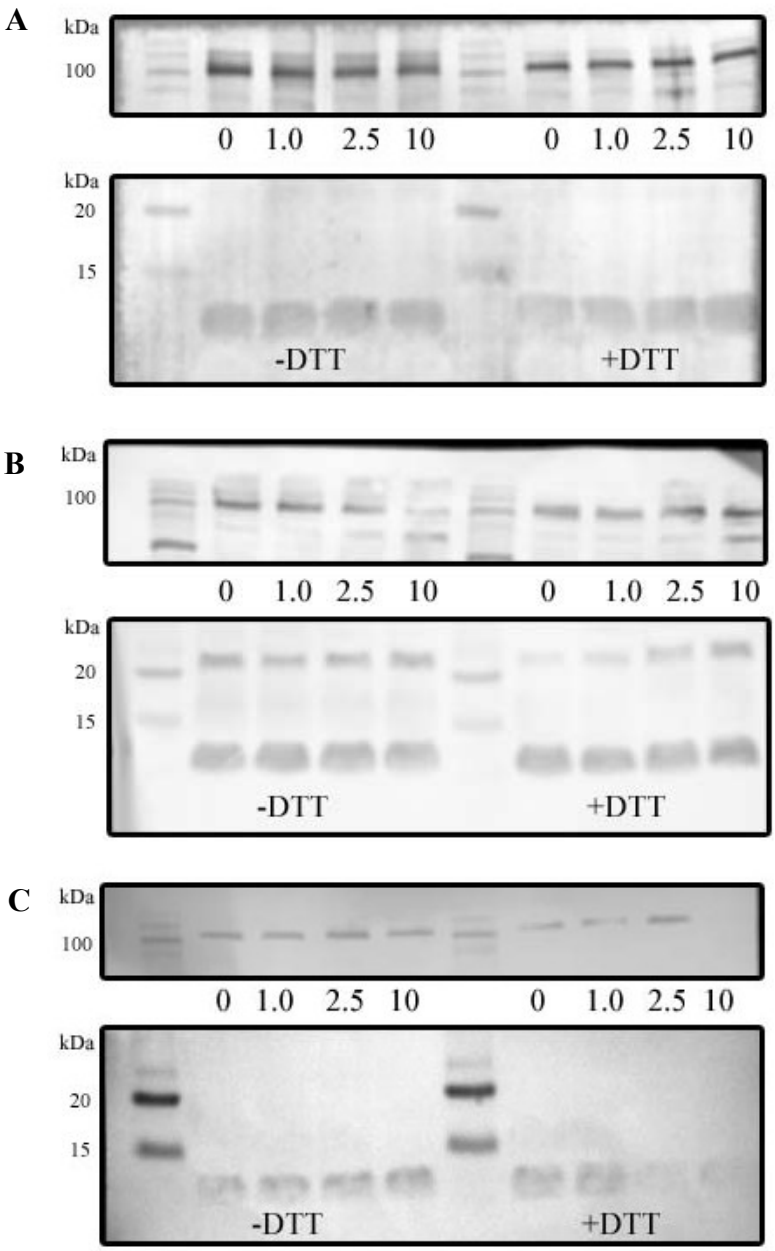

Figure 4-5. Immunoblot- SERCA2a + single cysteine PLN mutants ± AS/ HNO. 2mg/ml of coexpressed High Five™ cell microsomes containing SERCA2a and single cysteine PLN were treated with AS for 10 minutes at RT with a final concentration of (0, 1.0, 2.5, 10 μM), lanes labeled. The three panels represent the following microsomal coexpressions: (A) S2a+ 36C PLN (B) S2a+41C PLN (C) S2a+46C PLN. After the treatment with AS, the microsomes were mixed in a 1:1 ratio with a gel loading buffer containing either no DTT (-DTT) or 6 mg/ml DTT (+DTT). 30 μg of each microsome sample was electrophoresed on a 12% continuous gel and transferred onto a PVDF membrane. PLN was detected using the anti-PLN monoclonal antibody 2D12 while SERCA2a was detected using the anti-S2a antibody 2A7-A1. Molecular weight standards are shown in the most left lane in each gel.

Immunoblot resolution of HNO induced covalent bond formation

In previous SDS-PAGE experiments, insect cell microsomal samples were treated with Angeli's Salt at various concentrations and separated to detect potential HNO induced PLN intermediate migration species. In the event that any intermediate PLN migration species was caused by a disulfide bond, the addition of DTT after AS treatment should make any disulfide formed bands disappear on an immunoblot using anti-PLN antibody. However, since we were not able to detect any change in the migration pattern of PLN upon AS or DTT treatment, we decided to employ another treatment method to detect and/or confirm the presence of covalent disulfide bond links between PLN. Prior to loading the microsomes onto a denaturing gel, samples were incubated in boiling water after treatment with AS and/or DTT. Once heated above 90^{o}C PLN can easily dissociate into the five major electrophoretic mobilites: pentamer, tetramer, trimer, dimer, and monomer as detected on SDS-PAGE. Because PLN is stabilized by a non-covalent leucine-isoluecine zipper, heat is able to disrupt the bonds. If HNO truly creates a disulfide bond connecting two or more PLN residues, then there should be a resistance in PLN dissociation upon boiling.

Similar to the previous blots, each single cysteine mutant was pre-incubated with either 10 μM Angeli's Salt or post-incubated with 6mg/ml DTT. Figure 4-6 shows the results for the various treatment conditions (marked by "+") in each microsomal sample. Beginning with 36C PLN, there was no change in the migration pattern of PLN between the control (no treatments) nor the lane plus 10μM AS. This confirms the previously reported data in Figure 4-3. When the 36C PLN microsomes were boiled, there was no dissociation into other oligomeric forms other than the already present pentamer and monomer bands. Pre-treatment of 36C PLN microsomes with AS before boiling does not change the migration pattern. Again, similar to Figure 4-3, the post-treatment of DTT following AS did not cause any visible changes in 36C PLN. The addition of boiling after both AS and DTT treatments also showed no change in the pentamer or monomer bands of 36C PLN.

The data for 41C PLN seen in lanes 2, 3, 6 and 7 (Figure 4-6 "41C") are also consistent with the previously reported immunoblot data shown in Figure 4-3. In summary, there was no visible change in the migration pattern plus the addition of AS or DTT. There was a noticeable increase in the appearance of the pentamer band upon AS treatment (lane 3). It is questionable whether there was also a quantifiable decrease in the 41C PLN monomer upon AS treatment, as

the levels appeared to stay consistent. There was also a difference observed when the 41C PLN microsomes were subjected to boiling after +/- AS treatment. Without any AS treatment, the 41C PLN microsomes migrated only as a monomer when boiled. This was the case in the absence and presence of DTT. However, once the 41C PLN was pretreated with 10 μM AS and followed by subsequent boiling, the pentamer withstood dissociation and remained present indicating the presence of a covalent bond. The addition of DTT did not appear to change the presence of the pentamer. When the 41C PLN microsomes were treated with AS, DTT and boiled, the majority of PLN was only seen in the monomer form.

The results for 46C PLN (Figure 4-6 "46C") were similar to that seen in the 41C PLN microsomes. Boiling caused a dissociation of PLN into primarily only the monomeric form of PLN. Incubating the microsomes in 10 μM AS prior to boiling seemed to protect PLN from dissociation. The pre-treatment of 46C PLN microsomes followed by DTT did not change the apparent migration pattern with or without boiling similar to 36C PLN. This data is concurrent with the immunoblots shown in Figure 4-3. From this data, we can observe that only in the 41C PLN microsomes did the pentamer dissociate upon boiling. To gain a better understanding of these bonds, we repeated the same experiments using the double cysteine PLN mutant microsomes.

Figure 4-7, shows the immunoblot data of the double cysteine PLN mutants under the various treatment conditions of 10 μM AS, DTT, and/or boiling. In each of the three panels, the lanes labeled with only the AS and DTT treatments show a migration pattern that was consistent with the data in Figure 4-4. Pre-incubation with 10μM AS as compared to the non-treatment control did not cause a shift and change in PLN migration pattern. Logically, the lanes plus and minus DTT after AS did not show any changes either. For all three microsomal samples, the act of boiling prior to loading onto the SDS gel, showed almost a complete dissociation of PLN into only the monomer form. Only 36/41C PLN showed remnants of the pentamer and another migration form underneath this band which could be labeled a tetramer. In this 36/41C sample, the pre-incubation of AS prior to boiling caused these faint bands to nearly disappear and only the monomer is seen distinctively. None of the double cysteine mutants show a migration of PLN that was able to withstand boiling which would be indicative of a covalent bond formation.

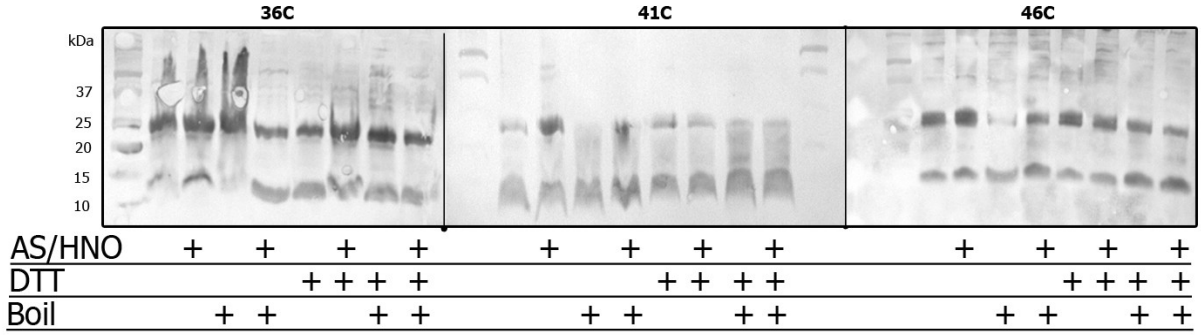

Figure 4-6. Immunoblot- Single cysteine PLN mutants treated with various conditions. The first lane in each panel shows molecular weight standards with the corresponding masses (kDa) on the left. AS/HNO (+) signifies whether the microsomal protein were treated with 10μM AS/HNO_{final} at room temperature for 10 minutes. DTT (+) signifies the microsomal samples were treated with 6 mg/ml DTT. Treatment with AS/HNO always preceded DTT treatment. Boil (+) signifies the submersion of the sample in boiling water for a duration of 1 minute after all treatments. 30 μgrams of each microsome sample were electrophoresed on a 12% continuous gel and then transferred onto a nitrocellulose membrane. PLN was detected using the anti-PLN monoclonal antibody 2D12.

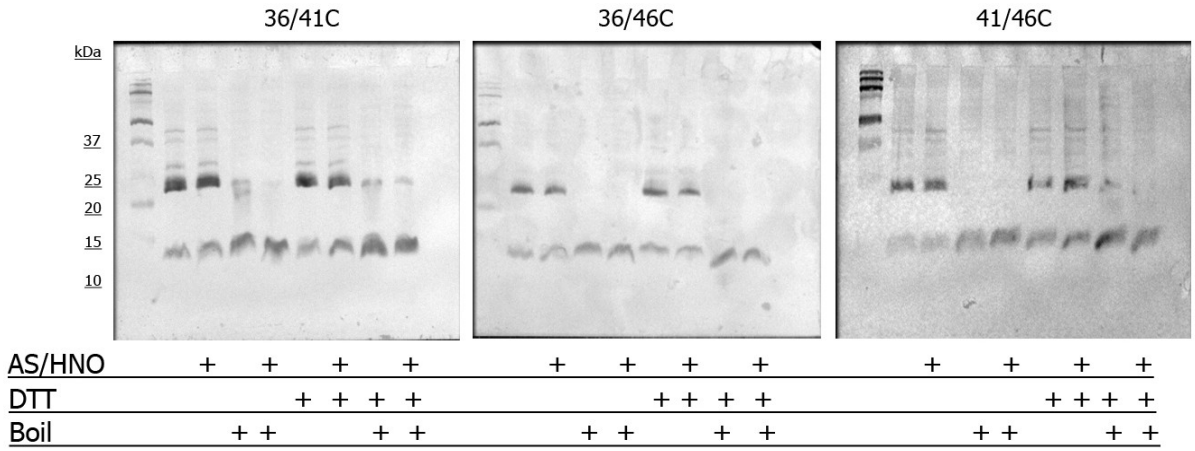

Figure 4-7. Immunoblot- Double cysteine PLN mutants treated with various conditions. The first lane in each panel shows molecular weight standards with the corresponding masses (kDa) on the left. AS/HNO (+) signifies the microsomal protein samples were treated with 10μM AS/HNO_{final} at RT for 10 minutes. DTT (+) signifies the microsomal samples were treated with 6 mg/ml DTT. Treatment with AS/HNO always preceded DTT treatment. Boil (+) signifies the submersion of the sample in boiling water for a duration of 1 minute after all treatments. 30 μg of each microsome were electrophoresed on a 12% continuous gel and transferred onto a nitrocellulose membrane. PLN was detected using the anti-PLN monoclonal antibody 2D12.

Discussion – Using SDS-PAGE to study HNO effect on PLN mobility

At first glance, there seems to be some inconsistencies between the SERCA2a activity data in Figure 4-1 and the immunoblot data shown in Figures 4-3 – Figure 4-7. The activation of SERCA2a + 41C PLN and SERCA2a + 46C PLN via AS/HNO treatment does not correlate with the observed oligomeric stability using the same AS treatment levels. There were no changes observed in the migration patterns of PLN or SERCA2a upon AS treatments in any of the PLN cysteine mutants created [36C, 41C, 46C, 36/41C, 36/46C, 41/46C]. This raises the possibility that SDS-PAGE assay used in this study does not accurately reflect the PLN oligomeric stability in the microsomal membranes even though this method has been used in the past to study PLN and estimate subunit structures (*85, 86*). Usually, accurate molecular weight values are difficult to obtain for small proteins based solely on the results of SDS gel electrophoresis, especially when the protein of interest is located in a membrane. However, previous analyses of PLN oligomeric stability using spectroscopic probes in lipid bilayers has shown that SDS-PAGE is very accurate in determining the oligomeric distribution of oligomers for PLN and its mutants (*66, 71*).

PLN is a multimeric protein that has an ability to dissociate into five major mobility forms (*67*). Wegener and Jones (1984) were to visualize all five forms of PLN on a denaturing polyacrylamide gel using a partially purified sample solubilized in 1.25% SDS and subjected to boiling for 1 minute prior to electrophoresis. However, when they changed the solubilization of the partially purified PLN sample to 2.5% SDS, just the monomeric form of PLN appeared. Moreover, they found that boiling highly purified PLN in a lower concentration of SDS (0.8%) was sufficient to convert PLN to no more than the monomeric form, however higher concentrations of SDS were required for the same effect in the partially PLN fraction.

We realized early in the project that SDS concentration played a major role in the visualization of other PLN mobility forms. Unlike the WT-PLN microsomes, the 36C and 46C PLN microsomes were sensitive to the higher levels of SDS and did not show any mobility form other than the monomer. While we decreased the final SDS concentration in our dissociation buffer from 6.5% to 2.2%, this might have not been enough of a decrease to visualize the formation of intermediate mobility forms within the microsomes. There were many immunoblots that showed a possible PLN dimer or trimer mobility upon HNO treatment, yet the bands were not clear enough to make an assertion. One of the current goals of the lab is to

perform an SDS titration study to empirically determine the lowest level of SDS required to visualize all other mobility forms in each PLN cysteine mutant sample.

In addition to the SDS investigation, a reconsideration of the immunoblot detection method and gel composition might assist in discernment of PLN mobility forms upon HNO treatment. The colorimetric detection method currently employed in the lab is not as sensitive as other chemiluminescent, radioactive, or fluorescent detection methods. Since most of the PLN electrophoretic mobilities are separated by only a few kDa, finding a system that will result in better separation and sensitive detection will be important to fully understand the role of HNO on PLN cysteines.

In the event that SDS optimization and an increase in immunoblot detection sensitivity does not allow for the visualization of higher oligomeric PLN species upon AS treatment, our hypothesis indicating the formation of disulfide bonds within PLN as the HNO mechanism is not fully disproven. A limitation to using SDS-PAGE to analyze HNO modification on PLN is the inability to visualize potential intramolecular disulfide bonds. An intramolecular disulfide bond between PLN cysteines within a single monomer would lower the amount of free thiols able to form any intermolecular disulfide bonds and thus additional mobilites such as dimers and trimers. Any HNO induced PLN modifications that are intramolecular could be verified by HPLC or a DTNB titration assay using a purified PLN sample (see Chapter VI).

It is also possible the mechanism of HNO modification on PLN does not include the complete formation of disulfide bonds but rather stops at producing a hydroxysulfinamides on each of the free thiols. An HNO induced production of a hydroxysulfinamides is a chemical modification that could alter the way PLN regulates SERCA2a, thus still being in line with our hypothesis. But, similar to the intramolecular bonds, we would need a purified PLN sample in order to determine which residues were modified by HNO to form this intermediate species.

Overall, there are some limitations to using SDS-PAGE analysis to study HNO modification of PLN cysteines in insect cell microsomes. Previous research has shown that one cannot completely depend on SDS-PAGE to assess oligomeric stability and inhibitory potency of PLN (*87*) as there is a lack of quantitative correlation the two. Spectroscopic studies have shown that the Ca^{2+}-ATPase depolymerizes PLN consistent with the migration pattern change observed in Figure 3-6. WT-PLN which is usually 10-20% monomer in SDS (*88*) is 40% monomeric in the presence of Ca^{2+}-ATPase (*89*). However, there are PLN mutants in which a decrease in

pentameric stability as evidence by SDS-PAGE has negligible inhibitory activity on SERCA2a (*69*). In simple terms, although some PLN cysteine mutants may have greatly decreased pentameric stability (36C and 46C), that does not translate into greater inhibitory activity. Karim et. al. discovered that the cysteine residues within PLN are not required for pentamer formation however specific chemical properties of the thiol groups do play a significant role in pentamer stability (*24*). Therefore, any chemical modification of these thiol groups by HNO would be expected to have an effect on PLN pentamer stability.

CHAPTER V

SUPPORTING EXPERIMENTATION

HNO versus nitrite

At physiological pH, Angeli's Salt decomposes into an equimolar amount of HNO and nitrite. Studies of AS decomposition in the myocyte yielded 25% nitrite generation after 16 minutes and identical results with 0.1 to 1 mM AS (*53*). Because our microsome experiments utilize 0.1 – 1.0 mM AS, about 25 to 250μM NO_2^- is expected at the time of functional analysis. Since both products are present in the microsomal sample after Angeli's Salt treatment, we decided to design a set of control experiments. The goal was to determine whether the presence of nitrite had any effect on the microsomes, to help us know whether the AS effects on SERCA2a and PLN are due solely to the HNO. Previous Mahaney lab members performed Ca^{2+}-ATPase activity assays on SERCA2a + WT-PLN microsomes treated with a range of nitrite (up to 10mM) and found nitrite induced no effect on the V_{max} or $K_{0.5}$ values of SERCA2a (not shown (Jackson et. al, unpublished observations)). For further confirmation, nitrite treated SERCA2a + WT-PLN microsomal samples were subjected to SDS-PAGE and immunoblotting to examine the effect of nitrite on migration pattern on SERCA2a and PLN (Figure 5-1). At physiological treatment levels, there was no change in the migration pattern of SERCA2a or PLN compared to the non-treatment control. When all of the generated data is considered, it is clear that any effect on SERCA2a activation after treatment with Angeli's Salt is due to the presence of HNO and not nitrite. This data supports previous reports indicating the non effect of nitrite using Angeli's Salt as an HNO donor (*53*).

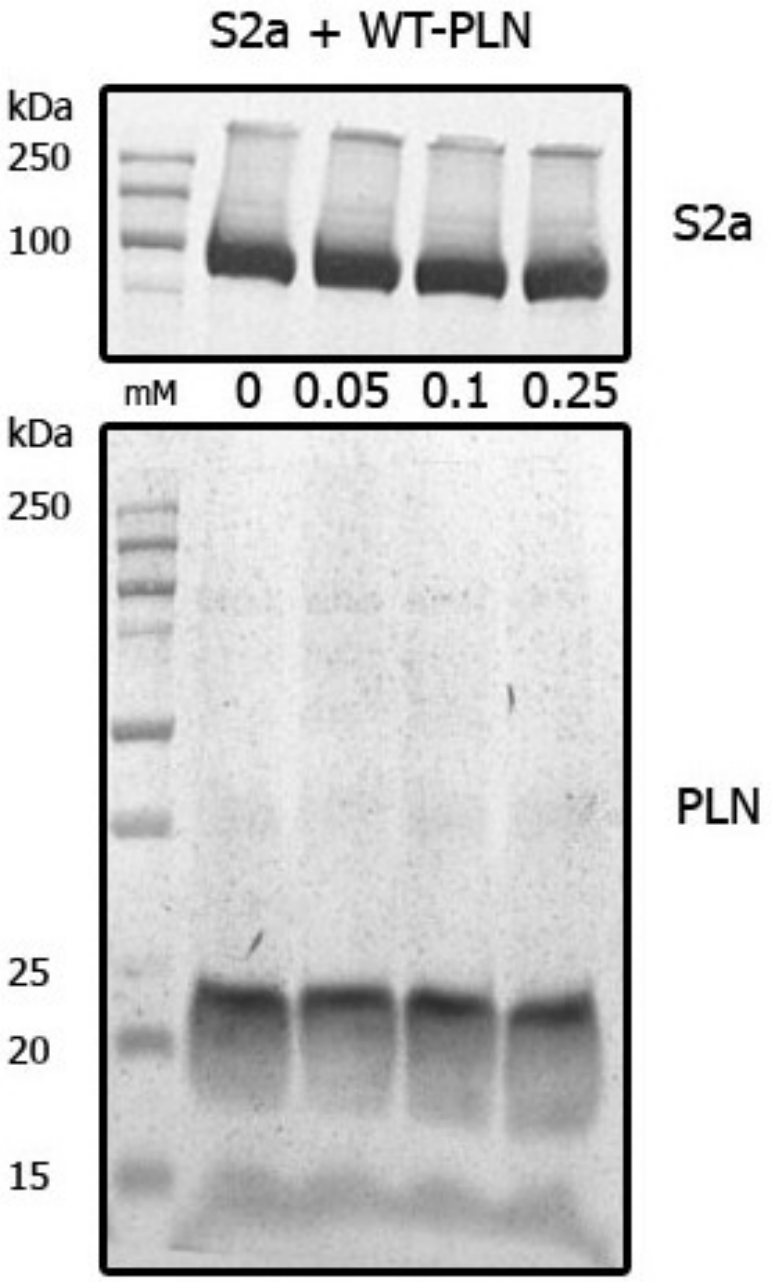

Figure 5-1. Immunoblot- Effect of nitrite on SERCA2a+WT-PLN microsomes. SERCA2a +PLN in insect cell microsomes were co expressed in High Five cells; microsomal fractions were isolated and subjected to treatment with nitrite at the indicated concentrations. Following treatment, 0.12 mg of the microsome samples were loaded on a 12% continuous polyacrylamide gel and subjected to SDS PAGE and immunoblotting. Top panel shows SERCA2a blot using 2A7-A1 antibody and the bottom panel shows the PLN blot using 2D12 antibody. The 1kb protein ladder (Bio-Rad) is shown in the most left lane.

Analysis of HNO effect on Wild-type S2a+PLN microsomes

Wild-type SERCA2a and PLN microsomes were created in order to assist in elucidating the role of the PLN cysteine mutants in their potential involvement in SERCA2a activation upon HNO treatment. Although studying the effect of HNO on wild-type S2a+PLN microsomes cannot conclusively confirm the role of cysteines in activation, the data will serve as a baseline value for cysteine mutant data comparison. Most of the ATPase activity data generated studying the effect of HNO on SERCA2a + WT-PLN was completed by Vidhya Sivakumaran, a previous graduate student. To summarize her work, she confirmed that SERCA2a activation by HNO is PLN dependent by showing a $K_{0.5}$ shift in the SERCA2a activity curve upon Angeli's Salt treatment similar to treating SERCA2a + PLN microsomes with anti-PLN antibody 2D12 (*90*). To follow up on her studies, SERCA2a + WT-PLN microsomes were subjected to SDS-PAGE and subsequent immunoblotting following glutathione pretreatment and Angeli's Salt treatment at various concentrations. This study was done to help determine a PLN sulfhydyl role in the mechanism of HNO action.

From previous knowledge, we know that HNO is highly thiophilic and targets thiol groups on selective proteins (*44*). In an effort to confirm that the effects seen on microsomal SERCA2a and/or PLN sulfhydryl groups are due to HNO, studies were performed in the presence of glutathione (GSH). We hypothesized that by enriching the reaction thiol content, the probability of competitively trapping HNO before it could target the critical thiol residues on PLN would be enhanced. In theory, if HNO treatment induces the formation of a disulfide bond or other chemical modification within PLN, then the presence of GSH before HNO treatment should prevent these HNO generated modifications.

SERCA2a + WT-PLN (2mg/ml) insect cell microsomes were pretreated with 10mM GSH and subsequently subjected to AS treatment at 0.1, 1.0, and 10mM. SDS-PAGE followed by immunoblot analysis was used to assess any changes in the migration pattern of SERCA2a and/or PLN due to the addition of AS with (+GSH) or without (-GSH) GSH pre-treatment (Figure 6- 2). In the non- pretreated samples, the results show a reciprocal correlation between the concentration of AS/HNO and the gradual disappearance of both monomeric SERCA2a (110 kDa) and PLN pentamers. As the concentration of AS increases, there is a decrease in SERCA2a and PLN pentamer levels, whereas the monomeric form of PLN is unaffected. At the two highest levels of AS used (1 and 10mM) we also observed some non-specific binding of both

SERCA2a and PLN. Pre-treatment with GSH preserves SERCA2a migration at all AS treatment levels with the slight exception of the very high 10mM treatment. The anti-PLN blot shows that GSH pre-treatment affects the pentamer/monomer ratio. At 0, 0.1, and 1.0 mM AS treatment, only the monomeric form of PLN is present. The 10mM AS treatment shows PLN migrating as both the pentamer and monomer. In addition, GSH treatment prevents the formation of the higher molecular weight non-specific binding of PLN at the top of the gel.

The results show that GSH pretreatment was able to reverse the AS-dependent change in SERCA2a and PLN migration. This confirms a role for PLN (and SERCA2a) cysteines in the mechanism of action of HNO. Furthermore, the results provide insight into the inhibitory effects of AS on SERCA2a activity even at levels as low as 0.1 mM AS, we observe a shift in SERCA2a migration away from the 110 kDa (monomer) form toward the highly aggregated form that does not enter the gel. Mahaney and Thomas (1991) reported a direct correlation between calcium pump aggregation and loss of enzyme activity. Here, in the presence of GSH, AS treatment (0-250 μM) has no inhibition effect on SERCA2a activity (Jackson et. al., unpublished observations), similar to the result shown in Figure 5-2, where AS had no effect on SERCA2a migration. Therefore, we conclude that PLN cysteines are modified during AS treatment, and that SERCA2a cysteine modifications by AS may be responsible for the observed inhibition of SERCA2a activity at higher levels of AS.

To confirm these conclusions, an additional experiment was completed in which WT-PLN microsomes were subjected to AS treatment followed by DTT before SDS-PAGE. With all three cysteines present, there is an increased chance that HNO can promote the formation of intra-molecular disulfide bonds or inter-molecular disulfide bonds within PLN. Because the migration pattern of PLN changes in the presence of SERCA (*89*), the results were not expected to match the co-expressed microsomal data in Figure 5-2 but provide an additional view of HNO modification on PLN. WT-PLN insect cell microsomes were pretreated with AS at 0.1, 1.0, and 10 mM for 20 minutes at room temperature. Before loading, the treated microsomes were mixed in a 1:1 ratio of gel loading buffer containing no DTT (-DTT) or 6 mg/ml DTT (+DTT). After immunological detection of PLN using the appropriate antibodies, it is clear that HNO induces the formation of disulfide bond crosslinks within PLN (Figure 5-3). Although faint, PLN dimer bands were visualized in all of the AS treatments starting at 0.1 mM AS. At 10 mM AS, two intermediate mobilites were seen on the blot. It would be premature to label these mobilites as

dimers, trimers, or tetramers as it is difficult to tell from the gel separation. Nevertheless, an argument can be made that these migration mobilites are the results of disulfide bond crosslinks as their appearance dissipates once DTT is added to the treated microsomes. The no treatment control lanes showed no higher MW forms, which further confirms the HNO induced results. This is consistent with Sivakumaran et. al. (unpublished results) that shows AS treatment of WT PLN induces the formation of trimer and tetramer forms of PLN within cardiomyocyte samples. Clearly additional microsome studies will help clarify this result.

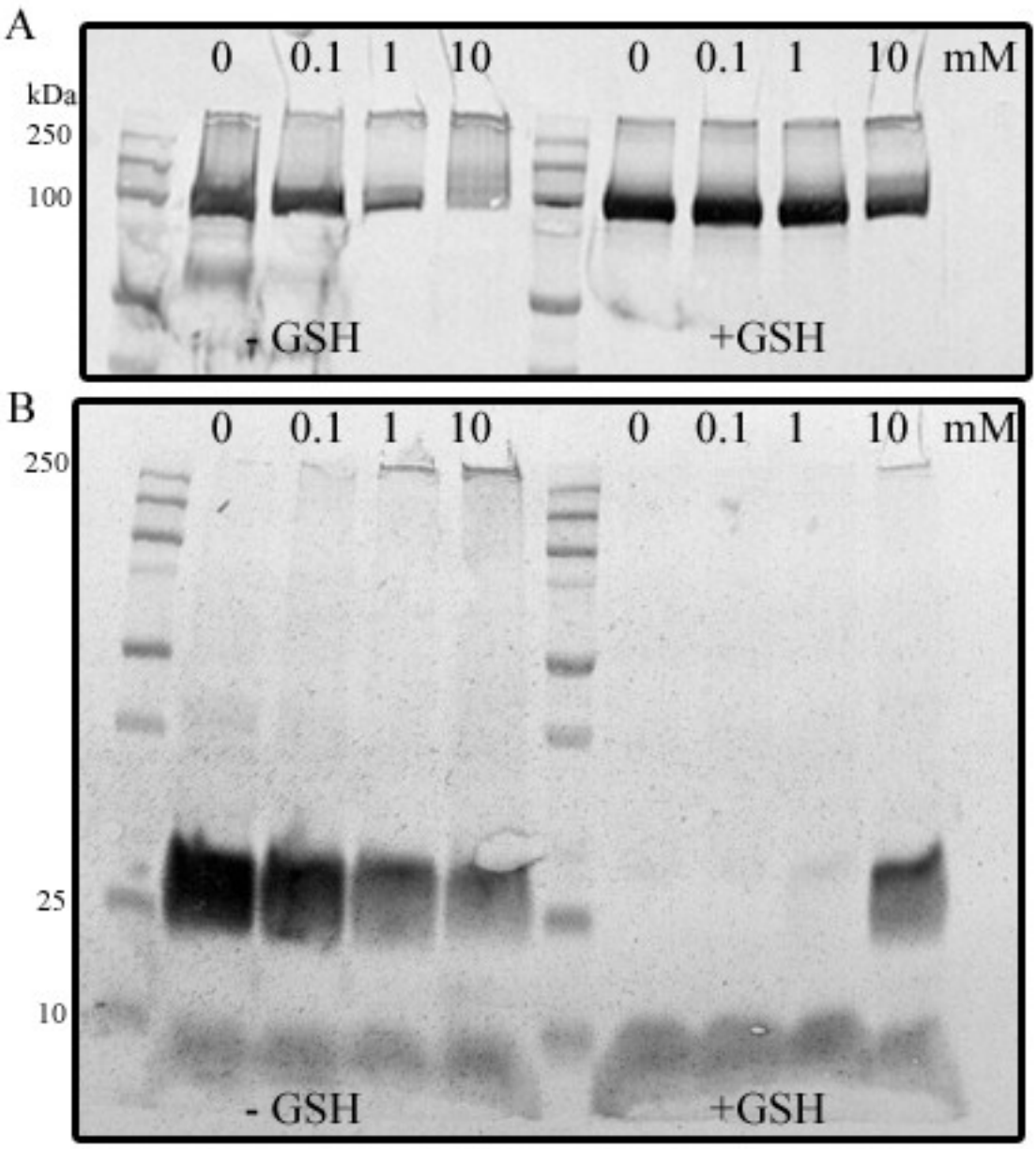

Figure 5-2. Immunoblot- Effect of glutathione on HNO treated SERCA2a + WT-PLN. SERCA2a +PLN insect cell microsomes were pre-treated with 10mM GSH and subsequently subjected to AS treatment at the indicated concentrations. As a control, a portion of the same microsomal prep was not pre-treated with GSH and only received the AS treatment. A total of 0.12 mg of protein was loaded on a 12% continuous polyacrylamide gel and subjected to SDS PAGE and immunoblotting. The bottom panel (B) shows the 2D12 (anti-PLN) blot while the upper panel (A) shows the 2A7-A1 (anti-SERCA2a) blot. The 1kb protein ladder (Bio-Rad) is shown in the most left lane.

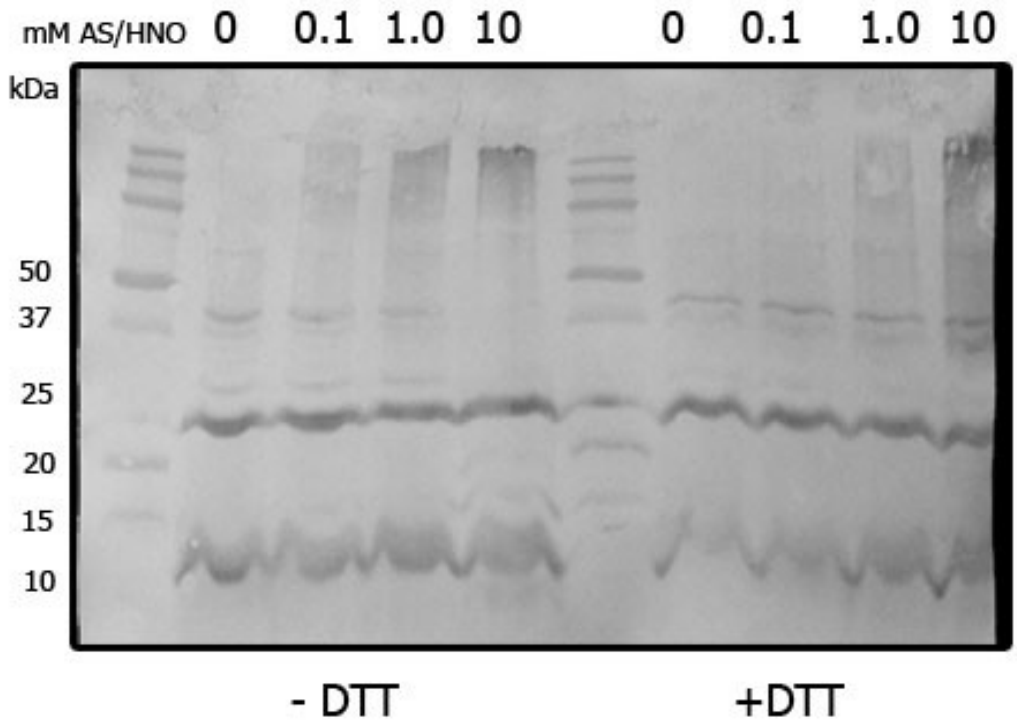

Figure 5-3. Immunoblot- WT-PLN ± AS/HNO. 2mg/ml of recombinant High Five cell WT-PLN microsomes were treated with AS for 20 minutes at RT with a final concentration of (0, 0.1, 1.0, 10 mM) as labeled on the lanes. 30 micrograms of each treated sample were loaded on a pre-cast10-20% gradient polyacrylamide gel (BIO-RAD), subjected to electrophoresis and transferred onto a nitrocellulose membrane. PLN was detected using the anti-PLN monoclonal antibody 2D12. The 1kb protein ladder (Bio-Rad) is shown in the most left lane.

Effect of HNO on null cysteine PLN microsomes

In 2007, Froehlich et. al established that the activation of SERCA2a by HNO was PLN dependent and that the thiols within PLN are critical to this process (*54*). It is for this reason; we decided to create a null cysteine PLN ($Ala^{36}Ala^{41}Ala^{46}$) sample to further test whether the PLN cysteine residues are the key to the proposed HNO functionality in the heart. Null cysteine PLN (Ala-PLN) has been previously characterized in other laboratories where the reported findings indicate that null cysteine PLN has complete SERCA2a regulatory capacity without altering SERCA2a kinetics (*91*) and exhibits a complete destabilization of the pentamer resulting in only a monomer migrational mobility (*24*). With the absence of PLN thiols, we suspect that HNO treatment will not elicit any effect on PLN stability or oligomerization.

As described in Chapter II, the null cysteine PLN microsomes were created using the baculovirus expression system after three point mutations were introduced in the pFASTBac™1-WT-PLN vector via site-directed mutagenesis. The null cysteine PLN microsomal sample was treated with various levels of Angeli's Salt for 10 minutes followed by SDS-PAGE and subsequent immunoblotting (Figure 5-4). Despite increasing levels of AS treatment, the Cys→Ala PLN microsomes only migrate as the monomeric form of PLN. There was no observed change between the control and the AS treated samples, further confirming the evidence that PLN cysteines are important for pentamer stability and thiols are important for HNO-mediated PLN effects. In order to further confirm the role of PLN cysteines in the activation of SERCA2a by HNO, the lab is working on creating a microsomal co-expression of SERCA2a + null cysteine PLN. A co-expressed microsomal sample will allow for AS treated activity assays.

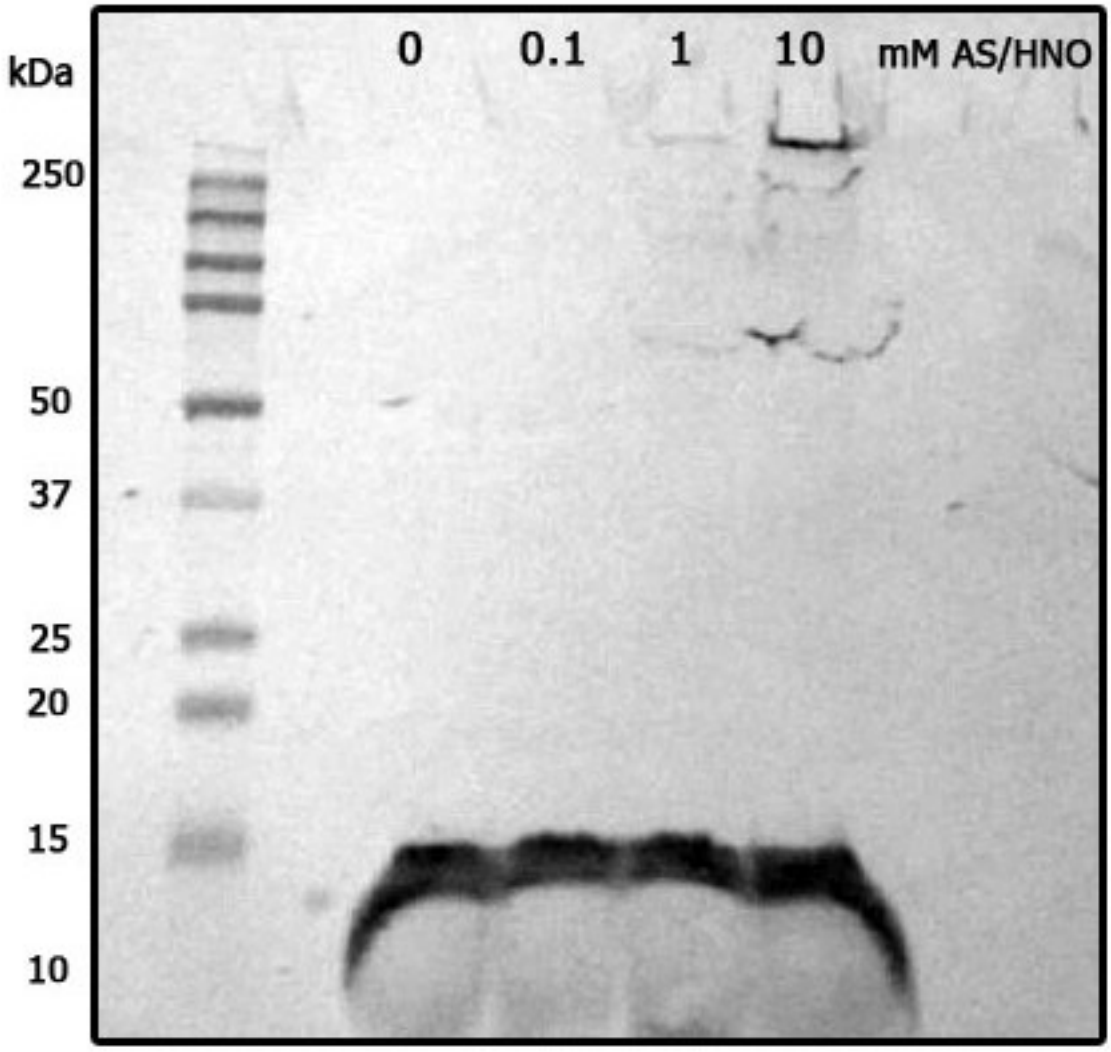

Figure 5-4. Immunoblot- Null cysteine PLN ± AS/HNO. 2mg/ml of recombinant High Five™ cell null cysteine PLN microsomes were treated with AS for 10 minutes at RT with a final concentration of (0, 0.1, 1.0, 10 mM) as labeled on the lanes. 30 micrograms of each treated sample were loaded on a 12% continuous polyacrylamide gel, subjected to electrophoresis and transferred onto a PVDF membrane. PLN was detected using the anti-PLN monoclonal antibody 2D12. The 1kb protein ladder (Bio-Rad) is shown in the most left lane.

Effect of HNO on SERCA2a + L37A PLN microsomes

Wild-type PLN exists in pentameric and monomeric forms, but the introduction of a mutation in a Leucine or Isoleucine amino acid residue on one face of the PLN transmembrane helix, such as Leu37 to Ala (L37A) or Ile40 to Ala (I40A), leads to a 94% monomer formation (*21*). These mutations have been shown to enhance the inhibitory function of PLN, by increasing greatly the monomeric fraction, supporting the theory that monomeric PLN is the inhibitory SERCA2a species (*92*). As a result, it was of interest to determine whether HNO effected the more potent inhibition of SERCA2a by superinhibitory monomeric form of PLN.

As previously described, SERCA2a ATPase activity displays a sigmoidal dependence on $[Ca^{2+}]$ which, using the Hill equation (methods), can provide the maximum activity of the sample at saturating Ca^{2+} (V_{max}) and the $[Ca^{2+}]$ required for half-maximal activity ($K_{0.5}$). Insect cell microsomes coexpressed with SERCA2a and L37A PLN were incubated in the absence (control, ■) or presence of either 2D12 (anti-PLN antibody,●), 0.1 mM AS (▲), or 1.0 mM AS (▼) (Figure 5-5). The top panel shows the activity data normalized to the maximum value while the bottom panel shows the raw activity data. The effects of HNO on the $K_{0.5}$ and V_{max} are summarized in the table within the bottom panel of Figure 5-1. As suspected, the ΔpK_{Ca} value for the S2a + L37A microsomes upon 2D12 treatment was 34% higher as compared to the S2a+ WT-PLN sample, supporting the previously reported data noting the superinhibitory effect of this particular mutation. Upon the addition of 0.1 mM or 1.0mM Angeli's Salt, there was a significant loss (~40%) of ATPase function in the co-expressed sample (bottom panel, ▼▲), compared to the control, untreated samples (bottom panel, ■). This data is consistent with the reported ATPase activity findings for all of our insect cell microsomes, including WT and mutant PLN. At saturating calcium, the V_{max} decreased by 47.8% and 33.2% for AS treatments of 0.1mM and 1.0 mM respectively. In contrast to the negative correlation trend seen in the PLN cysteine mutant microsomes, the higher level of AS treatment did not result in a lower V_{max}. To better show the effect of AS on SERCA2a $K_{0.5}$ values, as affected by PLN, the data were normalized to the maximum activity value. Upon normalization of the activity data, it is clear that only 1.0 mM AS causes the increase in calcium sensitivity in SERCA2a as evidence by the shift in the Calcium curve and a ΔpK_{Ca} similar to the 2D12 curve. A treatment with 0.1 mM AS which showed the most effect in certain SERCA2a plus cysteine mutant PLN microsomes did not have any apparent effect on the SERCA2a + L37A PLN. These results suggest a positive

correlation between the amount active PLN monomer and the concentration of AS needed to cause an effect. Since SERCA2a +L37A PLN microsomes contain mostly monomeric PLN, and only the higher concentration of AS increased the apparent calcium sensitivity of SERCA2a, the data suggest that the ability of PLN to form pentamers (or higher MW oligomers) is important for the HNO effect on SERCA2a activity.

In an effort to gain a full perspective on the effect of HNO on SERCA2a + L37A, we subjected the sample to Angeli's Salt and DTT treatments followed by the standard SDS-PAGE and immunoblot procedures (Chapter II). Insect cell microsomes coexpressed with SERCA2a and L37A PLN were incubated in the absence or presence of 6 mg/ml DTT preceded by and AS treatment of either 0.1 mM or 1.0 mM AS (Figure 5-6). Regardless of AS or DTT treatment, there was no change in the migration pattern of SERCA2a (~110 kDa). However, there were changes observed in the PLN migration pattern between the two AS treatments. As expected, the majority of PLN migrated as a monomer in the control (0 mM AS) microsomes. In the absence of DTT, SERCA2a + L37A PLN treated with 0.1mM AS showed a near identical PLN migration pattern as the control. Yet, when SERCA2a + L37A PLN microsomes were treated with 1.0 mM AS, PLN aggregates were detected at the top of the gel (not shown), and the pentamer mobility disappeared leaving only the monomer. With the addition of DTT, the appearance of the pentamer at 0.1 mM AS was diminished while there was a restoration of the pentamer and an increase in the monomer band at 1.0 mM AS. At first glance, we can presume that the addition of 1.0 mM AS induced PLN association via disulfide bond links because of the decreased monomer, absent pentamer and large aggregate binding reversed by DTT. These results support the activity data in Figure 5-5. We did not see much of a loss of monomeric L37A at 0.1 mM, so there is not much of an effect of AS on the enzyme activity. At 1.0 mM AS, there is less apparent inhibitory PLN, therefore there is less L37A PLN to interact with SERCA2a resulting in a shift in the $K_{0.5}$ as seen in Figure 5-5. Since the level of PLN expression was not quantitated, the correlation between the activity data and the immunoblot cannot be absolutely definitive, but the consistency builds a solid case for the effect of HNO on this sample.

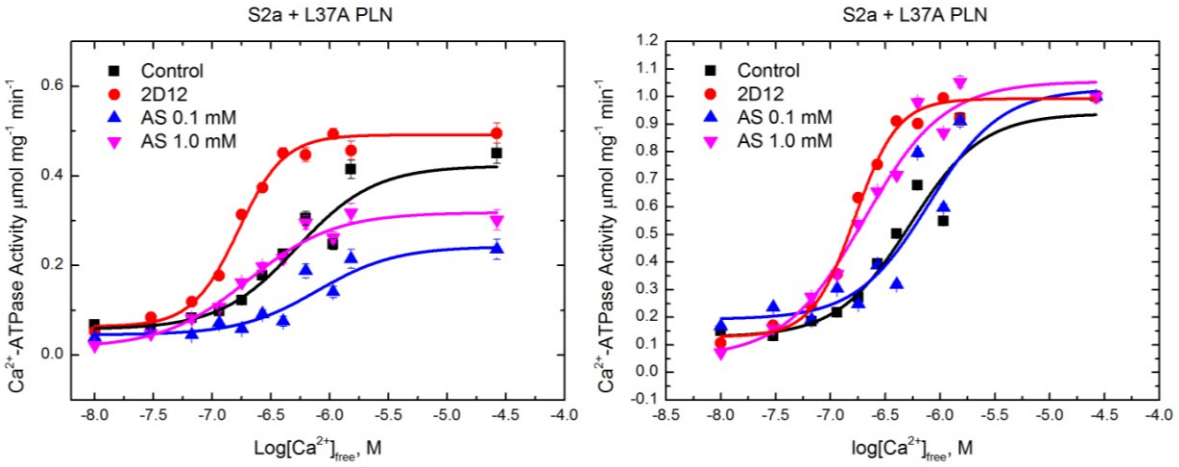

	V_{max} control	V_{max} + 0.1 mM AS	V_{max} + 1.0 mM AS	$K_{0.5}$ control	$K_{0.5}$ + 0.1 mM AS	$K_{0.5}$ + 1.0 mM AS	$K_{0.5}$ + 2D12
Sample Type	µmol mg SERCA2a^{-1} min^{-1}			(µM)			
SERCA2a + WT-PLN	0.68±0.05	0.37±0.03	N/A	0.48±0.50	0.18±0.30	N/A	0.28±0.04
SERCA2a + L37A PLN	0.45±0.02	0.24±0.02	0.30±0.02	0.53±0.07	0.57±0.05	0.20±0.03	0.16±0.05

Figure 5-5/ Table 5-1. SERCA2a+L37A PLN ATPase Activity as affected by AS/HNO. SERCA2a was co-expressed with L37A PLN in High Five insect cell microsomes. Samples were preincubated in the absence (control, ■) or the presence of either 2D12 (2D12, ●), 0.1mM AS/HNO (AS/HNO, ▲) , or 1.0mM AS/HNO (▼) for 15 minutes at room temperature. The left panel shows raw SERCA2a ATPase specific activity expressed in terms of mg of SERCA2a, according to the amount of total protein in the High Five cells for each sample. The top right panel shows the specific activities normalized to the V_{max} calculated from fitting the raw data to the Hill equation. The addition of AS/HNO at either level decreases the V_{max} similar to S2a+WT-PLN. Decreasing the [AS] results in a loss of the apparent shift in the $[Ca^{2+}]$ dependence of SERCA2a activity. All WT-PLN data listed in the table was collected by a previous graduate student, Vidhya Sivakumaran.

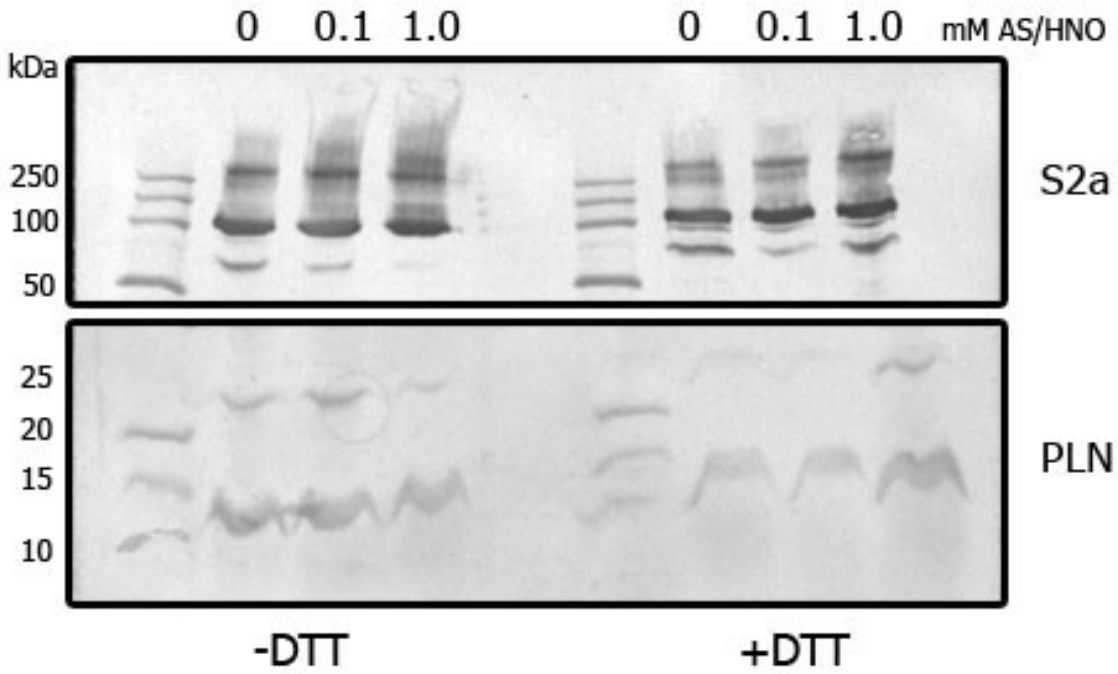

Figure 5-6. Immunoblot- SERCA2a + L37A PLN. 2mg/ml of recombinant High Five cell SERCA2a + L37A PLN microsomes were treated with AS for 20 minutes at RT with a final concentration of (0, 0.1, 1.0 mM) as labeled on the lanes. 30 micrograms of each treated sample were loaded on a pre-cast10-20% gradient polyacrylamide gel (BIO-RAD), subjected to electrophoresis and transferred onto a nitrocellulose membrane. PLN was detected using the anti-PLN monoclonal antibody 2D12. The 1kb protein ladder (Bio-Rad) is shown in the most left lane.

Effect of HNO on SERCA1

The Ca^{2+}-ATPase of skeletal muscle sarcoplasmic reticulum is denoted as the first isoform of the three isoforms found in the body. Much like the cardiac isoform, SERCA2a, SERCA1 is also an integral membrane protein that is responsible for actively transporting Ca^{2+} ions from the cytoplasm to the lumen of the sarcoplasmic reticulum to promote muscle relaxation. Most other details about these two forms of SERCA are very similar with a 96% homology at the amino acid level. However, unlike SERCA2a, PLN does not actively regulate the function of SERCA1 as the protein is not expressed in skeletal muscle. To gain a further understanding of the mechanism by which HNO activates SERCA2a, we decided to employ studies using crude skeletal SR preps naturally devoid of phospholamban.

SERCA1 activity was assessed using crude skeletal SR preparations as described in Chapter II. In congruence with the other activity data obtained using insect cell microsomes, there is an AS- dose-dependent inhibition of V_{max} observed upon AS treatment (Figure 5-7 A). The V_{max} values ranged from 1.6 μmol mg^{-1} min^{-1}(control) to 0.15 μmol mg^{-1} min^{-1} resulting in a 90% drop in V_{max} upon 10mM AS treatment. Treatment with 1.0 mM AS showed a 45% decrease in V_{max}, followed closely by 0.01 at 36% and finally 0.1 mM AS at 21% decrease. Although there was a V_{max} effect, there was not a change in the apparent calcium sensitivity of SERCA1 with all curves having a relative $K_{0.5}$ of ~0.6 μM. In addition, gel mobilities of SERCA1 were assessed in a Tris-Glycine SDS-PAGE system (Figure 5-7 B). Irrespective of AS treatment, each sample showed a major band at the expected SERCA molecular weight (~110kDa).

These control studies provide important support for our SERCA2a microsomal data. The results from all of the control studies build a strong case for the necessity of PLN in HNO-mediated SERCA2a activation. Like SERCA2a, SERCA1 has a number of reactive cysteine residues that, when modified, result in significant enzyme inhibition. A future goal of the lab for this project is to better understand which SERCA cysteine(s) are modified by AS, in hopes of finding ways to minimize HNO inhibition of SERCA. This would greatly increase the utility of HNO as a drug to stimulate Ca^{2+} cycling in cardiomyocytes.

A

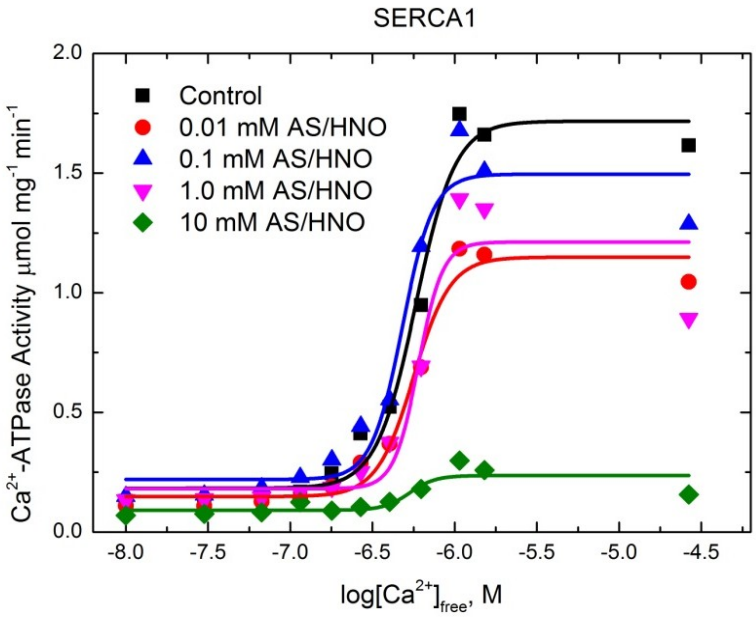

B

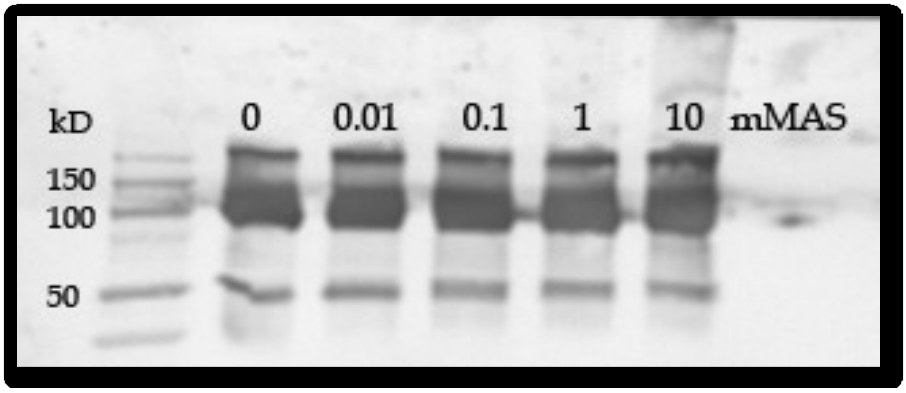

Figure 5-7. Effect of AS/HNO on SERCA1 ATPase Activity and migration pattern. (A) SERCA1 activity was assessed using crude skeletal SR preparations as described in Chapter III. The samples were treated with various levels of AS for 10 minutes at RT. The data are plotted as specific ATPase activity (µmol mg^{-1} min^{-1}) versus the log of free calcium (M). AS/HNO inhibits SERCA1 in a concentration – dependent manner but treatment does not affect Ca^{2+} sensitivity. Decreasing the [AS] relieves SERCA1 V_{max} inhibition but does not change the apparent shift in the $[Ca^{2+}]$ dependence of SERCA1. (B) Immunoblot of SERCA1 prep treated with various levels of AS/HNO. There is no effect on the migration pattern of SERCA1 upon treatment with AS/HNO. SERCA1 was detected using anti-SERCA antibody.

Chapter VI

SUMMARY AND FUTURE DIRECTIONS

The interaction between cardiac sacroplasmic Ca^{2+}-ATPase (SERCA2a) and phospholamban (PLN) is a key regulating factor in modulating the cardiac excitation-contraction coupling mechanism. In heart failure models, deviations in the inhibition of SERCA2a by PLN have been associated with anomalies in cardiac function. More recently, it has been proposed that modulation of the interaction between SERCA2a and PLN can be used as a potential pharmacological approach for heart failure. The aim of this research was to further study the therapeutic potential of the HNO donor Angeli's Salt by elucidating the mechanism by which it is able to modulate the SERCA2a: PLN interaction. HNO has been shown previously to uncouple PLN from SERCA2a, resulting in a stimulation of SERCA2a activity (*6, 54, 90*). These studies provided evidence that PLN cysteine residues were the key to HNO activation of SERCA2a. However, it was not known which of these PLN cysteines were responsible for this effect. Therefore, the goal of this study was to determine the role of each PLN cysteine in the mechanism of SERCA2a stimulation by HNO.

Our hypothesis stated that HNO uncouples PLN from the Ca^{2+}-ATPase via PLN disulfide bond formation making PLN unable to regulate the Ca^{2+}-ATPase, thus stimulating activity. For this purpose, we used the baculovirus expression system to express microsomes containing SERCA2a coexpressed with six different PLN cysteine mutant variants. In a null cysteine (Cys→Ala) PLN background, we replaced each alanine residue with a cysteine in all of the three cysteine transmembrane positions [36C, 41C, 46C, 36/41C, 36/46C, 41/46C]. The functional activities of SERCA2a in these microsomes was tested by an enzyme assay while the detection of physical changes were assessed using both the activity assay and an immunoblot technique.

In summary, we have supported previously reported literature by showing that HNO activation of SERCA2a is PLN dependent and that PLN cysteines are instrumental in this process. At various concentrations of Angeli's Salt (HNO donor) there were no changes observed in the PLN migration pattern of null cysteine PLN (Figure 5-4) or SERCA1 calcium sensitivity using native skeletal SR vesicles (SERCA1) (Figure 5-7). Our results using SERCA1 (no PLN) suggest HNO acts as an irreversible inhibitor of SERCA2a, decreasing V_{max} by decreasing the concentration of active enzyme units. The enzymes not inhibited by HNO have

the same Ca^{2+} sensitivity as control enzymes, as evidence by the lack of ΔpK_{Ca} upon the addition of HNO. This theory was also supported by our SERCA2a +L37A PLN results (Figure 5-5 and Figure 5-6) that showed a positive correlation between the amount active PLN monomer and the concentration of AS needed to cause an effect. Thus, the data suggest that the ability of PLN to form pentamers (or higher MW oligomers) is important for the HNO effect on SERCA2a activity. That is, PLN molecules must be in close proximity (or in contact) to facilitate the formation of disulfide bonded PLNs.

We have also been able to successfully determine which PLN cysteines are important in the mechanism of HNO activation of SERCA2a. Using the techniques described in Chapter II, we have concluded that the PLN cysteines at positions 41 and 46 are key residues in the mechanism of HNO activation of SERCA2a by PLN. At certain levels of AS treatment, SERCA2a + 41C and SERCA2a + 46C PLN microsomes displayed a sigmoidal activity curve that had a ΔpK_{Ca} similar to that of WT-PLN and 2D12 treated microsomes (Figure 4-1). In addition, the formation of HNO- induced covalent disulfide bonds was confirmed in 41C PLN, 46C PLN and WT-PLN. At 10 μM AS, the pentamer of 41C and 46C PLN microsomes were protected from dissociation after boiling but not in the presence of DTT (Figure 4-6). Furthermore, HNO-induced intermediate PLN migration mobilites (dimers-tetramers) were observed at 0.1-10 mM AS treatment. These species were not observed in the control or DTT treated samples confirming the disulfide bond.

Although these results clearly suggest HNO modification of PLN activity via disulfide bond formation, we are also aware that HNO could chemically modify PLN in a way that was undetectable using the techniques at our disposal. In addition to disulfide bond formation between two thiol groups, HNO could interact with a free thiol group to only form the intermediate hydroxysulfinamide. The presence of a hydroxysulfinamide would sterically perturb the interaction of PLN and SERCA2a independent of disulfide formation. If HNO interacts with PLN in this path, we would theoretically still observe SERA2a activation in co-expressed microsomes but observe no change in the migration pattern of PLN upon HNO treatment. However, if DTT reverses the HNO effect on SERCA2a activity, this would argue in favor of a disulfide bond and against sulfinamide formation, since DTT can't convert the sulfinamide back to a free sulfhydryl. Our data suggests that the mechanism in which HNO interacts with PLN is via disulfide bond formation. Without a purified PLN sample and the

double cysteine PLN mutants, we are not able to discern if these disulfide bonds are formed intra- or inter-molecularly. The current efforts to develop the SERCA2a + double cysteine PLN mutants and purify PLN for a reconstituted system will assist in clarification of the exact mechanism by which HNO modifies these residues.

Our studies were carried out using insect cell microsomes, which is a complex and heterogeneous environment. In order to understand how each PLN cysteine is modified (or not) and how this modification affects PLN function, one would need to study PLN in a purified system. However, that would take you further away from the native membrane system, with the possibility that the results would not completely translate to HNO action *in vivo*. Nevertheless, this is a basic biology attempt to help us fully understand how HNO truly interacts with proteins in the heart to create the HNO effects. Although we were not able to recreate the positive inotropic results that have been previously published in studies using whole hearts and/or isolated myocytes, the results of my research show that PLN cysteines are important in the mechanism of HNO induced activation of SERCA2a. Looking ahead, we will continue to investigate the role of HNO on PLN cysteines using various methods to quantify cysteine modification and assess the activity of SERCA2a via additional enzyme assays. In order to attribute observed changes to the effect of HNO and not Angeli's Salt, we also plan to use other HNO donors (*93*). Our first priority is the creation of the double cysteine PLN mutant microsomes and purification of PLN cysteine mutants for reconstitution in synthetic membrane systems (methodology in Chapter II). We will also use these new samples to study the effect of PLN cysteine mutants on SERCA2a protein-protein interaction and conformation changes, as affected by HNO. These details are outlined in the future work section below.

Future Work

Quantitation of PLN cysteine modifications

If HNO interacts with any PLN cysteines via our proposed mechanism to form disulfide bonds or hydroxysulfinamides, there would be a change in the amount of free/unreactive thiols. The Ellman's reagent or DTNB (5,5'-dithiobis-(2-nitrobenzoic acid)) is the most widely used chemical in biochemical research to quantify the number of thiol groups in proteins. Free thiols react with the compound by cleaving the disulfide bond to give 2-nitro-5-thiobenzoate (NTB^-),

which ionizes to NTB^{2-} dianion in water. The dianion has a yellow color that can be quantified in a spectrophotometer at 412nm using an extinction coefficient of 14.2 x 10^4 $M^{-1}cm^{-1}$. This reaction is rapid and stoichiometric, with the addition of one mole of thiol releasing one mole of NTB (*94*). This assay will be the most effective in quantifying free PLN thiols once the protein is purified. It would be difficult to accurately attribute HNO induced changes in thiol concentrations to only PLN using the microsomes generated by the baculovirus expression system because of the large amount of thiol containing proteins in these preparations. Therefore, we plan to use this assay with purified PLN (mutant and WT) reconstituted in model bilayers using the protocol developed by Karim et al. (*25*). Any sulfhydrl modified by HNO treatment (disulfide bond or sulfinamide) will not react with DTNB. By measuring the DTNB labeling of WT-PLN versus the cysteine mutants, we will be able to determine the site(s) of HNO reactivity. In order to determine an accurate account of which cysteine residues are modified by HNO, we will need to employ mass spectrometry techniques such as matrix-assisted laser desorption/ionization time-of-flight mass spectrometer (MALDI-TOF) or N-terminal sequencing.

Supplementary ATPase activity measurements

The malachite-green ammonium molybdate activity assay is a proven and reliable technique used by many standard biochemistry labs to measure the amount of free inorganic phosphate produced by an ATP hydrolyzing enzyme. However, since each assay can only measure one sample and treatment condition at a time, there is more room for experimental variations due to temperature fluctuations and other human error. Therefore, in addition to the established activity assay, we plan to employ a higher throughput measurement of Ca^{2+}-ATPase activity by an enzyme-linked NADH assay performed in a microtiter plate (200 µl total volume per well). We have obtained an established protocol from Razvan Cornea (University of Minnesota) who has successfully used this assay to measure Ca^{2+}-ATPase in reconstituted membranes (*75*). In summary, each well will contain 0.2-0.6 µg of Ca^{2+}-ATPase along with a buffer containing 50 mM inidazole, pH 7.0, 0.1 M KCl, 5 mM $MgCl_2$, 0.5 mM EGTA, 0.5 mM phosphoenolpyruvate, 2.5 mM ATP, 0.2 mM NADH, 2 IU of pyruvate kinase, 2 IU of lactate dehydrogenase, and 1-2 µg of calcium ionophore (A23187). The calcium ionophore is added such that no transported calcium is retained in the vesicles allowing the ATPase to operate freely and uninhibited by the finite calcium capacity. Each assay is done in triplicate at 12 different

free calcium concentrations. The decay of NADH absorbance is monitored at 340 nm on a SPECTRAmax microplate spectrophorometer to determine the rate of ATP hydrolysis. This assay has the advantage of being faster and more efficient allowing for multiple activity curves including the control and experimental to be run on one plate.

Reconstitution of PLN in synthetic membranes

The use of synthetic membranes to study the interaction between SERCA and PLN has been demonstrated by many labs (for example see refs. (*24, 64, 75, 91*)). To start the process of reconstitution, purified samples of our PLN cysteine mutants is required (see Chapter II for methodology). Once the purified PLN samples are obtained, reconstitution of PLN with SERCA into lipid membranes will be done using established protocols (*76*). Before reconstitution, the SDS in the purified PLN samples has to be exchanged for $C_{12}E_9$ using DEAE-cellulose chromatography. This is accomplished by adding ~2 mg of purified PLN in 10 ml buffer (20 mM MOPS, pH 7.0, 5% $C_{12}E_{9,}$) onto a DEAE-cellulose column (0.5 bed volume). PLN is eluted with 20 mM MOPS, pH 7.0, 5% $C_{12}E_9$, and 0.2 M NaCl. To reconstitute, 1 mg of extracted SR lipids are mixed with 30 µg of purified PLN in $C_{12}E_{9,}$ followed by the addition of 30 µl of 10% 1-*O*-octyl-β-D-glucopyranoside. Affinity-purified Ca^{2+}-ATPase (100µg) in $C_{12}E_9$ is mixed with detergent –lipid micelles at a Ca^{2+}-ATPase to PLN molar ratio of 1:5. The detergent is removed by the sequential addition of 3 portions of 80 µg Biobeads SM2 with stirring in 3 hours. The final reconstituted vesicles are concentrated by centrifugation at 100,000 x g for 30 minutes after removal of the Biobeads.

As discussed briefly in chapter III, the use of insect cell microsomes can be limiting in that the system can limit the types of experiments and thus questions that can be answered. It would be beneficial to have a reconstituted system in which Ca^{2+}-ATPase measurements can be made on membranes having identical concentrations of Ca^{2+} pump in the absence or presence of PLN like Reddy et. al (*75, 76*). This is difficult to achieve in cardiac SR samples where the (-) PLN control is usually estimated by phosphorylating PLN or by treatment with 2D12 which has been shown to only partially reverse the effect. In addition, the use of microsomes does not allow for fine control of SERCA2a and/or PLN expression level. Being able to change the level of either protein could be beneficial in modeling difference disease states in which the levels of SERCA2a and PLN are varied. The reconstitution system would allow for well-defined protein

levels and accurate measurements. The use of synthetic membranes is a catch 22 because it allows for a closer investigation of PLN and SERCA2a but this technique is even further away from the native cardiac environment. I believe that both are needed to fully understand the complexity of the effects on SERCA2a and its regulation by PLN.

SERCA2a protein-protein interaction and confirmational changes

We originally proposed to investigate if HNO-treated PLN cysteine mutants inhibit SERCA2a conformational changes and protein-protein interactions compared using fluorescence spectroscopy and electron paramagnetic resonance spectroscopy. These experiments have been moved to future studies due to limited quantity of microsomal protein created versus the amount of microsomal protein required per assay. With the revitalization of the baculovirus system planned, the lab should now be able to successfully create enough microsomes to perform the experiments.

Fluorescence spectroscopy using IAEDANS

In 2007, Waggoner et. al. showed that wild-type PLN inhibits the SERCA2a E2 to E1 conformational transition as it preferentially binds to the E2-like state of SERCA2a using fluorescent spectroscopy (*29*). We proposed to repeat these studies using our PLN cysteine mutants ± HNO treatment. The fluorescent probe that we plan to use is 5-(2-((iodoacetyl)amino)ethyl) aminonaphthalene-1-sulfonic acid (IAEDANS). The fluorescent intensity of IAEDANS bound to SERCA2a will change based on the SERCA2a conformational state due to the differences in exposure of the probe to the aqueous environment. Therefore, this probe can be used to measure the SERCA2a E2 to E1(Ca_2) transition as affected by the mutant cysteine PLN ± HNO treatment.

The Mahaney lab has previously established an IAEDANS labeling protocol for expressed microsomal proteins (*29*). Out of all microsomal proteins, this method labels only SERCA2a in a stoichiometric ratio of one probe per enzyme. The IAEDANS probe covalently binds to Cys^{674} which is located in the phosphorylation domain of SERCA2a. Once labeled, the enzyme is suspended in a buffer (100 mM KCl, 3 mM $MgCl_2$, 50 mM MOPS, pH 7.0, 25^oC) containing no Ca^{2+} and 1 mM EGTA. The initial fluorescence intensity (F_o) of the E_2 state is then measured at the λ_{max} of the probe, 465nm. Afterwards, 1mM $CaCl_2$ is added to the sample,

which results in a jump in ionized [Ca^{2+}] to a saturated level and shifts the SERCA2a to the E1(Ca_2) state and the new fluorescent intensity is recorded (F_i). The difference in fluorescent intensity between E2 and E1 states ($\Delta F/F_o$; $|F_o-F_i|$ normalized to the initial fluorescence intensity, (F_o) is expressed as a percent change to facilitate direct comparison between sample types. As a control, each co-expressed PLN cysteine mutant will be measured without HNO treatment. There is no evidence that HNO will chemically interact with the IAEDANS probe, nor is it likely that HNO will react with the sulfhydyl to which the IAEDANS probe is bound (*45*). If it is determined that HNO does affect the probe, we can utilize fluorescein isothiocyanate (FITC) as the fluorescent probe instead of IADEANS. Since FITC binds to SERCA2a at Lys^{514} there should not be any interference with HNO treatment.

Electron paramagnetic resonance spectroscopy (EPR)

Using saturation transfer EPR (ST-EPR) the Mahaney lab has shown that PLN inhibits SERCA2a by disrupting the protein-protein interactions within an enzyme oligomer, important for optimal activity (*9*). In this technique, a malemide spin probe will be attached to the SERCA2a such that the motion of the probe reflects the global rotation of the SERCA2a. We will be able to test if the PLN cysteine mutants affect SERCA2a rotational mobility upon HNO treatment. If HNO uncouples PLN from the SERCA2a we would expect to see increased amplitude for the E2-E1 conformational change and SERCA2a rotational mobility, similar to that of the SERCA2a in the absence of PLN. By testing individual cysteine mutants, we will determine which PLN sulfhydryls are central to the HNO mechanism. In combination with the activity studies, this data should confirm or refute our hypothesis on the physical mechanism of HNO stimulation of SERCA2a.

The Mahaney lab has already established a labeling protocol for the SERCA2a in expressed microsomes. This method labels only SERCA2a in a stoichiometric ratio of 1.2 moles MSL per mole of enzyme. EPR studies will be conducted at 25^oC, to match the conditions of the activity and fluorescent assays allowing for direct correlation. PLN inhibition of the SERCA2a is more pronounced at lower ionized Ca^{2+} (EGTA) levels therefore our experiments will focus on this range of free calcium. Each co-expressed PLN cysteine mutant sample will be studied with and without HNO treatment. The Angeli's Salt concentration used to treat the samples will be the same levels used in the activity assays to correlate these sets of data.

Is HNO the solution to heart failure?

In complex disease states such as cardiovascular disease, many complex pathways are involved and altered. Despite continuing therapeutic progress, there is still an unmet need to develop effective treatments aimed at decreasing the morbidity and mortality of heart failure. Although HNO has shown great potential as a pharmacological agent for heart failure it would be premature to think that an HNO centered therapy could improve all cardiovascular diseases. So far, HNO (as donated by Angeli's Salt) has shown to improve calcium cycling by interaction with a number of key proteins involved in controlling excitation/contraction coupling. These include the ryanodine receptor, which promotes Ca^{2+} release from the SR to stimulate cardiac muscle contraction, Troponin C, which responds to the increase cell Ca^{2+} levels and promotes myosin binding to actin for force generation, and PLN, which regulates Ca^{2+} transport into the SR and therefore muscle relaxation via SERCA2a. Thus, patients who suffer from cardiovascular diseases that involve impairment of left ventricular function and/or dysregulation of SERCA2a and PLN would theoretically benefit the most. The reported enhancements in cardiac function due to HNO have all been independent of the β- adrenergic system activation which has been implicated as the cause for the high mortality rates. Thus, there is no argument that the use of HNO to enhance the lives of patients suffering from certain cardiac failure would not be promising. But, because of the lack of knowledge in regards to the mechanism of action surrounding HNO, other types of therapy have emerged that target key calcium handling proteins and taken the forefront in becoming the next heart failure therapy.

A promising therapeutic strategy that has gained momentum in the last few years is the use gene therapy. For a complete review of the current heart failure gene therapy initiatives, go to references (*95-97*). To summarize, the advances in the understanding of the molecular basis of myocardial dysfunction have made the use of gene therapy a reality for combating congestive heart failure. The goal of gene therapy is to restore the function of cardiomyocytic signaling pathways that are consistently shown to be defective in heart failure such as β-adrenergic signaling and calcium cycling (*98*). The majority of gene therapy initiatives have been designed to improve cardiac function using SERCA2a as a target because of its importance in calcium cycling. To date, adenovirus-mediated gene transfer of SERCA2a to failing human cardiomyocytes have showed restored calcium transient and improved contraction and relaxation velocity to the level of non-failing myocytes (*99*). There has also been a recent successful

completion of a phase II clinical trial of intracoronary gene therapy of sarcoplasmic reticulum Ca^{2+}-ATPase in patients with advanced heart disease (*100*). These studies propel the case for gene therapy initiatives as a safe and effective method for heart failure treatment.

The use of small molecules to target PLN has also become a recent therapeutic approach to target the Ca^{2+} handling pathway in the failing heart. This year (2012), Tilgmann et. al. first reported the design of novel inhibitors of PLN (*101*). In addition to PLN inhibitors, the small molecule, Istraroxime, was discovered in 2006 and has shown to be a novel inotropic agent that enhances SERCA2a activity in heart failure models (*102*). Together, these findings open another perspective for the pharmacotherapy of heart failure.

I believe that these therapeutic areas of gene therapy and novel inhibitors are expanding rapidly and will undoubtedly lead to other targets for gene therapy approaches. The completion of successful phase I and II clinical trials and successful inhibition of key proteins suggests that these forms of therapy will be available much sooner than a HNO approach. This does not discount the work done to understand the pharmacological significance of HNO within the cardiomyocyte as we have gained considerable knowledge about excitation/contraction coupling and NO biology through these studies. As I alluded to earlier, there cannot be a one size fits all approach to cardiovascular treatments as there will always be limitations. For example, a limitation to using a gene therapy approach is that only one molecule can be targeted at a time; however, a limitation to using the HNO donor Angeli's Salt is that any sulfhydyl containing protein can be modified. Further studies are needed in both areas of research to fully evaluate them as effective therapeutic approaches to combat heart failure.

Conclusion

In experimental heart failure models, modulation of the interaction between SERCA2a and PLN has shown to be a potential therapeutic approach. Nitroxyl (HNO) has been shown to disrupt normal SERCA2a:PLN regulation in a positive way that increases SERCA2a activity in normal and failing hearts. It was our goal to elucidate the mechanism by which HNO causes this effect in cardiomyocytes. Through our studies, we conclude that PLN cysteines are critical in the mechanism of HNO-mediated activation of SERCA2a. These results are consistent with previous studies that show HNO activation of SERCA2a is PLN and thiol dependent (*54*). The results further establish the identity of PLN cysteine residues 41 and 46 as the sites that are

modified in the mechanism of HNO. These cysteines are probably involved in intramolecular disulfide bonds or hydroxysulfinamide formation. Further experimentation is needed to clarify which modification occurs. The techniques presented in this study are sensitive to the concentration of Angeli's Salt used to elicit a response as shown by the differences in our results and that of the original work stating HNO induced SERCA2a activation. Nevertheless, this study establishes the feasibility for application of these techniques to the analysis of other proteins within the SR that regulate excitation-contraction coupling. Furthermore, this study demonstrates the importance of experimental evidence in understanding the use of HNO as a potential pharmacological agent in combating congestive heart failure.

References

1. Bers, D. M. (2002) Cardiac excitation-contraction coupling, *Nature 415*, 198-205.
2. Walsh, R. A., (Ed.) (2005) *Molecular Mechanisms of Cardiac Hypertrophy and Failure*, Taylor & Francis, London.
3. Vafiadaki, E., Papalouka, V., Arvanitis, D. A., Kranias, E. G., and Sanoudou, D. (2009) The role of SERCA2a/PLN complex, Ca^{2+} homeostasis, and anti-apoptotic proteins in detrmining cell fate, *European Journal of Physiology 457*, 687-700.
4. Rossi, D., Barone, V., Giacomello, E., Cusimano, V., and Sorrentino, V. (2008) The Sarcoplasmic Reticulum: An Organized Patchwork of Specialized Domains, *Traffic 9*, 1044-1049.
5. Toyoshima, C., and Inesi, G. (2004) Structural basis of ion pumping by Ca2+-ATPase of the sarcoplasmic reticulum, *Annu. Rev. Biochem. 73*, 269-292.
6. Paolocci, N., Katori, T., Champion, H., St. John, M., Miranda, K., Fukuto, J. M., Wink, D. A., and Kass, D. A. (2003) Positive inotropic and lusitropic effects of HNO/NO- in failing hearts: independence from beta-adrenergic signaling, *Proc. Natl. Acad. Sci. 100*, 5537-5542.
7. Periasamy, M., Bhupathy, P., and Babu, G. J. (2008) Regulation of sarcoplasmic reticulum Ca2+ ATPase pump expression and its relevance to cardiac muscle physiology and pathology, *Cardiovasc Res 77*, 265-273.
8. Haghighi, K., Chen, G., Sato, Y., Fan, G.-C., He, S., Kolokathis, F., Pater, L., Paraskevaidis, I., Jones, W. K., II, G. W. D., Kremastinos, D. T., and Kranias, E. G. (2008) A human phospholamban promoter polymorphism in dilated cardiomyopathy alters transcriptional regulation by glucocorticoids, *Human Mutation 29*, 640-647.
9. Haghighi, K., Kolokathis, F., Gramolini, A. O., Waggoner, J. R., Pater, L., Lynch, R. A., Fan, G.-C., Tsiapras, D., Parekh, R. R., II, G. W. D., MacLennan, D. H., Kremastinos, D. T., and Kranias, E. (2006) A mutation in the human phospholamban gene, deleting arginine 14, results in lethal, hereditary cardiomyopathy, *Proc. Natl. Acad. Sci. 103*, 1388-1393.
10. Mattiazzi, A., Mundina-Weilenmann, C., Vittone, L., and Said, M. (2004) Phosphorylation of phospholamban in ischemia-reperfusion injury: Functional role of Thr^{17} residue, *Molecular and Cellular Biochemistry 263*, 131-136.
11. Minamisawa, S., Hoshijima, M., Guoxiang, C., Ward, C., Frank, K., Gu, Y., Martone, M. E., Wang, Y., Jr., J. R., Kranias, E., Giles, W. R., and Chien, K. R. (1999) Chronic phospholamban-sarcoplasmic reticulum calcium ATPase interaction is the critical calcium cycling defect in dilated cardiomyopathy, *Cell 99*, 313-322.
12. Wuytack, F., Raeymaekers, L., and Missiaen, L. (2002) Molecular physiology of the SERCA and SPCA pumps, *Cell Calcium 32*, 279-305.

13. MacLennan, D. H., Toyofuku, T., and Lytton, J. (1992) Structure-Function Relationships in Sarcoplasmic or Endoplasmic Reticulum Type Ca2+ Pumpsa, *Annals of the New York Academy of Sciences 671*, 1-10.

14. Toyoshima, C., Nakasako, M., Nomura, H., and Ogawa, H. (2000) Crystal structure of the calcium pump of sarcoplasmic reticulum at 2.6 [angst] resolution, *Nature 405*, 647-655.

15. MacLennan, D. H., and Kranias, E. G. (2003) Phospholamban: A crucial regulator of cardiac contractility, *Nature Reviews 4*, 566-577.

16. Wuytack, F. (2009) Half a century of ion-transport ATPases: the P- and V-type ATPases, *European Journal of Physiology 457*, 569-571.

17. Toyoshima, C., Nomura, H., and Tsuda, T. (2004) Lumenal gating mechanism revealed in calcium pump crystal structures with phosphate analogues, *Nature 432*, 361-368.

18. Karim, C. B., Stamm, J. D., Karim, J., Jones, L. R., and Thomas, D. D. (1998) Cysteine reactivity and oligomeric structures of phospholamban and its mutants, *Biochemistry 37*, 12074-12081.

19. MacLennan, D. H., Kimura, Y., and Toyofuku, T. (1998) Sites of Regulatory Interaction between Calcium ATPases and Phospholamban, *Annals of the New York Academy of Sciences 853*, 31-42.

20. Fujii, J., Maruyama, K., Tada, M., and Maclennan, D. H. (1989) Expression and Site-specific Mutagenesis of Phospholamban, *The Journal of Biological Chemistry 264*, 12950-12955.

21. Simmerman, H. K. B., and Jones, L. R. (1998) Phospholamban: Protein Structure, Mechanism of Action, and Role in Cardiac Function, *Physiol. Rev. 78*, 921-947.

22. Simmerman, H. K. B., Kobayashi, Y. M., Autry, J. M., and Jones, L. R. (1996) A Leucine Zipper Stabilizes the Pentameric Membrane Domain of Phospholamban and Forms a Coiled-coil Pore Structure, *J. Biol. Chem. 271*, 5941-5946.

23. Cornea, R. L., Autry, J. M., Chen, Z., and Jones, L. R. (2000) Reexamination of the Role of the Leucine/Isoleucine Zipper Residues of Phospholamban in Inhibition of the Ca2+ Pump of Cardiac Sarcoplasmic Reticulum, *J. Biol. Chem. 275*, 41487-41494.

24. Karim, C. B., Paterlini, M. G., Reddy, L. G., Hunter, G. W., Barany, G., and Thomas, D. D. (2001) Role of cysteine residues in structural stability and function of a transmembrane helix bundle, *Journal of Biological Chemistry 276*, 38814-38819.

25. Asahi, M., Kimura, Y., Kurzydlowski, K., Tada, M., and MacLennan, D. H. (1999) Transmembrane Helix M6 in Sarco(endo)plasmic Reticulum Ca^{2+}-ATPase Forms a Functional Interaction Site with Phospholamban., *J. Biol. Chem. 274*, 32855-32862.

26. Morita, T., Hussain, D., Asahi, M., Tsuda, T., Kurzydlowski, K., Toyoshima, C., and MacLennan, D. H. (2008) Interaction sites among phospholamban, sarcolipin, and the sarco(endo)plasmic reticulum Ca2+-ATPase, *Biochemical and Biophysical Research Communications 369*, 188-194.

27. Chen, Z., Akin, B. L., Stokes, D. L., and Jones, L. R. (2006) Cross-linking of C-terminal residues of phospholamban to the Ca2+ pump of cardiac sarcoplasmic reticulum to probe spatial and functional interactions within the transmembrane domain, *The Journal of Biological Chemistry 281*, 14163-14172.

28. Chen, L. T. L., Yao, Q., Soares, T. A., Squier, T. C., and Bigelow, D. J. (2009) Phospholamban Modulates the Functional Coupling between Nucleotide Domains in Ca-ATPase Oligomeric Complexes in Cardiac Sarcoplasmic Reticulum&#x2020, *Biochemistry 0*.

29. Waggoner, J. R., Huffman, J., Froehlich, J. P., and Mahaney, J. E. (2007) Phopholamban inhibits Ca-ATPase conformational changes involving the E2 intermediate, *Biochemistry 46*, 1999-2009.

30. Rossi, A. E., Boncompagni, S., and Dirksen, R. T. (2009) Sarcoplasmic Reticulum - mitochondrial symbiosis: bidirectional signaling in skeletal muscle, *Excercise Sport Science Review 37*, 29-35.

31. Negash, S., Chen, L. T., Bigelow, D. J., and Squier, T. C. (1996) Phosphorylation of phospholamban by cAMP-dependent protein kinase enhances interactions between Ca-ATPase polypeptide chains in cardiac sarcoplasmic reticulum membranes, *Biochemistry 35*, 11247-11259.

32. Mukherjee, R., and Spinale, F. G. (1998) L-type calcium channel abundance and function with cardiac hypertrophy and failure: a review, *J Mol Cell Cardiol 30*, 1899-1916.

33. Wickenden, A. D., Kaprielian, R., Kassiri, Z., Tsoporis, J. N., Tsushima, R., Fishman, G. I., and Backx, P. H. (1998) The role of action potential prolongation and altered intracellular calcium handling in the pathogenesis of heart failure, *Cardiovasc Res 37*, 312-323.

34. Richard, S., Leclercq, F., Lemaire, S., Piot, C., and Nargeot, J. (1998) Ca2+ currents in compensated hypertrophy and heart failure, *Cardiovasc Res 37*, 300-311.

35. Towbin, J. A. (N. E. Bowles) The failing heart, *Nature 415*, 227-233.

36. Chien, K. R., Jr., J. R., and Hoshijima, M. (2005) Calcium and heart failure: the cycle game, *Nature Medicine 9*, 508-509.

37. Schwinger, R. H., Munch, G., Bolck, B., Karczewski, P., Krause, E. G., and Erdmann, E. (1999) Reduced Ca(2+)-sensitivity of SERCA 2a in failing human myocardium due to reduced serin-16 phospholamban phosphorylation, *J Mol Cell Cardiol 31*, 479-491.

38. Schmitt, J. P., Ahmad, F., Lorenz, K., Hein, L., Schulz, S., Asahi, M., MacLennan, D. H., Seidman, C. E., Seidman, J. G., and Lohse, M. J. (2009) Alterations of Phospholamban Function Can Exhibit Cardiotoxic Effects Independent of Excessive Sarcoplasmic Reticulum Ca2+-ATPase Inhibition, *Circulation 119*, 436-444.

39. Schmitt, J. P., Kamisago, M., Asahi, M., Li, G. H., Ahmad, F., Mende, U., Kranias, E., MacLennan, D. H., and Seidman, J. G. (2003) Dilated Cardiomyopathy and Heart Failure Caused by a Mutation in Phospholamban, *Science 299*, 1410-1413.

40. (2008) Heart Disease and Stroke Statistics, (Association, T. A. H., Ed.).

41. Feelisch, M. (2003) Nitroxyl gets to the heart of the matter, *Proc. Natl. Acad. Sci. 100*, 4978-4980.

42. Feldman, A. M., Bristow, M. R., Parmley, W. W., Carson, P. E., Pepine, C. J., Gilbert, E. M., Strobeck, J. E., Hendrix, G. H., Powers, E. R., Bain, R. P., and et al. (1993) Effects of vesnarinone on morbidity and mortality in patients with heart failure. Vesnarinone Study Group, *N Engl J Med 329*, 149-155.

43. Packer, M., Carver, J. R., Rodeheffer, R. J., Ivanhoe, R. J., DiBianco, R., Zeldis, S. M., Hendrix, G. H., Bommer, W. J., Elkayam, U., Kukin, M. L., and et al. (1991) Effect of oral milrinone on mortality in severe chronic heart failure. The PROMISE Study Research Group, *N Engl J Med 325*, 1468-1475.

44. Fukuto, J. M., Dutton, A. S., and Houk, K. N. (2005) The chemistry and biology of nitroxyl (HNO): A chemically unique species with novel and important biological activity, *ChemBioChem 6*, 612-619.

45. Paolocci, N., Jackson, M. I., Lopez, B. E., Miranda, K., Tocchetti, C. G., Wink, D. A., Hobbs, A. J., and Fukuto, J. M. (2007) The pharmacology of nitroxyl (HNO) and its therapeutic potential: Not just the janus face of NO, *Pharmacology & Therapeutics 113*, 442-458.

46. Miranda, K. M., Paolocci, N., Katori, T., Thomas, D. D., Ford, E., Bartberger, M. D., Espey, M. G., Kass, D. A., Feelish, M., Fukuto, J. M., and Wink, D. A. (2003) A biochemical rationale for the discrete behavior of nitroxyl and nitric oxide in the cardiovascular system, *Proc. Natl. Acad. Sci. 100*, 9196-9201.

47. Irvine, J. C., Ritchie, R. H., Favaloro, J. L., Andrews, K. L., Widdop, R. E., and Kemp-Harper, B. K. (2008) Nitroxyl (HNO): the Cinderella of the nitric oxide story, *Trends in Pharmacological Sciences 29*, 601-608.

48. Shafirovich, V., and Lymar, S. V. (2002) Nitroxyl and its anion in aqueous solutions: Spin states, protic equilibria, and reactivities toward oxygen and nitric oxide, *Proc. Natl. Acad. Sci. 99*, 7340-7345.

49. Lanzetta, P. A., Alvarez, L. J., Reinach, P. S., and Candia, O. A. (1979) An improved assay for nanomole amounts of inorganic phosphate, *Analytical Biochemistry 100*, 95-97.

50. Espey, M. G., Miranda, K. M., Thomas, D. D., and Wink, D. A. (2002) Ingress and reactive chemistry of nitroxyl-derived species within human cells, *Free Radic Biol Med 33*, 827-834.

51. Porzio, M. A., and Pearson, A. M. (1977) Improved resolution of myofibrillar proteins with sodium dodecyl sulfate-polyacrylamide gel electrophresis, *Biochimica et Biophysica Acta 490*, 27-34.

52. Paolocci, N., Saavedra, W., Miranda, K., Martignani, C., Isoda, T., hare, J., Espey, M. G., Fukuto, J. M., Feelisch, M., Wink, D. A., and Kass, D. A. (2001) Nitroxyl anion exerts redox-sensitive positive cardiac inotropy in vivo by calcitonin gene-related peptide signaling., *Proc. Natl. Acad. Sci. 98*, 10463-10468.

53. Tocchetti, C. G., Wang, W., Froehlich, J. P., Huke, S., Aon, M. A., Wilson, G. M., Benedetto, G. D., O'Rourke, B., Gao, W. D., Wink, D. A., Toscano, J. P., Zaccolo, M.,

Bers, D. M., Valdivia, H. H., Cheng, H., Kass, D. A., and Paolocci, N. (2007) Nitroxyl improves cellular heart function by directly enhancing cardiac sarcoplasmic reticulum Ca^{2+} cycling, *Circulation Research 100*, 96-104.

54. Froehlich, J. P., Mahaney, J. E., Keceli, G., Pavlos, C. M., Goldstein, R., Redwood, A. J., Sumbilla, C., Lee, D. I., Tocchetti, C. G., Kass, D. A., Paolocci, N., and Toscano, J. P. (2008) Phospholamban Thiols Play a Central Role in Activation of the Cardiac Muscle Sarcoplasmic Reticulum Calcium Pump by Nitroxyl, *Biochemistry 47*, 13150-13152.

55. Wouters, M. A., George, R. A., and Haworth, N. L. (2007) "Forbidden" Disulfides: Their Role as Redox Switches, *Current Protein and Peptide Science 8*, 484-495.

56. Cheong, E., Tumbev, V., Abramson, J., Salama, G., and Stoyanovsky, D. A. (2005) Nitroxyl triggers Ca^{2+} release from skeletal and cardiac sarcoplamic reticulum by oxidizing ryanodine receptors, *Cell Calcium 37*, 87-96.

57. Akhtar, M. J., Lutz, C. A., and Bonner, F. T. (1979) Decomposition of Sodium Trioxodinitrate ($Na_2N_2O_3$) in the presence of added nitrite in aqueous solution, *Inorganic Chemistry 18*, 2369-2375.

58. Hughes, M. N., Cammack, R., and Lester, P. (1999) [30] Synthesis, chemistry, and applications of nitroxyl ion releasers sodium trioxodinitrate or Angeli's salt and piloty's acid, In *Methods in Enzymology*, pp 279-287, Academic Press.

59. Murphy, C. I., Piwnica-Worms, H., Grunwald, S., Romanow, W. G., Francis, N., and Fan, H.-Y. (2004) Expression of Proteins in Insect Cells Using Baculovirus Vectors, *Current Protocols in Molecular Biology 65*, 16.19.11-16.19.10.

60. Luckow, V. A., Lee, S. C., Barry, G. F., and Olins, P. O. (1993) Efficient generation of infectious recombinant baculoviruses by site-specific transposon-mediated insertion of foreign genes into a baculovirus genome propagated in Escherichia coli, *Journal of Virology 67*, 4566-4579.

61. Waggoner, J. R., Ginsburg, K. S., Mitton, B. A., Haghighi, K., Robbins, J., Bers, D. M., and Kranias, E. G. (2008) Phospholamban Overexpression in Rabbit Ventricular Myocytes Does Not Alter Sarcoplasmic Reticulum Calcium Transport, *Am J Physiol Heart Circ Physiol*, 00272.02008.

62. Gornall, A. G., Bardawill, C. J., and David, M. M. (1949) Determination of Serum Proteins by Means of the Biuret Reaction, *Journal of Biological Chemistry 177*, 751-766.

63. Mahaney, J. E., Autry, J. M., and Jones, L. R. (2000) Kinetics Studies of the Cardiac Ca-ATPase Expressed in Sf21 Cells: New Insights on Ca-ATPase Regulation by Phospholamban, *Biophysical Journal 78*, 1306-1323.

64. Yao, Q., Bevan, J. L., Weaver, R. F., and Bigelow, D. J. (1996) Purification of Porcine Phospholamban Expressed inEscherichia coli, *Protein Expression and Purification 8*, 463-468.

65. Waggoner, J. R., Huffman, J., Griffith, B. N., Jones, L. R., and Mahaney, J. E. (2004) Improved expression and characterization of Ca2+-ATPase and phospholamban in High-Five cells, *Protein Expression and Purification 34*, 56-67.

66. Cornea, R. L., Jones, L. R., Autry, J. M., and Thomas, D. D. (1997) Mutation and phosphorylation change the oligomeric structure of phospholamban in lipid bilayers, *Biochemistry 36*, 2960-2967.

67. Wegener, A. D., and Jones, L. R. (1984) Phosphorylation-induced mobility shift in phospholamban in sodium dodecyl sulfate-polyacrylamide gels. Evidence for a protein structure consisting of multiple identical phosphorylatable subunits, *Journal of Biological Chemistry 259*, 1834-1841.

68. Rath, A., Glibowicka, M., Nadeau, V. G., Chen, G., and Deber, C. M. (2009) Detergent binding explains anomalous SDS-PAGE migration of membrane proteins, *Proceedings of the National Academy of Sciences 106*, 1760-1765.

69. Kimura, Y., Kurzydlowski, K., Tada, M., and MacLennan, D. H. (1997) Phospholamban Inhibitory Function Is Activated by Depolymerization, *J. Biol. Chem. 272*, 15061-15064.

70. Zvaritch, E., Backx, P. H., Jirik, F., Kimura, Y., de Leon, S., Schmidt, A. G., Hoit, B. D., Lester, J. W., Kranias, E. G., and MacLennan, D. H. (2000) The Transgenic Expression of Highly Inhibitory Monomeric Forms of Phospholamban in Mouse Heart Impairs Cardiac Contractility, *Journal of Biological Chemistry 275*, 14985-14991.

71. Thomas, D. D., Reddy, L. G., Karim, C. B., Li, M., Cornea, R. L., Autry, J. M., Jones, L. R., and Stamm, J. D. (1998) Direct Spectroscopic Detection of Molecular Dynamics and Interactions of the Calcium Pump and Phospholamban, *Annals of the New York Academy of Sciences 853*, 186-194.

72. Phelan, M. L., Sif, S., Narlikar, G. J., and Kingston, R. E. (1999) Reconstitution of a core chromatin remodeling complex from SWI/SNF subunits., *Mol. Cell 3*, 247-253.

73. Zhang, Y., Ng, H. H., Erdjument-Bromage, H., Tempst, P., Bird, A., and Reinburg, D. (1999) Analysis of the NuRD subunits reveals a histone deacetylase core complex and a connection with DNA methylation, *Genes Dev. 13*, 1924-1935.

74. Murphy, C. I., Piwnica-Worms, H., Grunwald, S., Romanow, W. G., Francis, N., and Fan, H.-Y. (2004) Expression and Purification of Recombinant Proteins Using the Baculovirus System, *Current Protocols in Molecular Biology 65*, 16.11.11-16.11.14.

75. Reddy, L. G., Cornea, R. L., Winters, D. L., McKenna, E., and Thomas, D. D. (2003) Defining the Molecular Components of Calcium Transport Regulation in a Reconstituted Membrane System, *Biochemistry 42*, 4585-4592.

76. Reddy, L. G., Jones, L. R., Cala, S. E., O'Brian, J. J., Tatulian, S. A., and Stokes, D. L. (1995) Functional Reconstitution of Recombinant Phospholamban with Rabbit Skeletal Ca-ATPase, *Journal of Biological Chemistry 270*, 9390-9397.

77. Trieber, C. A., Douglas, J. L., Afara, M., and Young, H. S. (2005) The Effects of Mutation on the Regulatory Properties of Phospholamban in Co-Reconstituted Membranes&#x2020, *Biochemistry 44*, 3289-3297.

78. Einarson, M. B., Pugacheva, E. N., and Orlinick, J. R. (2007) Preparation of GST Fusion Proteins, *Cold Spring Harbor Protocols 2007*, pdb.prot4738.

79. Bichet, P., Mollat, P., Capdevila, C., and Sarubbi, E. (2000) Endogenous Glutathione-Binding Proteins of Insect Cell Lines: Characterization and Removal from Glutathione S-Transferase (GST) Fusion Proteins, *Protein Expression and Purification 19*, 197-201.

80. Davies, A. H., Jowett, J. B. M., and Jones, I. M. (1993) Recombinant baculovirus vectors expressing glutathione-S-transferase fusion proteins, *Bio/Technology 11*, 933-936.

81. Mahaney, J. E., Albers, R. W., Waggoner, J. R., Kutchai, H. C., and Froehlich, J. P. (2005) Intermolecular Conformational Coupling and Free Energy Exchange Enhance the Catalytic Efficiency of Cardiac Muscle SERCA2a following the Relief of Phospholamban Inhibition†, *Biochemistry 44*, 7713-7724.

82. Mahaney, J. E., Autry, J. M., and Jones, L. R. (2000) Kinetics Studies of the Cardiac Ca-ATPase Expressed in Sf21 Cells: New Insights on Ca-ATPase Regulation by Phosholamban, *Biophysical Journal 78*, 1306-1323.

83. Ma, X. L., Gao, F., Liu, G. L., Lopez, B. L., Christopher, T. A., Fukuto, J. M., Wink, D. A., and Feelisch, M. (1999) Opposite effects of nitric oxide and nitroxyl on postischemic myocardial injury, *Proc Natl Acad Sci U S A 96*, 14617-14622.

84. Wink, D. A., Feelisch, M., Fukuto, J., Chistodoulou, D., Jourd'heuil, D., Grisham, M. B., Vodovotz, Y., Cook, J. A., Krishna, M., DeGraff, W. G., Kim, S., Gamson, J., and Mitchell, J. B. (1998) The cytotoxicity of nitroxyl: possible implications for the pathophysiological role of NO, *Arch Biochem Biophys 351*, 66-74.

85. Louis, C. F., Maffitt, M., and Jarvis, B. (1982) Factors that modify the molecular size of phospholamban, the 23,000-dalton cardiac sarcoplasmic reticulum phosphoprotein, *Journal of Biological Chemistry 257*, 15182-15186.

86. Le Peuch, C. J., Haiech, J., and Demaille, J. G. (1979) Concerted regulation of cardiac sarcoplasmic reticulum calcium transport by cyclic adenosine monophosphate dependent and calcium-calmodulin-dependent phosphorylations, *Biochemistry 18*, 5150-5157.

87. Reddy, L. G., Autry, J. M., Jones, L. R., and Thomas, D. D. (1999) Co-reconstitution of Phospholamban Mutants with the Ca-ATPase Reveals Dependence of Inhibitory Function on Phospholamban Structure, *Journal of Biological Chemistry 274*, 7649-7655.

88. Li, M., Reddy, L. G., Bennett, R., Silva, N. D., Jr., Jones, L. R., and Thomas, D. D. (1999) A fluorescence energy transfer method for analyzing protein oligomeric structure: application to phospholamban, *Biophys J 76*, 2587-2599.

89. Reddy, L. G., Jones, L. R., and Thomas, D. D. (1999) Depolymerization of phospholamban in the presence of calcium pump: a fluorescence energy transfer study, *Biochemistry 38*, 3954-3962.

90. Sivakumaran, V. (2010) In *Biochemistry*, Virginia Tech, Blacksburg, VA.

91. Karim, C. B., Marquardt, C. G., Stamm, J. D., Barany, G., and Thomas, D. D. (2000) Synthetic null-cysteine phospholamban analouge and the corresponding transmembrane domain inhibit the Ca-ATPase, *Biochemistry 39*, 10892-10897.

92. Autry, J. M., and Jones, L. R. (1997) Functional Co-expression of the Canine Cardiac Ca2+Pump and Phospholamban in Spodoptera frugiperda (Sf21) Cells Reveals New Insights on ATPase Regulation, *Journal of Biological Chemistry 272*, 15872-15880.

93. Sha, X., Isbell, T. S., Patel, R. P., Day, C. S., and King, S. B. (2006) Hydrolysis of Acyloxy Nitroso Compounds Yields Nitroxyl (HNO), *Journal of the American Chemical Society 128*, 9687-9692.

94. Ellman, G. L. (1959) Tissue sulfhydryl groups, *Arch Biochem Biophys 82*, 70-77.

95. Lompre, A. M., Hajjar, R. J., Harding, S. E., Kranias, E. G., Lohse, M. J., and Marks, A. R. (2010) Ca2+ cycling and new therapeutic approaches for heart failure, *Circulation 121*, 822-830.

96. Lipskaia, L., Chemaly, E. R., Hadri, L., Lompre, A. M., and Hajjar, R. J. (2010) Sarcoplasmic reticulum Ca(2+) ATPase as a therapeutic target for heart failure, *Expert Opin Biol Ther 10*, 29-41.

97. Kawase, Y., Ladage, D., and Hajjar, R. J. (2011) Rescuing the failing heart by targeted gene transfer, *J Am Coll Cardiol 57*, 1169-1180.

98. Kairouz, V., Lipskaia, L., Hajjar, R. J., and Chemaly, E. R. (2012) Molecular targets in heart failure gene therapy: current controversies and translational perspectives, *Annals of the New York Academy of Sciences 1254*, 42-50.

99. del Monte, F., Harding, S. E., Schmidt, U., Matsui, T., Kang, Z. B., Dec, G. W., Gwathmey, J. K., Rosenzweig, A., and Hajjar, R. J. (1999) Restoration of contractile function in isolated cardiomyocytes from failing human hearts by gene transfer of SERCA2a, *Circulation 100*, 2308-2311.

100. Jessup, M., Greenberg, B., Mancini, D., Cappola, T., Pauly, D. F., Jaski, B., Yaroshinsky, A., Zsebo, K. M., Dittrich, H., and Hajjar, R. J. (2011) Calcium Upregulation by Percutaneous Administration of Gene Therapy in Cardiac Disease (CUPID): a phase 2 trial of intracoronary gene therapy of sarcoplasmic reticulum Ca2+-ATPase in patients with advanced heart failure, *Circulation 124*, 304-313.

101. Tilgmann, C., Pollesello, P., Ovaska, M., Kaivola, J., Pystynen, J., Tiainen, E., Yliperttula, M., Annila, A., and Levijoki, J. (2012) Discovery and Structural Characterization of a Phospholamban-Binding Cyclic Peptide and Design of Novel Inhibitors of Phospholamban, *Chemical Biology & Drug Design*, no-no.

102. Micheletti, R., Palazzo, F., Barassi, P., Giacalone, G., Ferrandi, M., Schiavone, A., Moro, B., Parodi, O., Ferrari, P., and Bianchi, G. (2007) Istaroxime, a stimulator of sarcoplasmic reticulum calcium adenosine triphosphatase isoform 2a activity, as a novel therapeutic approach to heart failure, *Am J Cardiol 99*, 24A-32A.

Appendix A:

Oligonucleotide Primers for Site- Directed Mutagenesis

Site-directed mutagenesis procedures are outlined in Chapter II: Materials and Methodology. The following table of primers was used to create PLN cysteine mutant variants in the baculovirus (pFASTBac™1) and pGEXT2T –vector system for expression of recombinant proteins. The underlined segments refer to the position of the new cysteine codon to be generated with mutagenic primers. As a reminder, 36/46C PLN primers were not created and are therefore not listed because a primer could not be created to span the distance between the two locations. Results showing HNO effect on the oligomeric stability and migration pattern using the mutant variants are discussed in Chapter IV. These mutant variants were also co-expressed with SERCA2a in insect cell microsomes and use to understand the effect of HNO on PLN and SERCA2a activation, those results can also be seen in Chapter III. In Table A-1, all primers are listed, both forward (5' - 3') and reverse (5' - 3', reverse complement).

Variant	Primer	Oligonucleotide Sequence (5'-3')	Template
36C	Forward	CTTCAGAACCTATTTATCAATTTCTGTCTCATCTTAATAGCCCTCTTGCT	pGEX2T
	Reverse	AGCAAGAGGGCTATTAAGATGAGACAGAAATTGATAAATAGGTTCTGAAG	
41C	Forward	CCTATTTATCAATTTCGCTCTCATCTTAATATGCCTCTTGCTGATTGCC	pGEX2T
	Reverse	GGCAATCAGCAAGAGGCATATTAAGATGAGAGCGAAATTGATAAATAGG	
46C	Forward	CATCTTAATAGCCCTCTTGCTGATTTGCATCATCGTGATGC	pGEX2T
	Reverse	GCATCACGATGATGCAAATCAGCAAGAGGGCTATTAAGATG	
36/41C	Forward	CCTATTTATCAATTTCTGTCTCATCTTAATATGCCTCTTGCTGATTGCC	pGEX2T
	Reverse	GGCAATCAGCAAGAGGCATATTAAGATGAGACAGAAATTGATAAATAGG	
41/46C	Forward	CTCATCTTAATATGCCTCTTGCTGATTTGCATCATCGTGATGCT	pGEX2T
	Reverse	AGCATCACGATGATGCAAATCAGCAAGAGGCATATTAAGATGAG	
36C	Forward	TCTTCAGAACCTATTTATAAATTTCTGTCTCATTTTAATATGTCTCTTGTTGATCTG	pFASTBac™1
	Reverse	CAGATCAACAAGAGACATATTAAAATGAGACAGAAATTTATAAATAGGTTCTGAAGATTTTG	
41C	Forward	CTATTTATAAATTTCGCTCTCATTTTAATATGTCTCTTGTTGATCGCCATCATTGTG	pFASTBac™1
	Reverse	CACAATGATGGCGATCAACAAGAGACATATTAAAATGAGAGCGAAATTTATAAATAG	
46C	Forward	GCTCTCATTTTAATAGCTCTCTTGTTGATCTGCATCATTGTGATGCTTCTCTGAAGATCTAGAG	pFASTBac™1
	Reverse	CTCTAGATCTTCAGAGAAGCATCACAATGATGCAGATCAACAAGAGAGCTATTAAAATGAGAGC	
36/41C	Forward	TTCAGAACCTATTTATAAATTTCTGTCTCATTTTAATATGTCTCTTGTTGATCTG	pFASTBac™1
	Reverse	CAGATCAACAAGAGACATATTAAAATGAGACAGAAATTTATAAATAGGTTCTGAA	
41/46C	Forward	TCGCTCTCATTTTAATATGTCTCTTGTTGATCTGCATCATTGTGATGCTTCTCTGAGATC	pFASTBac™1
	Reverse	GATCTCAGAGAAGCATCACAATGATGCAGATCAACAAGAGACATATTAAAATGAGAGCGA	
WT-PLN	Forward	CAAAATCTTCAGAACCTATTTATAAATTTCTGTCTCATTTTAATATGTCTCTTGTTGATCTG	pFASTBac™1
	Reverse	CAGATCAACAAGAGACATATTAAAATGAGACAGAAATTTATAAATAGGTTCTGAAGATTTTG	

Table A-1. Primers for site-directed mutagenesis

Appendix B:

Fair Use and Public Domain Figure Citations

Figure 1-1 ..... [fair use]
Bers, D. M. (2002). "Cardiac excitation-contraction coupling." Nature **415**: 198-205. (accessed March 14, 2012) Fair use determination attached.

Figure 1-2 ..... [used with permission]
Toyoshima, C., et.al. (2000). "Crystal structure of the calcium pump of sarcoplasmic reticulum at 2.6 [angst] resolution." Nature **405**: 647-655. http://www.nature.com/nature/journal/v405/n6787/full/405647a0.html (accessed June 4, 2012) Licensing attached.

Figure 1-4 ..... [used with permission]
Karim, C. B., Paterlini, M. G., Reddy, L. G., Hunter, G. W., Barany, G., and Thomas, D. D. (2001) Role of cysteine residues in structural stability and function of a transmembrane helix bundle, *Journal of Biological Chemistry 276*, 38814-38819. (accessed on May 25, 2012). Permission letter from ASMB attached.

Figure 1-5 ..... [used with permission]
MacLennan, D. H., and Kranias, E. G. (2003) Phospholamban: A crucial regulator of cardiac contractility, Nature Reviews 4, 566-577. www.nature.com/reviews/molcellbio. (accessed Apil 20, 2009). Licensing attached.

Draft 09/01/2009

(Questions? Concerns? Contact Gail McMillan, Director of the Digital Library and Archives at Virginia Tech's University Libraries: gailmac@vt.edu)

(Please ensure that Javascript is enabled on your browser before using this tool.)

Virginia Tech ETD Fair Use Analysis Results

This is not a replacement for professional legal advice but an effort to assist you in making a sound decision.

Name: Chevon Thorpe

Description of item under review for fair use: Figure 1. Bers, D. M., Cardiac excitation-contraction coupling. Nature 2002, 415, 198-205.

Report generated on: 05-14-2012 at : 15:54:15

Based on the information you provided:

Factor 1

Your consideration of the purpose and character of your use of the copyright work weighs: ***in favor of fair use***

Factor 2

Your consideration of the nature of the copyrighted work you used weighs: ***in favor of fair use***

Factor 3

Your consideration of the amount and substantiality of your use of the copyrighted work weighs: ***in favor of fair use***

Factor 4

Your consideration of the effect or potential effect on the market after your use of the copyrighted work weighs: ***in favor of fair use***

Based on the information you provided, your use of the copyrighted work weighs: *in favor of fair use*

NATURE PUBLISHING GROUP LICENSE
TERMS AND CONDITIONS

Jun 04, 2012

This is a License Agreement between Chevon N Thorpe ("You") and Nature Publishing Group ("Nature Publishing Group") provided by Copyright Clearance Center ("CCC"). The license consists of your order details, the terms and conditions provided by Nature Publishing Group, and the payment terms and conditions.

All payments must be made in full to CCC. For payment instructions, please see information listed at the bottom of this form.

License Number	2921970107227
License date	Jun 04, 2012
Licensed content publisher	Nature Publishing Group
Licensed content publication	Nature
Licensed content title	Crystal structure of the calcium pump of sarcoplasmic reticulum at 2.6 Å resolution
Licensed content author	Chikashi Toyoshima, Masayoshi Nakasako, Hiromi Nomura, Haruo Ogawa
Licensed content date	Jun 8, 2000
Volume number	405
Issue number	6787
Type of Use	reuse in a thesis/dissertation
Requestor type	academic/educational
Format	electronic
Portion	figures/tables/illustrations
Number of figures/tables/illustrations	1
Figures	Figure 2. Architecture of the sarcoplasmic reticulum Ca2+-ATPase.
Author of this NPG article	no
Your reference number	
Title of your thesis / dissertation	The Role of Phospholamban Cysteines in the Activation of the Cardiac Sarcoplasmic Reticulum Ca2+ Pump by Nitroxyl (HNO)
Expected completion date	Jun 2012
Estimated size (number of pages)	140
Total	0.00 USD
Terms and Conditions	

Terms and Conditions for Permissions

Nature Publishing Group hereby grants you a non-exclusive license to reproduce this material for this purpose, and for no other use, subject to the conditions below:

1. NPG warrants that it has, to the best of its knowledge, the rights to license reuse of this material. However, you should ensure that the material you are requesting is

original to Nature Publishing Group and does not carry the copyright of another entity (as credited in the published version). If the credit line on any part of the material you have requested indicates that it was reprinted or adapted by NPG with permission from another source, then you should also seek permission from that source to reuse the material.

2. Permission granted free of charge for material in print is also usually granted for any electronic version of that work, provided that the material is incidental to the work as a whole and that the electronic version is essentially equivalent to, or substitutes for, the print version. Where print permission has been granted for a fee, separate permission must be obtained for any additional, electronic re-use (unless, as in the case of a full paper, this has already been accounted for during your initial request in the calculation of a print run). NB: In all cases, web-based use of full-text articles must be authorized separately through the 'Use on a Web Site' option when requesting permission.

3. Permission granted for a first edition does not apply to second and subsequent editions and for editions in other languages (except for signatories to the STM Permissions Guidelines, or where the first edition permission was granted for free).

4. Nature Publishing Group's permission must be acknowledged next to the figure, table or abstract in print. In electronic form, this acknowledgement must be visible at the same time as the figure/table/abstract, and must be hyperlinked to the journal's homepage.

5. The credit line should read:
   Reprinted by permission from Macmillan Publishers Ltd: [JOURNAL NAME] (reference citation), copyright (year of publication)
   For AOP papers, the credit line should read:
   Reprinted by permission from Macmillan Publishers Ltd: [JOURNAL NAME], advance online publication, day month year (doi: 10.1038/sj.[JOURNAL ACRONYM].XXXXX)

   Note: For republication from the *British Journal of Cancer*, the following credit lines apply.
   Reprinted by permission from Macmillan Publishers Ltd on behalf of Cancer Research UK: [JOURNAL NAME] (reference citation), copyright (year of publication) For AOP papers, the credit line should read:
   Reprinted by permission from Macmillan Publishers Ltd on behalf of Cancer Research UK: [JOURNAL NAME], advance online publication, day month year (doi: 10.1038/sj.[JOURNAL ACRONYM].XXXXX)

6. Adaptations of single figures do not require NPG approval. However, the adaptation should be credited as follows:

   Adapted by permission from Macmillan Publishers Ltd: [JOURNAL NAME] (reference citation), copyright (year of publication)

   Note: For adaptation from the *British Journal of Cancer*, the following credit line applies.
   Adapted by permission from Macmillan Publishers Ltd on behalf of Cancer Research UK: [JOURNAL NAME] (reference citation), copyright (year of publication)

7. Translations of 401 words up to a whole article require NPG approval. Please visit http://www.macmillanmedicalcommunications.com for more information. Translations of up to a 400 words do not require NPG approval. The translation should be credited as follows:

   Translated by permission from Macmillan Publishers Ltd: [JOURNAL NAME] (reference citation), copyright (year of publication).

   Note: For translation from the *British Journal of Cancer*, the following credit line applies.
   Translated by permission from Macmillan Publishers Ltd on behalf of Cancer Research UK: [JOURNAL NAME] (reference citation), copyright (year of publication)

We are certain that all parties will benefit from this agreement and wish you the best in the use of this material. Thank you.

Special Terms:

v1.1

If you would like to pay for this license now, please remit this license along with your payment made payable to "COPYRIGHT CLEARANCE CENTER" otherwise you will be invoiced within 48 hours of the license date. Payment should be in the form of a check or money order referencing your account number and this invoice number RLNK500792056.
Once you receive your invoice for this order, you may pay your invoice by credit card. Please follow instructions provided at that time.

Make Payment To:
Copyright Clearance Center
Dept 001
P.O. Box 843006
Boston, MA 02284-3006

For suggestions or comments regarding this order, contact RightsLink Customer Support: customercare@copyright.com or +1-877-622-5543 (toll free in the US) or +1-978-646-2777.

Gratis licenses (referencing $0 in the Total field) are free. Please retain this printable license for your reference. No payment is required.

NATURE PUBLISHING GROUP LICENSE TERMS AND CONDITIONS

Jun 04, 2012

This is a License Agreement between Chevon N Thorpe ("You") and Nature Publishing Group ("Nature Publishing Group") provided by Copyright Clearance Center ("CCC"). The license consists of your order details, the terms and conditions provided by Nature Publishing Group, and the payment terms and conditions.

All payments must be made in full to CCC. For payment instructions, please see information listed at the bottom of this form.

License Number	2922100804470
License date	Jun 04, 2012
Licensed content publisher	Nature Publishing Group
Licensed content publication	Nature Reviews Molecular Cell Biology
Licensed content title	Calcium: Phospholamban: a crucial regulator of cardiac contractility
Licensed content author	David H. MacLennan, Evangelia G. Kranias
Licensed content date	Jul 1, 2003
Volume number	4
Issue number	7
Type of Use	reuse in a thesis/dissertation
Requestor type	academic/educational
Format	electronic
Portion	figures/tables/illustrations
Number of figures/tables/illustrations	1
High-res required	no
Figures	Box 2 | Sarcolipin is a phospholamban homologue. Adapted the image to delete the sarcolipin and modified the amino acid colors to highlight only the cysteine residues.
Author of this NPG article	no
Your reference number	
Title of your thesis / dissertation	The Role of Phospholamban Cysteines in the Activation of the Cardiac Sarcoplasmic Reticulum Ca2+ Pump by Nitroxyl (HNO)
Expected completion date	Jun 2012
Estimated size (number of pages)	140
Total	0.00 USD
Terms and Conditions	

Terms and Conditions for Permissions

Nature Publishing Group hereby grants you a non-exclusive license to reproduce this material for this purpose, and for no other use, subject to the conditions below:

1. NPG warrants that it has, to the best of its knowledge, the rights to license reuse of this material. However, you should ensure that the material you are requesting is original to Nature Publishing Group and does not carry the copyright of another entity (as credited in the published version). If the credit line on any part of the material you have requested indicates that it was reprinted or adapted by NPG with permission from another source, then you should also seek permission from that source to reuse the material.

2. Permission granted free of charge for material in print is also usually granted for any electronic version of that work, provided that the material is incidental to the work as a whole and that the electronic version is essentially equivalent to, or substitutes for, the print version. Where print permission has been granted for a fee, separate permission must be obtained for any additional, electronic re-use (unless, as in the case of a full paper, this has already been accounted for during your initial request in the calculation of a print run). NB: In all cases, web-based use of full-text articles must be authorized separately through the 'Use on a Web Site' option when requesting permission.

3. Permission granted for a first edition does not apply to second and subsequent editions and for editions in other languages (except for signatories to the STM Permissions Guidelines, or where the first edition permission was granted for free).

4. Nature Publishing Group's permission must be acknowledged next to the figure, table or abstract in print. In electronic form, this acknowledgement must be visible at the same time as the figure/table/abstract, and must be hyperlinked to the journal's homepage.

5. The credit line should read:
   Reprinted by permission from Macmillan Publishers Ltd: [JOURNAL NAME] (reference citation), copyright (year of publication)
   For AOP papers, the credit line should read:
   Reprinted by permission from Macmillan Publishers Ltd: [JOURNAL NAME], advance online publication, day month year (doi: 10.1038/sj.[JOURNAL ACRONYM].XXXXX)

   Note: For republication from the *British Journal of Cancer*, the following credit lines apply.
   Reprinted by permission from Macmillan Publishers Ltd on behalf of Cancer Research UK: [JOURNAL NAME] (reference citation), copyright (year of publication) For AOP papers, the credit line should read:
   Reprinted by permission from Macmillan Publishers Ltd on behalf of Cancer Research UK: [JOURNAL NAME], advance online publication, day month year (doi: 10.1038/sj.[JOURNAL ACRONYM].XXXXX)

6. Adaptations of single figures do not require NPG approval. However, the adaptation should be credited as follows:

   Adapted by permission from Macmillan Publishers Ltd: [JOURNAL NAME] (reference citation), copyright (year of publication)

   Note: For adaptation from the *British Journal of Cancer*, the following credit line applies.
   Adapted by permission from Macmillan Publishers Ltd on behalf of Cancer Research

UK: [JOURNAL NAME] (reference citation), copyright (year of publication)

7. Translations of 401 words up to a whole article require NPG approval. Please visit http://www.macmillanmedicalcommunications.com for more information.
Translations of up to a 400 words do not require NPG approval. The translation should be credited as follows:

   Translated by permission from Macmillan Publishers Ltd: [JOURNAL NAME] (reference citation), copyright (year of publication).

   Note: For translation from the *British Journal of Cancer*, the following credit line applies.
   Translated by permission from Macmillan Publishers Ltd on behalf of Cancer Research UK: [JOURNAL NAME] (reference citation), copyright (year of publication)

We are certain that all parties will benefit from this agreement and wish you the best in the use of this material. Thank you.

Special Terms:

v1.1

If you would like to pay for this license now, please remit this license along with your payment made payable to "COPYRIGHT CLEARANCE CENTER" otherwise you will be invoiced within 48 hours of the license date. Payment should be in the form of a check or money order referencing your account number and this invoice number RLNK500792384.
Once you receive your invoice for this order, you may pay your invoice by credit card. Please follow instructions provided at that time.

Make Payment To:
Copyright Clearance Center
Dept 001
P.O. Box 843006
Boston, MA 02284-3006

For suggestions or comments regarding this order, contact RightsLink Customer Support: customercare@copyright.com or +1-877-622-5543 (toll free in the US) or +1-978-646-2777.

Gratis licenses (referencing $0 in the Total field) are free. Please retain this printable license for your reference. No payment is required.

11200 Rockville Pike
Suite 302
Rockville, Maryland 20852

August 19, 2011

American Society for Biochemistry and Molecular Biology

To whom it may concern,

It is the policy of the American Society for Biochemistry and Molecular Biology to allow reuse of any material published in its journals (the Journal of Biological Chemistry, Molecular & Cellular Proteomics and the Journal of Lipid Research) in a thesis or dissertation at no cost and with no explicit permission needed. Please see our copyright permissions page on the journal site for more information.

Best wishes,

Sarah Crespi

American Society for Biochemistry and Molecular Biology
11200 Rockville Pike, Rockville, MD
Suite 302
240-283-6616
JBC | MCP | JLR